Combining effects of one tumor-stroma recognizing TCR with one cancer-cell specific TCR for eradication of solid tumors

Inaugural-Dissertation to obtain the academic degree

Doctor rerum naturalium (Dr. rer. nat.)

Submitted to the Department of Biology, Chemistry, Pharmacy

of Freie Universität Berlin

by

Steven Patrick Wolf

Berlin 2020

The dissertation “Combining effects of one tumor-stroma recognizing TCR with one cancer-cell specific TCR for eradication of solid tumors” was prepared under the direction of Prof. Dr. Thomas Blankenstein and Prof. Dr. Hans Schreiber in the period from September 2015 till June 2020 at the Max-Delbrück-Centrum für Molekulare Medizin in der Helmholtz-Gemeinschaft Berlin, Germany and at The University of Chicago in Chicago, Illinois, USA.

1st Reviewer	Prof. Dr. Thomas Blankenstein
	Freie Universität Berlin
2nd Reviewer	Prof. Dr. Hans Schreiber
	University of Chicago
Date of defense	12 November 2020

“Dripping water hollows out stone, not through force but through persistence.”

— Publius Ovidius Naso (Ovid, 43 B.C. – A.D. 17), Epistulae Herodium

Acknowledgement

I would like to thank my supervisors Prof. Dr. Thomas Blankenstein and Prof. Dr. Hans Schreiber for giving me the opportunity to do my PhD. I am very grateful to both of them and that I got this chance in life. Both have always taken their time to discuss my projects and guided me to earn my degree. I am especially thankful to Prof. Dr. Hans Schreiber who invited me to The University of Chicago and exposed me to the scientific community in the USA.

Special thanks also to Prof. Dr. Matthias Leisegang who helped me in the early stages of my research project, had always time to discuss scientific questions and supported me throughout the entire time as much as possible. I also thank Dr. Kazuma Kiyotani for his valuable help, suggestions and critical discussions.

I would also like to thank the members of Prof. Dr. Hans Schreiber's laboratory for their interactions and help on a daily basis. They made the work on my research project much more enjoyable. I like to thank Karin Schreiber for her valuable discussions about experimental design, planning and execution. I am grateful to Madeline Steiner, she was very supportive of me, took always time to discuss scientific problems and some of my experiments would have never worked without her assistance and problem solving creativity. I would also like to thank Markus Diehl who took projects over and freed some of my time. Yanran He helped me to arrive in Chicago and get used to the new environment in- and outside the laboratory and I thank her for her time, discussions and kindness.

Many thanks to all the people I met during my time at The University of Chicago and at the Max Delbrück Center in Berlin. Everyone helped me in their own way during my thesis and made this dissertation possible.

In the end I would like to thank my parents, Simone Wolf and Holger Wolf. They both had it not always easy with me but made my journey possible and supported my decisions on the way. I would have accomplished nothing if it would not have been for their believes in me.

Table of Content

1. Summary

Adoptive transfer of T cells, engineered with antigen-specific receptors, is clinically used against acute lymphoblastic leukemia and certain types of large-B-cell lymphomas. Reliable and efficient use of such T cells against solid tumors has not been established yet. However, adoptive transfer of autologous, tumor infiltrating T cells (TILs) can eradicate established solid tumors in some patients. A limitation with this form of therapy is that isolation and expansion of TILs fails in the majority of patients and success seems to depend on the presence of a mutant neoantigen-specific T cell population in the transferred TIL product. Mutant neoantigen-specific T cells can be found in almost all analyzed cancer types. Furthermore, TCR genes can be isolated from TILs and used for viral transduction of patient-derived, autologous peripheral blood lymphocytes (PBLs). As of yet, it is unknown how many different TCRs from T cell clonotypes of the polyclonal TIL response are needed to achieve cure. Therefore, the main objective of this thesis was to determine the requirements for mutant neoantigen-specific TCR-transduced T cells to achieve eradication of established solid tumors by adoptive transfer. For this, unmanipulated murine tumors were targeted using TCRs that recognized autochthonous, naturally occurring mutant neoantigens. Using such animal models, it was possible to show that tumors can be eradicated with just two cancer-specific TCR clonotypes. One TCR had to target the cancer cells directly by recognition of a cancer-specific MHC class I restricted antigen, while the second TCR had to target a MHC class II restricted mutant neoantigen presented by cells of the tumor stroma. It shows that both TCR clonotype are sufficient and essential to achieve tumor rejection because a combination of two TCRs targeting independent MHC class I restricted mutant neoantigens was not as efficient and led to tumor escape even though the tumor that had been targeted was developed from a cancer cell clone, seemingly lacking tumor heterogeneity. Targeting only the tumor stroma with a MHC class II restricted mutant neoantigen-specific TCR led to tumor destruction followed by long-term growth arrest but never eradicated the tumor. This effect was caused by regression of tumor vasculature and depended on tumor stroma recognition only. For tumor eradication, direct cancer cell recognition was essential because lack of surface expression of MHC class I molecules by cancer cells led to failure of tumor rejection despite the presence of both TCR clonotypes. These data created the hypothesis that a four cell-type interaction is required for effective elimination of solid tumors (**Figure 1**) and gives insights that simplifications for translation into clinical applications may be possible without sacrificing efficacy for adoptive, mutant neoantigen-specific, TCR-redirected T cell transfer.

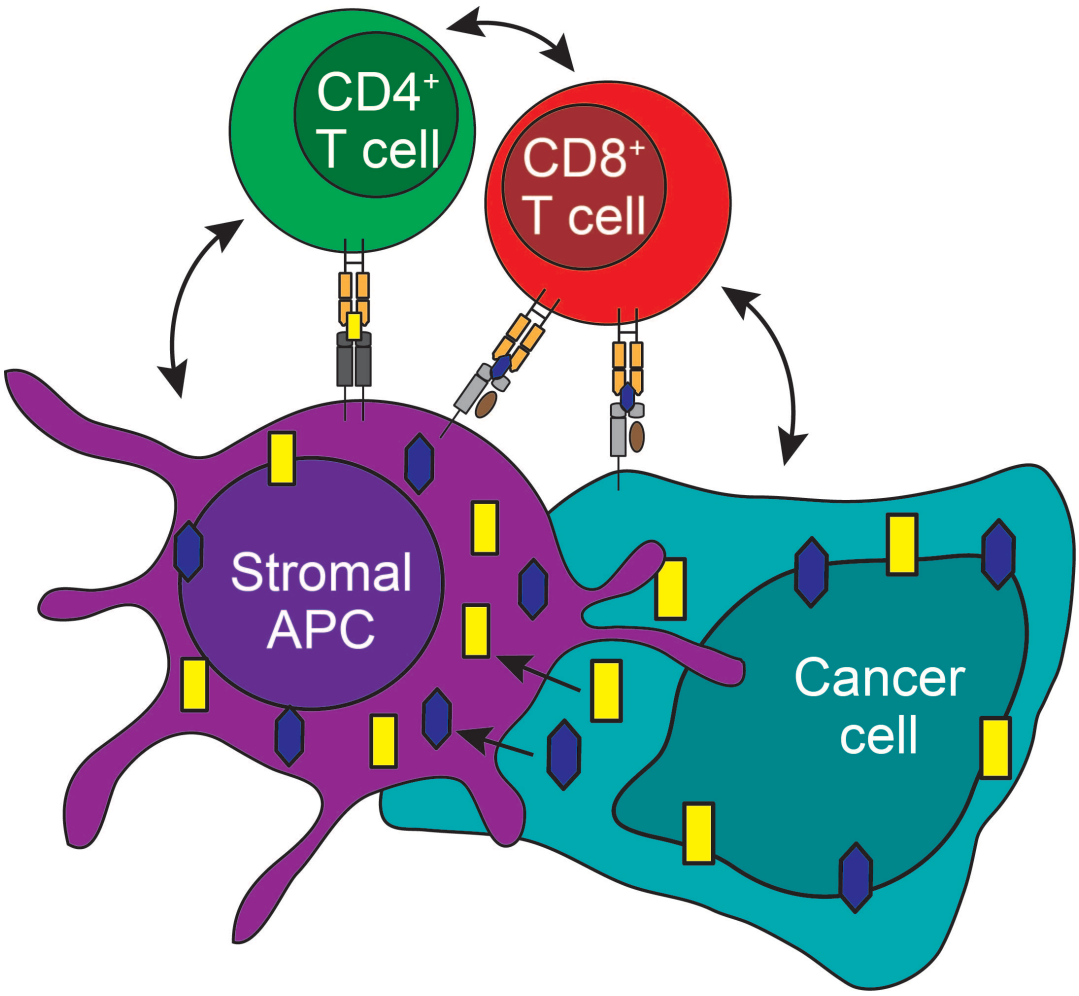

Figure 1. Hypothesized four-cell type interaction. Cancer cells harbor cancer specific mutant neoantigens which can be targeted by specific T cells. Adjacent antigen presenting cells (APC) in the tumor stroma pick up and present the mutant neoantigens on MHC class I (blue) and II (yellow) to T cells. Once T cells engage, a four-cell type interaction is formed, where direct cell to cell interactions (illustrated by arrows, for more detail see Figure 7) are possible.

2. Zusammenfassung

Der adoptive Transfer von T-Zellen, modifiziert mit antigen-spezifischen Rezeptoren, wird gegenwärtig zur Behandlung von akuter lymphatischer Leukämie und großzelligen B-Zell-Lymphomen genutzt, während ein zuverlässiger und effizienter Einsatz gegen solide Tumoren noch nicht etabliert wurde. Zurzeit werden zur Behandlung von soliden Tumoren tumorinfiltrierende Lymphozyten (TILs) genutzt. Diese Therapieform ist jedoch abhängig von der erfolgreichen Isolierung und Expansion der TILs. In Patienten, bei welchen die TIL-Therapie erfolgreich war, wurden neoantigen-spezifische T Zellen im TIL-Produkt entdeckt und es wird vermutet, dass diese speziellen T-Zellen Einfluss auf den Erfolg der adoptiven T-Zelltherapie nehmen. Die spezifischen T-Zellrezeptor (TCRs) Gene können isoliert und für die virale Transduktion von T-Zellen, die aus dem Blut vom Patienten stammen, genutzt werden. Momentan ist unklar, wie viele verschiedene T-Zellklone von einer polyklonen TIL-Antwort für die erfolgreiche Therapie benötigt werden. Hauptziel dieser Dissertation war es, die Voraussetzungen zu ermitteln, um solide Tumore mit adoptiven Transfer von neoantigen-spezifischen, TCR-modifizierten T-Zellen zu eliminieren. Im Mausmodell wurden etablierte und unmanipulierte Tumore mit TCRs behandelt, die natürlich vorkommende, mutierte Neoantigene erkennen. Dadurch wurde herausgefunden, dass die Eliminierung von Tumoren mit nur zwei TCR-Klonotypen erreicht werden kann. Ein TCR erkennt krebsspezifische Antigene, die auf MHC Klasse I präsentiert wurden, während der zweite TCR ein mutiertes Neoantigen erkennt, welches auf MHC Klasse II von Tumorstromazellen präsentiert wurde. Sie zeigt, dass beide TCR Klonotypen ausreichen und essentiell sind für die Krebsbehandlung, weil die Verwendung von zwei TCRs, die unabhängige MHC Klasse I beschränkte Neoantigene erkannten, unzureichend war und zum Relapse führte, obwohl Tumore behandelt wurden, die aus einem Krebszellklon stammten, welcher wenig bis keine Tumorheterogenität aufwies. Ein alleiniger Angriff auf das Tumorstroma durch einen MHC Klasse II abhängigen TCR verursachte eine Tumorverkleinerung und eine längerfristige Wachstumskontrolle des Tumors, ohne ihn zu eliminieren. Dieser Effekt wurde durch die Verringerung der Tumorvaskularität ausgelöst und war abhängig von der Erkennung des Tumorstromas. Wenn Krebszellen aufgrund mangelnder MHC Klasse I Oberflächenexpression nicht direkt erkannt werden konnten, war eine Tumoreliminierung nicht möglich, auch wenn beide TCR-Klonotypen vorhanden waren. Aus diesen Beobachtungen wurde die Vierzelltypeninteraktionshypothese abgeleitet, welche eine Voraussetzung für die erfolgreiche Behandlung von Tumoren sein könnte. Die in dieser Dissertation dargelegten Ergebnisse zeigen, dass die Verwendung von neoantigen-spezifischen, TCR-modifizierten T-Zellen als adoptive T-Zelltherapie vereinfacht und dadurch die klinische Anwendung erleichtert werden kann.

3. Introduction

In 2017, cancer was the second most common cause of death in the world (**Figure 2**, data are acquired from Institute of Health Metrics and Evaluation (IHME), Global Burden of Disease (GBD), (Collaborators 2017)). According to the GBD, 10 million people around the world died of it which means that every sixth death in the world in 2017 was caused by cancer. The National Cancer Institute (NCI, USA) defines cancer as a collection of disease in which abnormal cells continuously divide and start to invade surrounding tissue. This abnormality can start in any cell type in the body. The GBD states that almost 50 % of cancer deaths come from people which are 70 years or older (**Figure 3,** data are acquired from Institute of Health Metrics and Evaluation (IHME), Global Burden of Disease (GBD) (Collaborators 2017)) and this number is predicted to rise as health care, quality of life and life expectancy advance among the world (United Nations, Department of Economic and Social Affairs).

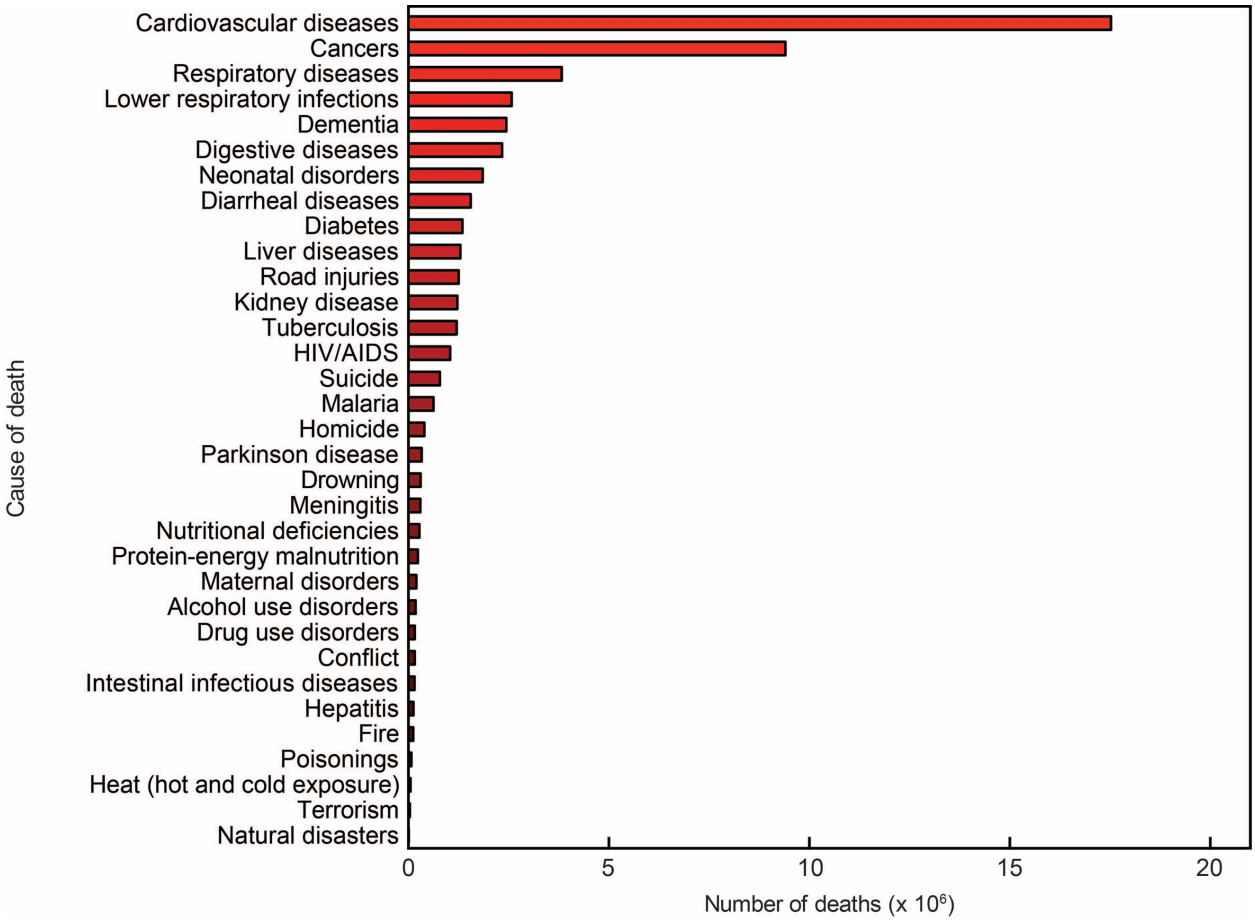

Figure 2. Worldwide causes of death. Cancer is the second most common cause of death worldwide, behind cardiovascular diseases. Modified from (Roser 2020).

The 5-year survival rate represents a prognostic statistic as one measure to follow improvement of cancer treatment over time. It estimates the chance of survival in the 5 years after the day of diagnosis. The SEER (Surveillance, Epidemiology and End Results Program) cancer statistic review from the National Cancer Institute (NCI, USA) provides data for the 5-year survival rate of any type of cancer since 1970. Surprisingly, it becomes evident that cancer therapy progresses very slowly, as the overall 5-year survival rate in cancer from 1970 – 1977 was 50 % and increased only to 67 % between 2007 - 2013. Some cancers such as prostate cancer advanced significantly from 67 % to 98 %, others, such as pancreatic cancer advanced only slightly from 2.5 % to 8 %. At the moment, survival rates depend highly on the type of cancer and stage at first diagnosis. Even though radiation and chemotherapy remain first line standard treatments, immunotherapies, a form of therapy which uses the patient's immune system to treat cancer, are on the rise and can result in increased 5-year survival rate and can cure, independent of cancer type (Sathyanarayanan and Neelapu 2015).

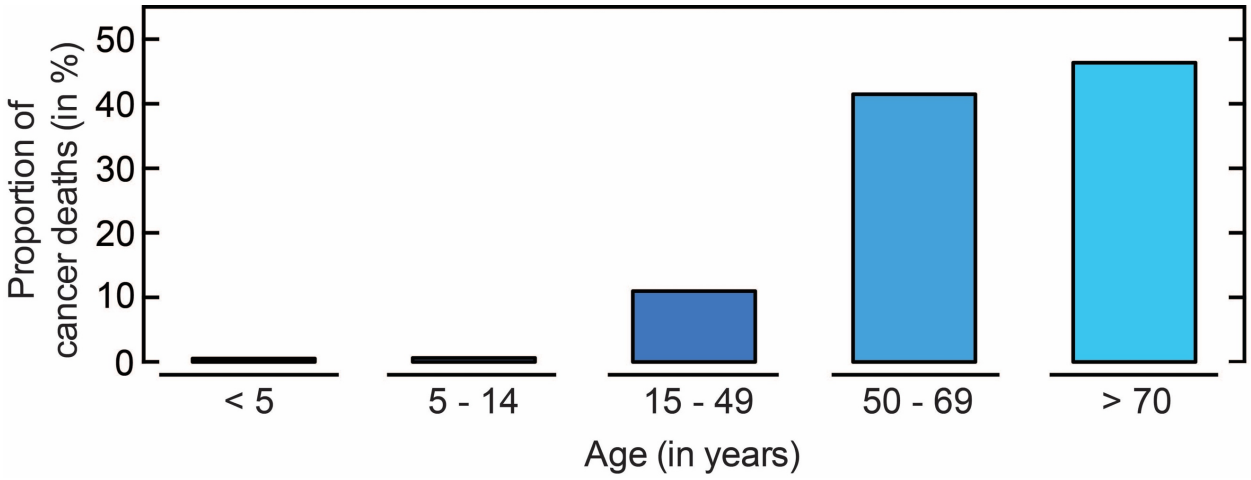

Figure 3. Cancer deaths by age. Cancer is a major issue in the older population, as most patients who die of cancer are over 50 years old. Modified from (Roser 2020)

3.1 Cancer development

Cancer as a disease summarizes a type of uncontrolled cell growth, which invades neighboring tissue and does not longer follow the regulation system of the body. External and internal factors, such as carcinogens, mutagens, hormones, injury or infections can influence the regulation system of cells. Every type of cancer starts with cells that acquired mutations or irreversible epigenetic changes by an initial transforming event that cause abnormal function of the highly regulated cell system and allows them to proliferate uncontrolled (Vogelstein, Fearon et al. 1988,

Vogelstein, Papadopoulos et al. 2013). Continuous proliferation increases the chance of obtaining new mutations which could give the abnormal cell an additional survival advantage and thus will be able to compete over space with other healthy cells. In 1935, Haldane estimated the spontaneous mutation rate in humans to 10^{-5} (Haldane 2004), meaning that 1 cell in 100,000 cells acquires a random mutation. Using fluctuation analysis, Luria and Delbrück showed in 1943 (Luria and Delbruck 1943) that selection of variants was not due to adaptation but due to randomly occurring events. Today, the spontaneous mutation rate is estimated at 10^{-5} to 10^{-6} for healthy cells and 10^{-4} to 10^{-6} in cancerous cells (Tomlinson, Novelli et al. 1996, Jackson and Loeb 1998). Mutations can also cause a cell to die. After one mitosis (cell division) two different cell types can arise, a living and a dying cell. Therefore, tumor growth is initially an equilibrium of surviving and dying cell populations. After a distinct time period, the number of living cells outweighs those that die and the tumor starts to grow. This tumor growth kinetic is characterized by the Gompertzian growth equation (Gompertz 1825). Laird used the Gompertzian growth model to describe tumor growth (Laird 1964). Subsequently clinical data validated the Gompertzian growth model (Norton 1988). This concept describes the doubling time of the tumor mass as a sigmoidal curve. The initial lag phase describes the equilibrium of cell gain and loss and transfers into an exponential phase of tumor growth. In the end, growth reaches a plateau because the organism cannot provide enough nutrients for himself and the whole tumor mass and eventually dies (**Figure 4**).

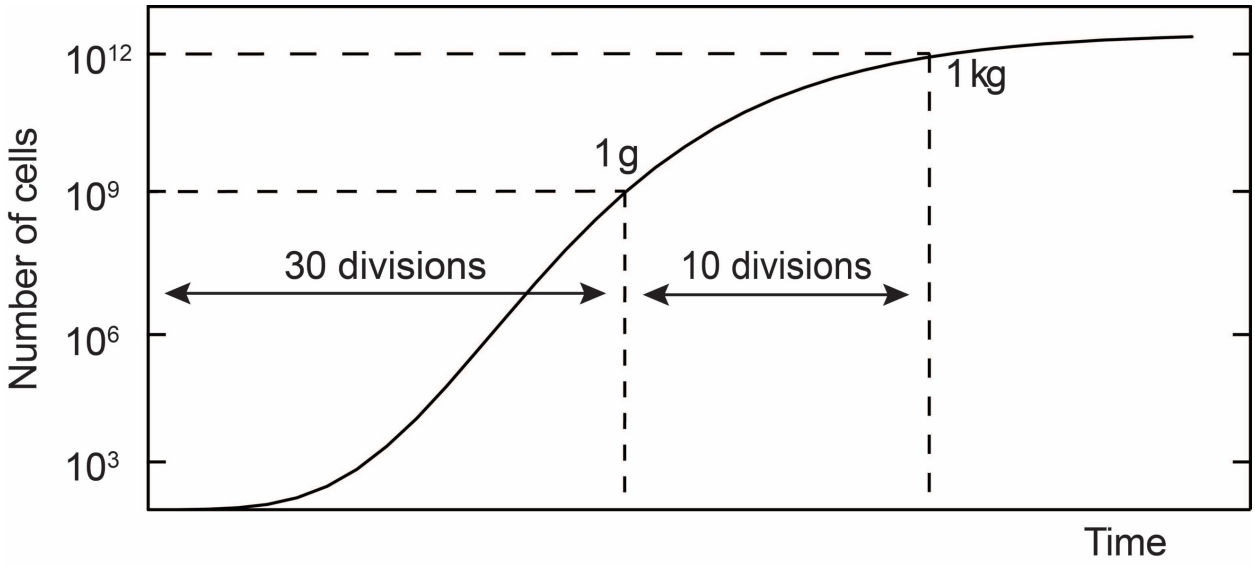

Figure 4. Idealized gompertzian tumor growth model. Shown is increase in cancer cells over time. Indicated is tumor mass and cell number at point of diagnosis (10^9 cells, 1 g) and when patients are in critical condition (10^{12} cells, 1 kg). Cell number, mass and time are estimated and usually common for most cancers. Modified from (Freiberg 1997).

In the clinic, when cancer is first diagnosed in patients, the cancer tissue has approximately a mass of 1 g or a size of about 1 cm in diameter, which equals about 10^9 tumor cells (Freiberg 1997). Tumor cells at the stage of diagnosis underwent approximately 30 viable cell divisions and only 10 more viable cell divisions are left before death. If a spontaneous mutation rate of 10^{-4} is considered, at least 10^5 out of 10^9 cancer cells display different mutation signatures, have distinct survival phenotypes and therefore most of the cancer heterogeneity has already been established. The development of distinct cancer cell clones is supported by modern sequencing data (Gerlinger, Rowan et al. 2012, Govindan, Ding et al. 2012, Govindan 2014) and fits the clonal evolution theory (Nowell 1976). In this concept, dividing cancer cells acquire new mutations over time and behave at one point different than the progenitor they arose from. From this stage forward, their descendants create a new branch were some lineages will die off and other take new spatial spaces within the developing tumor leading to tumor heterogeneity (**Figure 5**).

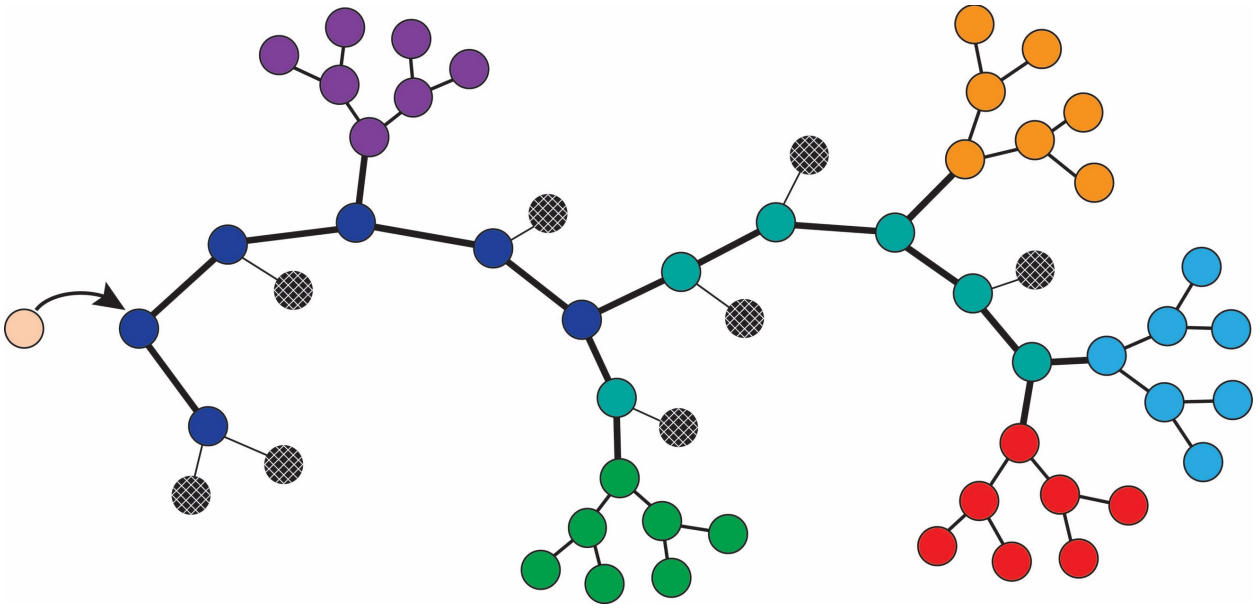

Figure 5. Clonal evolution theory. In the beginning, a cell transforming event occurs (arrow). Over time some cancer cell clones expand, while others become extinct or stay dormant (black checkered). Certain clones acquire new heritable phenotypes and some of these may be the result of additional mutations, that allow subclones to gain a growth advantage and adjust to changes in the tumor environment. Modified from (Nowell 1976).

In addition, the model of cancer stem cells, which divide indefinitely and are supposed to be the main driver of tumor growth, was introduced (Steel 1984). This concept may complement the clonal evolution theory but has been criticized because evidence shows that cancer growth does not depend on rare cancer stem cells (Kelly, Dakic et al. 2007). Collectively, the concepts on

tumor development explain that tumors of the same histologic type differ between patients (intertumor heterogeneity) and that there are even differences between individual tumor sites of one patient tumor mass (intratumor heterogeneity) (de Bruin, McGranahan et al. 2014, Zhang, Fujimoto et al. 2014, Liu, Dang et al. 2018) which are critical barriers for successful cancer therapy (Skipper 1971).

3.2 The adaptive immune response

A characteristic of the immune system is to distinguish healthy cells of the host (self) from non-self cells, e.g. bacteria, parasites and virus-infected cells. In a healthy individual, the differentiation between self and non-self is the basic principle that drives immune responses. For this, the vertebrate immune system can be divided into the innate and the adaptive immune response. The innate immune response represents the initial line of defense for the host. It recognizes a variety of pathogen-associated molecular patterns (PAMPs), which are conserved molecule motifs within a class of microbes and are identified by pattern recognition receptors (PRRs). These germ-line encoded receptors enable for a standardized, rapid response due to expression on multiple different cell types of the innate immune response (reviewed in (Schenten and Medzhitov 2011). In contrast, the adaptive immune response can identify molecules, named “antigens” (Jerne 1960), which are often unique and specific for a certain pathogen. An antigen is any kind of structure or substances that can be bound by antigen receptors and causes an immune response. The adaptive immune system uses a vast variety of antigen-receptors, which undergo somatic recombination of multiple and diversely encoded germ-line segments and are thus specifically made for every target (Tonegawa 1983, Samelson, Lindsten et al. 1985). This leads to an initially slow, but then gradually increasing immune response, because every single cell has made a different antigen-receptor and has to undergo clonal expansion, upon activation, before a sufficient number of effector cells is available to clear the pathogen. The main cells of the adaptive immune system are B cells and T cells. B cells use B cell receptors (BCR) to recognize their targets and after activation expand exponentially before secreting antibodies as the final effector molecule. T cells use T cell receptors (TCR) for target recognition and directly interact with the non-self, invading cells. For a review of the basics of the innate and adaptive immune system see (Janeway 1989). T cells recognize with their TCR short peptide molecules that bind to specific sides of the major histocompatibility complex (MHC) molecules and form a three body complex. Each TCR is able to identify the specific structure of a certain peptide-MHC (pMHC) (Garboczi, Ghosh et al. 1996, Garcia, Degano et al. 1996). This TCR-pMHC interaction is responsible for the hosts ability to distinguish self from non-self. T cells recognize their antigenic

target and are activated when the TCR binds successfully to the pMHC complex, which usually also requires the additional engagement of the CD4 or CD8 co-receptor with the pMHC (Miceli and Parnes 1991, Chien and Davis 1993). Hence, cells that are infected (e.g. by virus or bacteria) or transformed (cancer cells) present non-self pMHC and are being recognized by T cells. Two main T cell subsets are known, $CD8^+$ and $CD4^+$ T cells. In several diseases, $CD8^+$ T cells seem to be the main effector cell because they kill their targets upon activation. T cells which are $CD4^+$ are mainly regulators of effective $CD8^+$ T cell responses and are needed for the generation of high affinity antibodies by B cells. Thus, in most cases $CD8^+$ T cells and B cells depend on $CD4^+$ T cells for a powerful immune response.

3.2.1 Major histocompatibility complexes

In order to independently regulate $CD8^+$ and $CD4^+$ T cells, the immune system developed two different pathways for antigen presentation by distinct MHCs. MHC class I is expressed on all nucleated cells and presents peptide motifs that originate from cell endogenous proteins. It consists of one α-chain with three domains (α_1, α_2 and α_3) and is stabilized by the non-polymorphic β_2-microglobulin (Bjorkman, Saper et al. 1987). Proteins, which are no longer needed, damaged or dysfunctional will be degraded in a cell's cytosol by the proteasome. The proteasome is an enzyme complex which is able to break peptide bonds by proteolysis. It therefore generates short peptides which can be taken apart further by peptidases to produce single amino acids, which in return are used to build new proteins. However, not all created short peptides are initially recycled. Some peptides are transported into the endoplasmic reticulum (ER), where they are further processed and loaded onto MHC class I molecules. The stable pMHC class I molecules are transported in vesicles to the cell surface where they can be recognized by $CD8^+$ T cells (**Figure 6A**). In this sense, cells present their intrinsic protein composition on MHC class I, which is therefore representing the endogenous pathway of antigen presentation. In contrast, MHC class II covers the exogenous pathway of antigen presentation. MHC class II molecules are heterodimers, consisting of one α- and one β-chain (Brown, Jardetzky et al. 1993) and are only expressed by specialized cells named antigen-presenting cells (APC) (Rowley and Fitch 2012), which are dendritic cells (DC), B cells and macrophages. These cell types ingest molecules via endocytosis and are able to present peptide fragments on MHC class II. Endocytosis is a general term of active transport from cell surrounding material into the cell. Internalized material is transported in vesicles which develop into early and late endosomes and become later lysosomes.

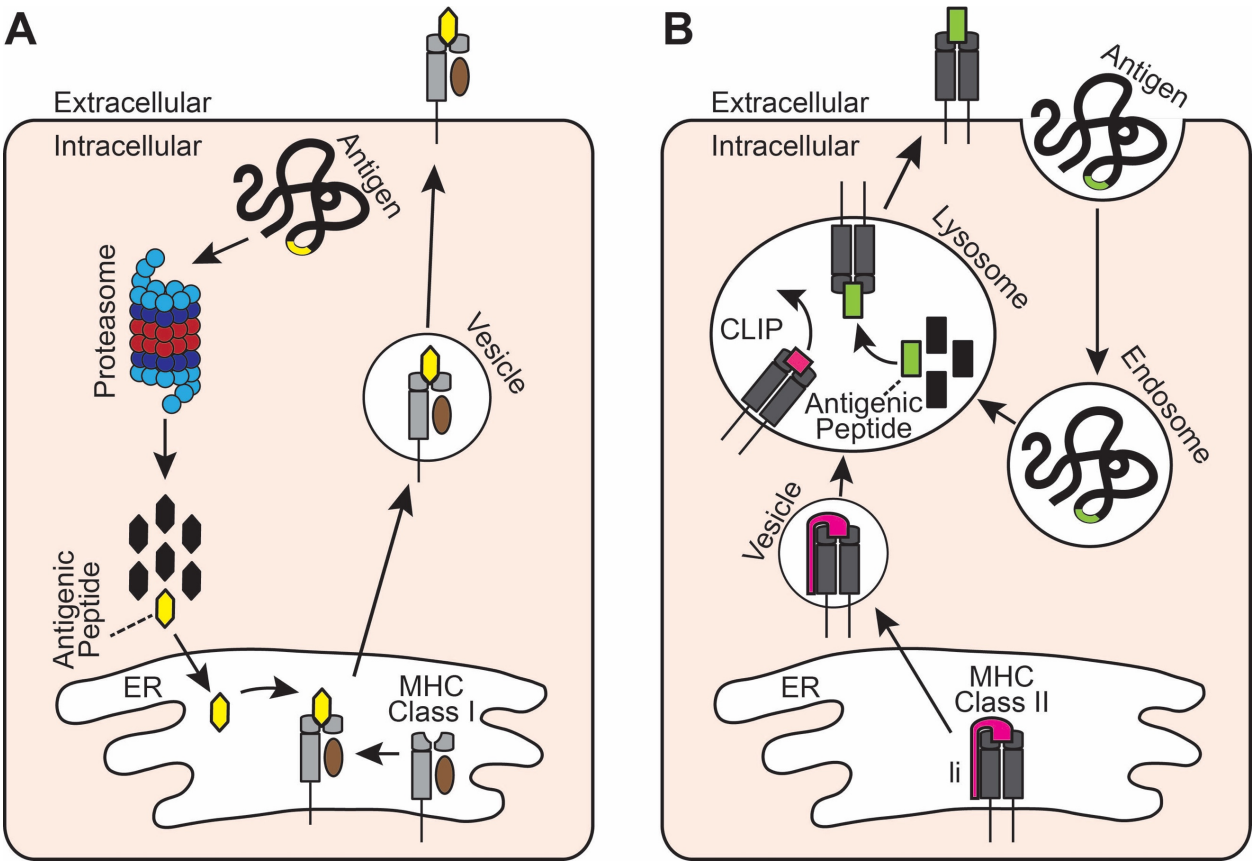

Figure 6. MHC class I and II antigen presentation pathways. (A) Any kind of cell endogenous protein, including viral proteins, are degraded by the proteasome. Degraded peptides are transported into the endoplasmic reticulum (ER) where they are loaded onto MHC class I. Peptide loaded MHC class I complexes are then transported to the cell surface and can be recognized by $CD8^+$ T cells. **(B)** Exogenous molecules are ingested via endocytosis and transported in endosomes. MHC class II molecules are assembled in the ER around the invariant chain (Ii) which acts as a chaperone. MHC II molecules are transported in vesicles and fuse with endosomes into lysosomes where antigens and Ii are digested. After degradation of Ii a CLIP (class II associated invariant chain peptide) is left which is exchanged with peptides from the digested antigen. Peptide loaded MHC class II molecules are then transported to the cell surface and can be recognized by $CD4^+$ T cells.

During those stages, different peptidases are activated and digest proteins into short peptide fragments and single amino acids which can be used for new protein synthesis. Some peptide fragments will be loaded onto MHC class II and transferred back to the cell surface where the pMHC class II molecules can be recognized by $CD4^+$ T cells (**Figure 6B**). This way, the diverse pMHCs on the surface of APCs represent the antigenic properties of their surrounding area which can be identified by T cells. Both MHC pathways are reviewed in (Cresswell 1994).

3.2.2 Antigen-presenting cells and the three cell type interaction

APCs are specialized in antigen presentation and T cell activation. The DC, a very rare (< 1 %) subgroup of APCs, is thought to be essential for primary T and B cell responses and link the innate and adaptive immune response (Rowley and Fitch 2012). DCs are distributed throughout the whole body where they sample their surroundings by permanent endocytosis and influx of molecules. Activation of DCs is followed by PAMP recognition and activated DCs advance to nearby lymph nodes (LN) where they present antigens to passing T cells. DCs express both MHC class I and II molecules and can therefore interact with both T cell subsets. They need the interaction with $CD4^+$ T cells to get fully activated and transfer the help signal to $CD8^+$ T cells, which is needed for successful stimulation. Once $CD8^+$ T cells receive the help signal and are switched on, they are the final effector cell which kills their recognized targets. The basic concept for successful T cell activation is the “two signal model” (Bretscher and Cohn 1970). In this concept, the first signal is generated by TCR-pMHC engagement and the second signal is derived from co-receptors which come mainly from activated DCs through help from $CD4^+$ T cells. One major co-receptor/ligand interaction is the CD28-CD80/CD86 interaction. T cells express the co-receptor CD28 while APCs express the ligands CD80 and CD86. This signal is important for priming and activation of T cells (for a more detailed explanation on the CD28-CD80/CD86 interaction see the review from (June, Bluestone et al. 1994)). The “two signal model” was improved and adjusted over the years (Bretscher 1999, Bretscher 2019). It was the first step to the current understanding that T cell activation is tightly regulated by multiple different signals and three additional pathways for transfer of help are exemplified in **Figure 7**. One major pathway for priming of $CD8^+$ T cell goes over CD40/CD40L interactions (Schoenberger, Toes et al. 1998). CD40 is expressed on the surface of APCs and $CD8^+$ T cells, while CD40L is expressed on $CD4^+$ T cells. Upon engagement of CD40 on APCs, they upregulate MHC molecules and produce cytokines needed for T cell proliferation and differentiation (Cella, Scheidegger et al. 1996, Koch, Stanzl et al. 1996). The signal transmitted through CD40L into $CD4^+$ T cells is required for differentiation and effector function (Grewal, Xu et al. 1995, van Essen, Kikutani et al. 1995). Over this axis, direct cell to cell interactions between APC and $CD4^+$ T cell and between $CD4^+$ T cell and $CD8^+$ T cell are possible. Over the CD27/CD70 pathway another direct cell to cell interaction and transfer of help from APCs to T cells is possible. CD27 is expressed by T cells, while APCs express its ligand CD70 and expression of CD70 by $CD8^+$ T cells has also been reported (Brugnoni, Airo et al. 1997). This axis mediates T cell priming, expansion and prevents apoptosis (Gravestein, Nieland et al. 1995, Arens, Tesselaar et al. 2001, Bullock and Yagita 2005, Feau, Garcia et al. 2012).

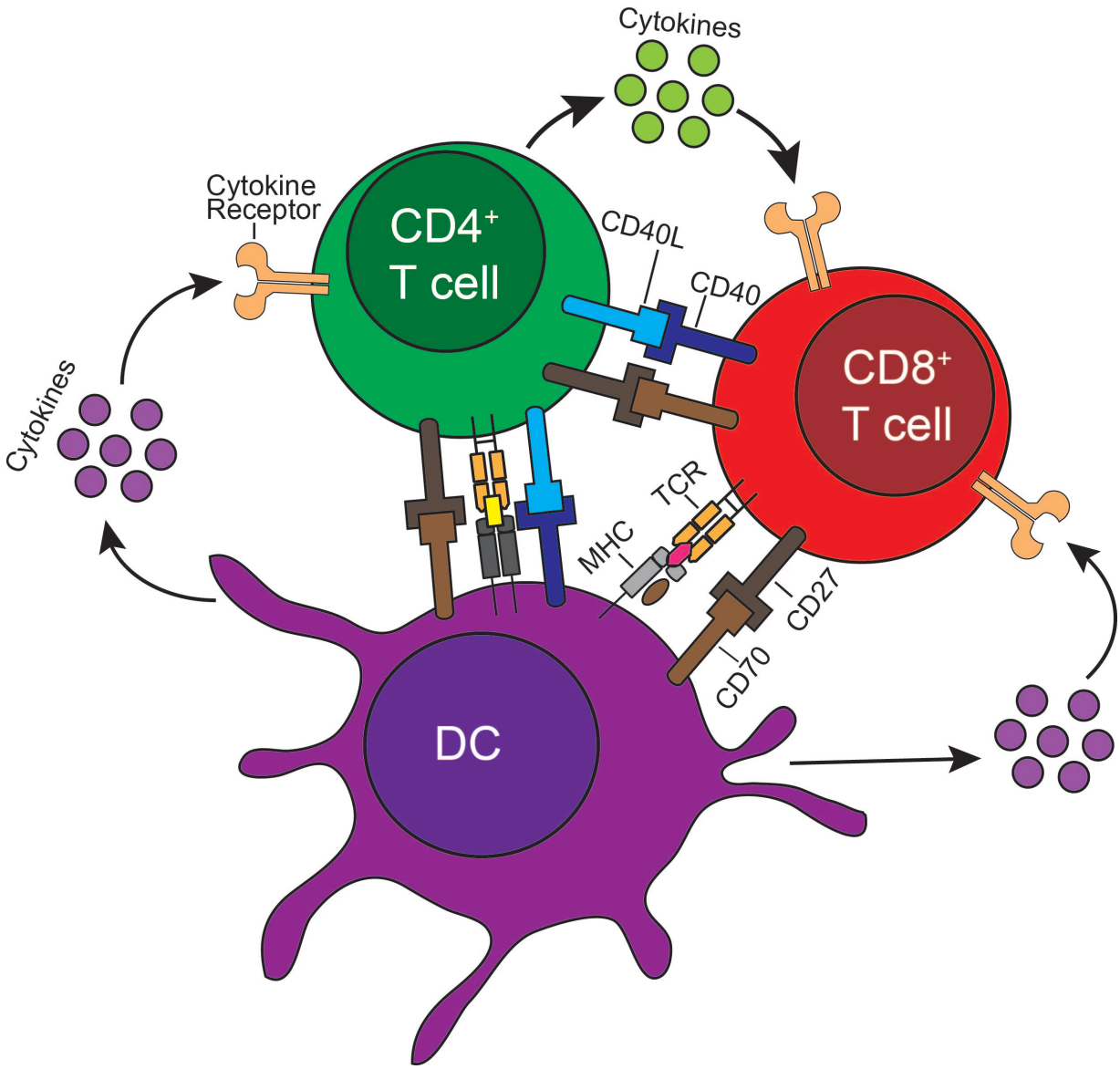

Figure 7. Exemplified signal delivery among the three-cell type interaction. DC present antigen on MHC class I and II to $CD8^+$ and $CD4^+$ T cells. Help signals from $CD4^+$ T cells to DC and $CD8^+$ T cells is transmitted via CD40/CD40L and CD70/CD27 interaction. Activated DC and $CD4^+$ T cells produce different cytokines which act on cytokine receptors to fully activate both, $CD4^+$ and $CD8^+$ T cells.

The last pathway introduced, transfers signal over soluble mediators, such as chemokines, interferons, interleukins and lymphokines and are summarized with the term “cytokines” (Cohen, Bigazzi et al. 1974). They act through cell surface receptors and are important regulators for cell differentiation, proliferation, migration, effector function and priming (Paul and Seder 1994, Cohen and Cohen 1996) and can also mediate tumor destruction (Briesemeister, Sommermeyer et al. 2011, Kammertoens, Friese et al. 2017). The effects of multiple different cytokines are well

studied and cannot be comprehensively introduced here. Although it was early on excepted that for an efficient immune response the three cell types (APC, $CD8^+$ and $CD4^+$ T cell) have to interact, the kinetics of interaction remain uncertain (Mitchison and O'Malley 1987). There is evidence that the initial interaction takes place only between $CD4^+$ T cells and DCs and that afterwards the DC alone is able to fully trigger $CD8^+$ T cells (Ridge, Di Rosa et al. 1998). Other suggest that all three cell types have to interact together at the same time (Smith, Wilson et al. 2004). There are different concepts explaining the interactions between these three cell types but there is always the basis that the natural, unmanipulated immune response depends on the interaction between DCs, $CD4^+$ and $CD8^+$ T cells, particularly in LNs.

3.2.3 Selection of T cell receptors

The activation of T cells is tightly regulated and only occurs under specific conditions. Once T cells are activated through TCR-pMHC interaction of the cognate antigen, they fulfill their function, e.g., in the case of $CD8^+$ T cells, they move from secondary lymphoid organs to the periphery and kill antigen-expressing target cells (Mavilio, Ferrari et al. 1994, Bunnell, Muul et al. 1995). The TCR was discovered in 1984 (Hedrick, Cohen et al. 1984, Yanagi, Yoshikai et al. 1984) and consists of an α- and β-chain or γ- and δ-chain ($\gamma\delta$ T cells are likely to be associated with the innate immune response and not discussed here (Brandes, Willimann et al. 2005)). Upon pMHC recognition, the heterodimer congregates with the CD3$\varepsilon\delta$, CD3$\varepsilon\gamma$ and CD3ζ to transfer an activation signal (Van Wauwe, De Mey et al. 1980, Chang, Kung et al. 1981, Borst, Alexander et al. 1983). Signal strength is amplified by co-receptors, e.g. CD4/CD8 and CD28 (Hansen 1980, Eichmann, Jonsson et al. 1987, Janeway, Haque et al. 1987, Ledbetter, June et al. 1987, Moretta, Poggi et al. 1987, Clevers, Alarcon et al. 1988).TCRs are made from multiple and diversely encoded germ-line segments by somatic recombination (Samelson, Lindsten et al. 1985). The α-chain is rearranged between variable (V) and joining (J) gene segments (Sim, Yague et al. 1984). The β-chain is rearranged between variable (V), diversity (D) and joining (J) gene segments (Chien, Gascoigne et al. 1984). The highly diverse region between V-J in the α-chain and V-D-J in the β-chain are named “complementarity determining region 3 (CDR3) equivalent” (Davis and Bjorkman 1988) and are central for TCR-antigen binding. In mice, about 100 V and 50 J gene segments for the α-chain and 25 V, 2 D and 12 J gene segments for the β-chain have been determined and calculate to about 10^{15} possible TCR combinations (Davis and Bjorkman 1988). Therefore, chances are high that TCRs are generated which can recognize self-antigens. Thus, TCRs are not automatically only specific to non-self antigens. In order to prevent activation

of T cells against self-antigens, the immune system has a self/non-self selection step during the T cell maturation process. The T cell selection and maturation process takes place in the thymus where thymocytes (T cell progenitors) are selected and mature into naïve T cells. The thymic selection involves MHC class I and II positive epithelial cells of the thymus which present self-antigens to thymocytes and thus guide the maturation process which consists of two steps (Sha, Nelson et al. 1988). The first step is the “positive selection” (McDuffie, Born et al. 1986). During that phase, the TCR generated by the immature T cells is tested for its activity. If an immature T cell is able to generate a functional TCR, meaning the TCR is not only able to recognize pMHC molecules but the TCR to pMHC affinity is also strong enough to transfer a stimulus, it will receive survival signals. The positive selection step ensures that only T cells with physiologically useful TCRs survive, while others die. The second step is the “negative selection” (Kappler, Roehm et al. 1987). During that phase TCRs that recognize self-antigens presented on MHC will be selected and the T cells which generate those TCRs receive a signal to undergo apoptosis and die. Afterwards, matured naïve T cells are released from the thymus and move to the periphery to surveil the body for non-self antigens. This process of clonal elimination is the foundation for “self-tolerance” (Kappler, Roehm et al. 1987) and ensures that the matured naïve T cells are able to distinguish self from non-self.

3.3 Cancer-specific antigens and cancer immunotherapy

Traditional cancer treatments (surgery, chemotherapy and radiation therapy) are established first and second line treatments against cancer. However, unless surgery can remove the cancer completely the standard second line therapies are rarely curative. An exception seems to be childhood leukemia that is often cured by combination chemotherapy. The search for more effective treatments of advanced cancers lead to the development of immunotherapy. In experimental mouse tumor models, it was shown that tumors induce immune responses and can be used to immunize mice of the same strain the tumor was induced in (Gross 1943). Between 1950 and 1970, the first experiments proved that immunized mice can develop a tumor-specific immune response which lead to rejection of transplanted tumor fragments and/or tumor cells (Foley 1953, Baldwin 1955, Prehn and Main 1957, Klein, Sjogren et al. 1960, Globerson and Feldman 1964). Cancer-specific antigens are also called “unique” or “individually specific” because usually a tumor, that developed in one host, cannot be used to immunize against a tumor from a second host, even though both hosts are from the same strain and both tumors were induced by the same carcinogen (Basombrio 1970, Basombrio and Prehn 1972). Further investigations using cytolytic T cell clones revealed that a single cancer cell harbors multiple

different, independent unique cancer-specific antigens (Wortzel, Philipps et al. 1983). Subsequently, it was proven that these antigens are indeed cancer-specific since they were not found on normal cells of the same host the tumors were derived from (Ward, Koeppen et al. 1989, Ward, Koeppen et al. 1990). These individual cancer-specific antigens were discovered to represent nonsynonymous single nucleotide variants (nsSNV) (Monach, Meredith et al. 1995, Wölfel, Hauer et al. 1995). The exchange of one nucleotide, which results into one single amino acid substitution, was enough for T cells to specifically distinguish self from non-self. In addition, insertion/deletion mutations (indels) can cause frameshifts in the amino acid sequence and, therefore, also cause the generation of cancer-specific antigens (Turajlic, Litchfield et al. 2017). In recent years, cancer-specific antigens have been referred to as neoantigens, specifically as mutant neoantigens (Lennerz, Fatho et al. 2005). It was confirmed in human cancer patients that targeting mutant neoantigens is required for effective cancer immunotherapy (Tran, Robbins et al. 2017). Multiple different approaches of immunotherapy, with their own advantages and disadvantages, try to unlock mutant neoantigen specific T cells for cancer eradication.

3.3.1 Immune-checkpoint blockade therapy

Immune-checkpoint blockade therapy uses antibodies to block immune-checkpoint surface molecules. Immune checkpoints are important controllers of self-tolerance and deliver as co-receptors either a stimulatory or inhibitory signal to T cells. The composition of engaged co-receptors in addition to the TCR-pMHC interaction determines duration and strength of the T cell response. As much as stimulatory co-receptors are needed to activate T cells, as much are inhibitory co-receptors needed to prevent hyperactivation which can result into non-specific target recognition and activation of T cells (Wolf, Schimpl et al. 2001, Ghosh, Koralov et al. 2010, Wehrens, Mijnheer et al. 2011). The two main studied costimulatory pathways are CD80/CD86/CTLA-4 and PD-1/PDL1 interactions (**Figure 8**). Cytotoxic T lymphocyte associated antigen 4 (CTLA-4) interacts with CD80 and CD86 presented by DCs and competes with CD28 over those ligands. It is upregulated by T cells after stimulation and delivers an inhibitory signal opposed to the activation signal by CD28 and thus dampens the T cell response by e.g. inhibition of proliferation (Linsley, Greene et al. 1992).

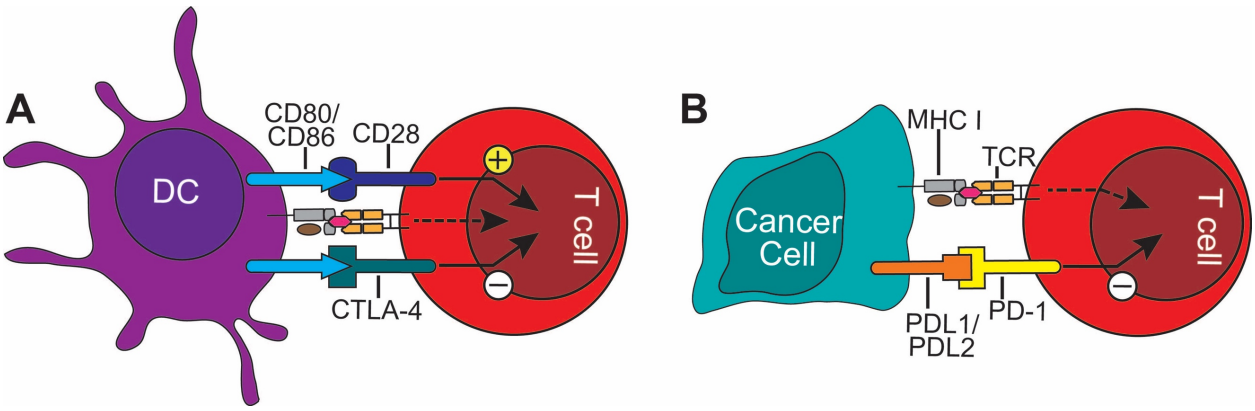

Figure 8. Co-receptors as immune checkpoints regulate the T cell response activation and inhibition. T cells recognize cognate antigen which delivers an activation signal. Additional stimulatory signals from co-receptors (e.g., CD80/86 and CD28 interaction) are needed for complete T cell function. The amplitude of activation induces the inhibitory regulation, e.g. CTLA-4 (cytotoxic T-lymphocyte-associated antigen 4). CTLA4 functions as a signal dampener to maintain a consistent level of T cell activation. By contrast, PD1 (programmed cell death protein 1) is constantly expressed by activated T cells and an inflammatory environment induces the expression of PD1 ligands (PDL1/PDL2), e.g. by cancer cells and block T cell activity. Blockade of the PD1 and CTLA-4 pathways are so far the main targets of immune-checkpoint blockade therapy.

Mice knocked out for the CTLA-4 gene showed enhanced T cell proliferation and developed severe autoimmunity (Tivol, Borriello et al. 1995, Waterhouse, Penninger et al. 1995). PD-1 is constantly expressed on activated T cells and induces apoptosis upon engagement (Ishida, Agata et al. 1992, Agata, Kawasaki et al. 1996). Mice lacking the PD-1 gene also develop autoimmune diseases (Nishimura, Nose et al. 1999). The ligand to PD-1, PD-L1 or B7-H1, is expressed on DCs, mediates negative T cell regulation (Dong, Zhu et al. 1999) and is expressed by cancer cells to evade immune responses (Dong, Strome et al. 2002). Inhibitory regulation can also be mediated indirectly by the environment that cancer cells create to grow (Whiteside 2008, Gajewski, Schreiber et al. 2013, Binnewies, Roberts et al. 2018). By blocking inhibitory co-receptors with blocking antibodies, T cells receive no longer inhibitory signals and are able to kill the cancer cells. In the recent years, many immune-checkpoint drugs have been approved for treatment but are so far only effective against certain types of cancers, e.g. melanoma and lung cancer (Ribas and Wolchok 2018). One major issue with this therapy is that it is neither antigen-specific nor restricted to the tumor milieu. Therefore, it causes severe side effects, such as hepatitis and colitis (Phan, Yang et al. 2003, Postow 2015). Therapy relies also on reactivating T cells that are already inside the tumor or make them migrate and infiltrate the tumor. Some cancers are poorly infiltrated because they generate a barrier against T cell infiltration, e.g. release of chemokines by DCs is inhibited (Lanitis, Dangaj et al. 2017). Although highly infiltrated

tumors have a better chance of responding, treatment can still fail. T cells can be inherently dysfunctional and as a result of continuous antigen stimulation be irreversibly programmed not to respond (Schietinger, Philip et al. 2016, Philip, Fairchild et al. 2017). Those T cells cannot be unlocked by immune-checkpoint blockade therapy.

3.3.2 Cancer-specific vaccination

Between 1950 and 1960 it was proven that mice can develop a cancer-specific immune response. First it was shown that normal tissue of the same mouse which developed the tumor cannot be used to immunize against the autochthonous tumor (Prehn and Main 1957). The issue was that genetic differences between inbred mice could not be completely excluded. Therefore, to prove that the tumor-induced immune response was truly cancer-specific, it was shown that the same mouse which developed the tumor (primary host) can develop an immune response against its own autochthonous tumor (Klein, Sjogren et al. 1960). However, the genetic origin of the targeted antigens remained unknown. Today, the idea of cancer-specific vaccination is to stimulate the immune system of a cancer patient with their own mutant neoantigens to either induce a new, cancer-specific response or to reactivate the already developed immune response. The first step includes the sequencing of the patient's tumor, followed by prediction of which mutant neoantigen might be a good candidate for induction of an effective immune response (Hundal, Carreno et al. 2016). After mutant neoantigen candidates have been predicted, they can be used in different ways to induce an immune response. The first approach used DCs from the patient and loaded them *in vitro* with mutant neoantigen peptides before reinfusing them (Carreno, Magrini et al. 2015). In recent clinical trials, the use of synthetic long peptide (SLP) cocktail as vaccines was tested (Ott, Hu et al. 2017, Keskin, Anandappa et al. 2019). The SLP needs to be ingested by APCs, which than digest the SLP and present them on MHC. Therefore, antigen presentation happens already *in vivo* which could be an advantage over *in vitro* loaded DCs. A different approach uses mutant neoantigen encoded DNAs or RNAs as vaccines (Sahin, Derhovanessian et al. 2017). The external DNA or RNA will be taken up by endocytosis from APCs, translated into short mutant neoantigen peptides and presented on MHC to induce a specific T cell response. This form of vaccination depends on the APCs to translate the DNA/RNA before it is being degraded. However, cancer-specific vaccination relies again on T cells that can be inherently dysfunctional as a result of continuous antigen stimulation (Schietinger, Philip et al. 2016, Philip, Fairchild et al. 2017).

3.3.3 Tumor infiltrating lymphocytes

T cells which infiltrate tumors (tumor infiltrating lymphocytes, TILs) can be isolated and expanded *in vitro* (Rosenberg and Dudley 2009). If TILs are found that recognize the patient tumor cells, the cancer-specific TIL population is expanded further and reinfused into the same patient (**Figure 9**). Adoptive T cell transfer (ATT) evolved from the finding that adoptively transferred lymphocytes could transfer immune responses into another host (Delorme and Alexander 1964). Delorme and Alexander showed that transfer of lymphocytes from immunized rats into chemically induced, tumor-bearing rats slowed down tumor growth and even caused tumor rejection in some cases. Later, it was shown that adoptive T cell transfer of spleen cells from immune hosts can cure and reject disseminated viral-induced lymphomas (Fefer 1969). In 1982, it was shown that murine immune lymphocytes can be cultured and expanded with IL-2 for five to seven days and still be used to transfer an immune response into another host (Eberlein, Rosenstein et al. 1982). Next, it was discovered that tumor-reactive TILs can be isolated and cultured from human melanoma patients (Muul, Spiess et al. 1987).

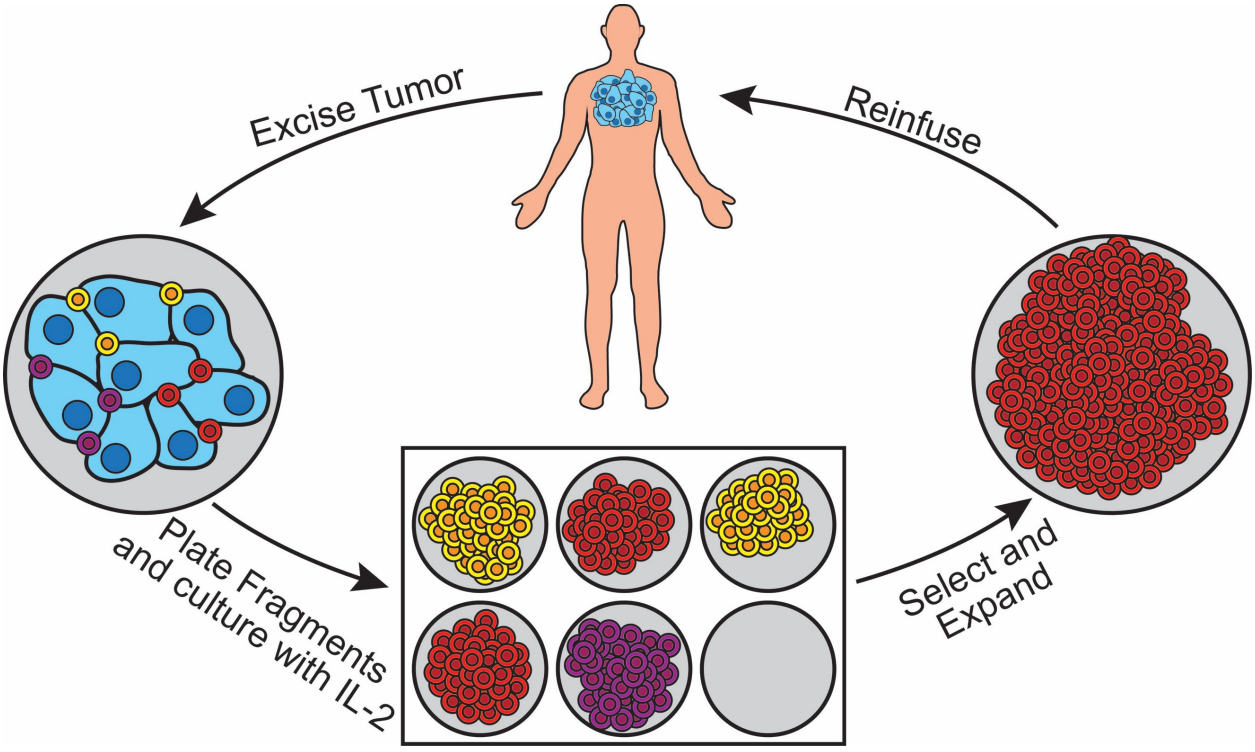

Figure 9. Generation of Tumor infiltrating lymphocytes used for adoptive T cell transfer. Patient tumor tissue is excised and used to establish multiple, different TIL cultures. Cultured TILs are examined for tumor-reactivity and specificity. Reactive TIL cultures are expanded further and reinfused into the patient.

The first adoptive TIL transfer in human melanoma patients yielded some success, as 60 % of the patients treated showed a partial response (Rosenberg, Packard et al. 1988). Over the years, the treatment procedure advanced (Dudley, Wunderlich et al. 2002) but the overall therapeutic efficiency of treated cancer patients did not improve substantially so far (Dudley, Wunderlich et al. 2005). TIL recovery rate differs between patients and between types of tumors. Only for metastatic melanoma, studies report that it is possible to expand TILs in 75 % to 97 % of the patients (Rohaan, van den Berg et al. 2018). An objective response occurs in about 40 % to 70 % of metastatic melanoma patients who received a TIL product (Rohaan, van den Berg et al. 2018) but they are rarely curative. Inefficiency of TIL therapy may result from *in vitro* expanded T cells that revert to a non-responsive state when reexposed to cognate antigen in the tumor environment after reinfused into the tumor bearing host (Schietinger, Delrow et al. 2012, Philip, Fairchild et al. 2017). At the moment, phase 3 clinical trials investigate the optimal procedure for TIL therapies and whether they have an advantage over immune-checkpoint blockade therapy in the treatment of melanoma patients (Rohaan, van den Berg et al. 2018). Thus, it remains unclear whether TIL therapy can become an approach for all cancer patients.

3.3.4 CAR and TCR gene therapy

In CAR and TCR gene therapy, peripheral blood T cells are expanded and engineered to express cancer-reactive or cancer-specific antigen receptors before being reinfused into the patient. At the moment CAR (chimeric antigen receptor) therapy in the clinic is effective against acute lymphoblastic leukemia and certain types of large-B-cell lymphomas using CARs specific for the B cell surface marker CD19 (Kochenderfer, Wilson et al. 2010, Sadelain, Brentjens et al. 2015, Davila and Brentjens 2016, Chavez, Bachmeier et al. 2019) or in multiple myeloma with CARs against the B cell maturation antigen (BCMA), summarized in an review from (D'Agostino and Raje 2020) The difference of a CAR to a TCR is that the CAR consists of a single-chain variable fragment (scFv) derived from the heavy and light chains (V_H and V_L) of an antibody linked over a transmembrane region to an intracellular signaling domain of CD28 and/or 4-1BB with CD3 (**Figure 10**), thereby imitating a stimulatory signal of a TCR (Gross, Waks et al. 1989, Eshhar, Waks et al. 1993, Kowolik, Topp et al. 2006). By engineering T cells, e.g. by viral transduction with CARs, they are able to express an engineered receptor which recognizes surface molecules independent of MHC presentation while still being properly stimulated. The idea of engineering T cells and giving them new specificities originated when it was shown that it is possible to transfer a TCR with its associated specificity (Dembic, Haas et al. 1986).

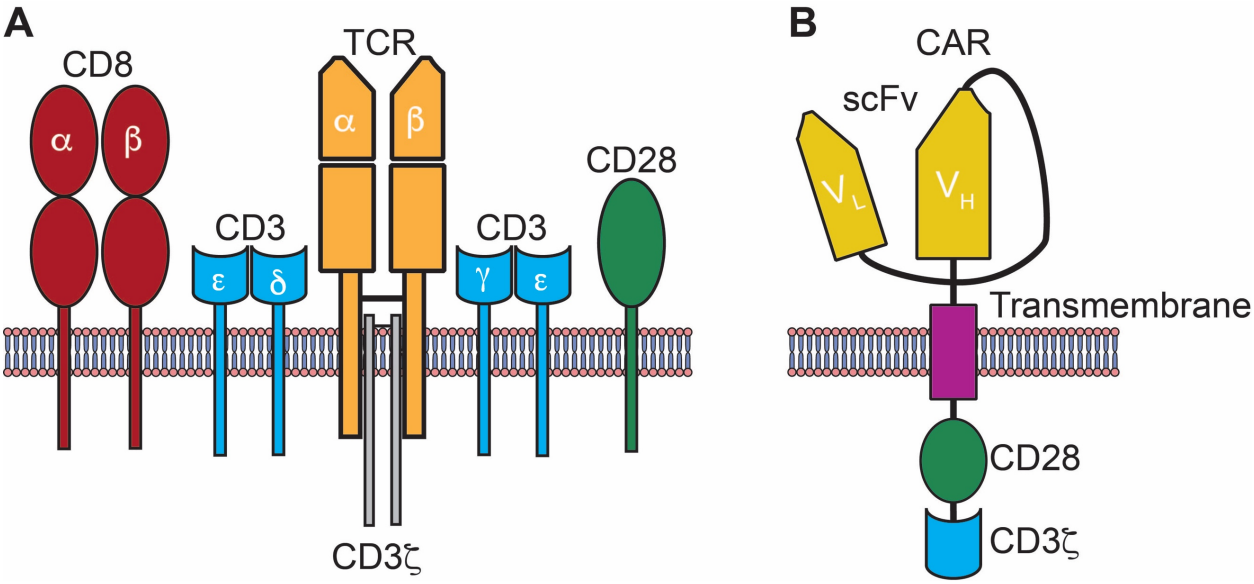

Figure 10. Structural comparison of activation signal between TCR wand CAR. (A) The T cell receptor (TCR) consists of α- and β-chain. Upon peptide-MHC recognition, the two TCR chains associate with δ-, γ- and ε-chains of the CD3 complex to transfer an activation signal over the CD3ζ-chain into the T cell by intracellular signaling cascades. In addition, CD8 binds to the MHC class I molecule to further strengthen the activation signal. Co-receptor engagement, e.g. of CD28, amplify the stimulatory signal further to fully activate the T cell by upregulation of effector-associates genes. (**B**) Chimeric antigen receptor (CAR) is made of a single chain variable fragment (scFv) composed from heavy (V_H) and light (V_L) antibody chains fused to a transmembrane linked to the co-stimulatory signals from CD28 and CD3 ζ-domains that transfer the stimulation signal by effector signaling cascades.

With the development of retroviral transduction, transfer of receptors into human T cells became highly efficient (Mavilio, Ferrari et al. 1994, Bunnell, Muul et al. 1995). CD19 CAR therapy is the prototype of CAR gene therapies and many clinical trials have been conducted so far (Kochenderfer and Rosenberg 2013). The main issue is that while CAR T cells are very effective against CD19 positive hematopoietic malignancies, there has generally been little success in CAR treatment of solid tumors (Martinez and Moon 2019). A major concern in treatment of solid tumors has been the choice of the targeted antigen. When T cells were engineered with an anti-ERBB2 CAR (αHER2) and used to treat HER2 overexpressing tumors, the αHER2 CAR T cells recognized HER2 positive, normal tissue which lead to strong side effects and eventually killed the patient (Morgan, Yang et al. 2010). Similar issues were observed when T cells were transduced with an affinity matured TCR against MAGE-A3 (Morgan, Chinnasamy et al. 2013), a testis antigen which can be overexpressed on tumors. MAGE-A3-directed T cells cross-reacted with the Titin antigen which is expressed on heart muscle cells and killed the patient (Cameron, Gerry et al. 2013). It is believed now that targeting cancer-specific antigens, e.g. mutant

neoantigens would be safe and effective (Tran, Robbins et al. 2017), in particular when the engineered receptor has been derived from the patient's own repertoire. CARs can only bind to cell surface antigens, which limits the pool of truly cancer-specific antigens because most are intracellular proteins that carry point mutations that are presented by MHC and therefore can only be recognized by TCRs. It was demonstrated in pre-clinical models that targeting mutant neoantigens with syngeneic, TCR-transduced T cells can be safe and effective against solid tumors (Leisegang, Engels et al. 2016, Leisegang, Kammertoens et al. 2016). However, the targeted mutant neoantigen, needed to be expressed evenly and at high levels. When the autochthonous, unmanipulated tumor was targeted relapse of antigen-negative variants occurred, which is more representative for human tumors and relapse remains to be the major challenge for development of curative treatments.

3.4 Scientific objective

In this dissertation, it was aimed to determine and characterize conditions for successful cancer immunotherapy of solid tumors targeting natural, unmanipulated mutant neoantigens by adoptive transfer of TCR-transduced T cells. Presented is evidence that $CD8^+$ T cells alone are not sufficient to cure cancers and that the combination with $CD4^+$ T cells is required when unmanipulated, autochthonous solid tumors are targeted. For this, two independent preclinical murine tumor models 8101 and 6132A, were used. Both tumor models were neither cultivated over a long period of time nor were they immunoselected in immunocompetent hosts, so that after transplantation into mice or for use in cell culture experiments, they remained representative to a part of the original, autochthonous cancer. For both tumor models, cancer-specific $CD8^+$ T cell clones were available (Ward, Koeppen et al. 1989, Dubey, Hendrickson et al. 1997) and the TCR genes had been isolated, cloned into a retroviral vector and provided by the laboratory of Prof. Dr. Matthias Leisegang (Leisegang, Engels et al. 2016). In the 6132A tumor model, a cancer-specific $CD4^+$ T cell clone was also available (Monach, Meredith et al. 1995). In this thesis, TCRs isolated from $CD8^+$ T cells that recognize MHC class I restricted antigens are referred to as $CD8^+$TCRs and if isolated from a $CD4^+$ T cell recognizing MHC class II restricted antigens as $CD4^+$TCRs.

3.4.1 The 8101 tumor model

The 8101 tumor was developed by repeated exposure of an immunocompetent C57BL/6 mice to UV light. The growing tumor mass was minced and fragments were adapted in culture to generate the 8101 cancer cell line (Dubey, Hendrickson et al. 1997). In addition, heart-lung-fibroblasts as

autologous control were adapted in culture from the same mouse. The 8101 tumor has been a valuable model to study the success of immune cancer therapy on heterogeneous, large tumors (Dubey, Hendrickson et al. 1997, Schreiber, Wu et al. 2001, Schreiber, Arina et al. 2012, Arina, Schreiber et al. 2014, Arina, Idel et al. 2016, Leisegang, Engels et al. 2016, Schreiber, Karrison et al. 2020). When the primary 8101 cancer cell line was established, two 8101-specific $CD8^+$ T cell clones from immune C57BL/6 wild-type mice, recognizing different independent antigens were generated (Dubey, Hendrickson et al. 1997). It was found that one $CD8^+$ T cell clone recognizes the serine to phenylalanine substitution at position 551 in the DEAD-Box Helicase protein 5, causing the immunodominant, H-$2K^b$ restricted mutant neoantigen mDDX5 (also known as mp68) with a IC_{50} to H-$2K^b$ of 0.48 nM (Schreiber, Arina et al. 2012). It was proven that adoptive T cell transfer with $CD8^+$ T cells transduced with the isolated anti-mDDX5 $CD8^+$TCR gene (introduced as 1D9) can eradicate large and long established solid 8101 tumors (Leisegang, Engels et al. 2016) which demonstrates the potential of adoptive transfer of TCR-transduced T cells in cancer immunotherapy. However, relapse occurred when the autochthonous, unmanipulated 8101 tumor was targeted. The escape variants lost expression of mDDX5 but it could not be solved whether tumor escape was due to pre-existent antigen negative variants or due to downregulation of expression because antigen negative variants were already found in the primary 8101 culture (Dubey, Hendrickson et al. 1997). Interestingly, the authors found a second $CD8^+$ T cell clone which was able to recognize mDDX5 negative variants and named this 8101-specific antigen “B”. In the laboratory of Prof. Dr. Matthias Leisegang, Charité – Universitätsmedizin Berlin, the antigen B-specific TCR sequence was determined and found to recognize the serine to phenylalanine substitution at position 1,490 in the Neuron Navigator 3 protein, creating the H-$2D^b$ restricted mutant neoantigen mNav3 (VSPTNLFQF). The IC_{50} of mNav3 to H-$2D^b$ predicted by NetMHC is 156 nM. The anti-mNav3 $CD8^+$TCR was provided for further studies because targeting of both mutant neoantigens could be a more powerful approach and might not select for antigen-loss variants because relapse is less likely.

3.4.2 The 6132A tumor model

The C3H/HeN tumor model 6132A was UV-induced in immunocompetent C3H/HeN mice (Ward, Koeppen et al. 1989). The growing tumor mass was minced and fragments were adapted in culture to generate the 6132A cancer cell line. In addition, Heart-Lung-Fibroblasts as autologous control were adapted in culture from the same mouse. For this model, a 6132A-specific $CD4^+$ T cell hybridoma was generated from 6132A-immunized C3H/HeN mice (Monach, Meredith et al. 1995). This hybridoma was found to recognize the lysine to histidine substitution at position 47 in

the ribosomal protein L9 (mRPL9) and is restricted to MHC class II I-E^k. It was shown that adoptive T cell transfer of mRPL9-specific $CD4^+$ T cells can prevent outgrowth of 6132A tumors even though the cancer cells do not express MHC class II molecules (Mumberg, Monach et al. 1999). With the hybridoma, the value of ribosomal proteins as targets in immunotherapy was evaluated (Beck-Engeser, Monach et al. 2001, Philip, Schietinger et al. 2010). The anti-mRPL9 TCR gene was isolated and a retroviral vector was provided for studies against established 6132A tumors. Furthermore, for the investigation whether one $CD8^+$TCR combined with one $CD4^+$TCR is required and sufficient for tumor eradication, TCR genes from 6132A cancer cell specific $CD8^+$ T cell clones which were generated from immune C3H/HeN mice (Ward, Koeppen et al. 1989) were also isolated. Two different TCR sequences were isolated and TCR vectors were made. The $CD8^+$TCRs were named after their T cell clone origin and specificity, anti-6132A-A1 and anti-6132A-A4. TCR genes were also isolated from $CD4^+$ and $CD8^+$ T cells specific for the UV-induced C3H tumor model 6139B (Ward, Koeppen et al. 1989, Beck-Engeser, Monach et al. 2001). For the 6139B tumor model another $CD4^+$ T cell hybridoma was generated and found to be specific for the histidine to tyrosine mutation at position 96 in the ribosomal protein L26 (Beck-Engeser, Monach et al. 2001) which was also I-E^k restricted. Additionally, a $CD8^+$ T cell clone that specifically recognizes antigen “A” on the 6139B cancer cell line was also used (Ward, Koeppen et al. 1989). Both TCRs, the anti-mRPL26 $CD4^+$TCR and the anti-6139B-A $CD8^+$TCR, were used as TCR controls for the combinational treatment against 6132A. All TCR-encoding vectors to study effects of adoptive T cell therapy in 6132A-bearing mice were also provided by the laboratory of Prof. Dr. Matthias Leisegang.

3.4.3 Research approach

At first, the 8101 tumor model was investigated because evidence already excised that this tumor can be rejected if targeted mutant neoantigen is highly and evenly expressed in established tumors (Leisegang, Engels et al. 2016). In addition, it was reported that B6 $Rag^{-/-}$ mice, transgenic for the anti-mDDX5 $CD8^+$TCR, developed tumors when challenged with the original 8101 cancer cell line but did not develop tumors when an 8101 clone (Clone 12) was used (Schreiber, Karrison et al. 2020). Thus, the single $CD8^+$TCR anti-mDDX5 was sufficient to prevent outgrowth when the targeted mutant neoantigen (mDDX5) was homogenously expressed among all cancer cells. Therefore, it was analyzed whether established and unmanipulated tumors developed from Clone 12 can also be treated with the anti-mDDX5 $CD8^+$TCR. Since the probability of cancer cells to escape treatment from targeting a single mutant neoantigen is estimated to be 10^{-4} (Tomlinson, Novelli et al. 1996, Jackson and Loeb 1998), which would be one cell in 10,000, it was also tested

whether tumors developed from Clone 12 could be rejected when two $CD8^+$TCRs targeting two independent mutant neoantigens (mDDX5 and mNav3) were used together for adoptive T cell transfer. Afterwards, it was investigated whether the original, unmanipulated and heterogeneous 8101 cancer cell line can be successfully treated by adoptive T cell transfer. For this, it was determined whether polyclonal $CD8^+$ T cells alone or in combination with polyclonal $CD4^+$ T cells had to be used and whether a single $CD8^+$TCR together with polyclonal $CD4^+$ T cells could be sufficient for successful therapy. Furthermore, it was evaluated whether polyclonal $CD4^+$ T cells alone could have an effect against established 8101 tumors.

In the 6132A tumor model, it was investigated whether one $CD4^+$TCR could also have effects against established tumors. The underlying mechanisms, whether $CD4^+$ T cells could cause tumor vessel regression and could be stroma dependent were further investigated. For the analysis whether stroma recognition is required, a model which used double $CD4^+$TCR T cells was established. The spleen cells of TCR75-transgenic mice were used for $CD4^+$TCR-transduction. The TCR75 is an anti-BALB/c $CD4^+$TCR that recognizes the BALB/c specific K^d 15mer peptide QEGPEYWEEQTQRAK presented on the B6 MHC class II haplotype I-A^b and is able to reject BALB/c skin grafts within 15 days after adoptive T cell transfer (Honjo, Xu et al. 2004). TCR75 $CD4^+$ T cells transduced with the anti-mRPL9 $CD4^+$TCR would be able to recognize both the I-A^b restricted K^d peptide from BALB/c origin and the I-E^k restricted mRPL9 peptide from 6132A cancer cells and could therefore be used to distinguish B6 and C3H stroma. Furthermore, it was examined whether established 6132A tumors could be treated with $CD8^+$TCRs only and whether a combination with one $CD4^+$TCR was needed and sufficient for tumor eradication. In the end, it was analyzed whether direct cancer cell recognition was required for eradication of established tumors and the hypothesis of the four-cell type interaction between cancer cell, APC, $CD8^+$ and $CD4^+$ T cell was proposed.

4. Materials

4.1 Mouse strains

Female and male mice were 3 to 8 months old and bred and maintained in a specific pathogen-free barrier facility at The University of Chicago according to Institutional Animal Care and Use Committee (IACUC) guidelines. Animal experiments were approved by the IACUC of The University of Chicago. Littermates of the same sex were randomly assigned to experimental groups on the day of adoptive T cell transfer.

Table 1. Mouse strains.

Name	Strain	Vendor
B6 wild type	C57BL/6	Jackson Laboratory
B6 Rag1$^{-/-}$	B6.129S7-Rag1^{tm1Mom}	Jackson Laboratory
B6 CD4$^{-/-}$	B6.129S2-Cd4a^{tm1Mak}	Jackson Laboratory
B6 CD8$^{-/-}$	B6.129S2-Cd8a^{tm1Mak}	Jackson Laboratory
OT-I Rag1$^{-/-}$	B6.129S7-Rag1^{tm1Mom} Tg(TcraTcrb)1100Mjb	University of Chicago
TCR75 Rag1$^{-/-}$	B6.129S7-Rag1^{tm1Mom}Tg(CD2-Tcra,-Tcrb)75Bucy	University of Chicago
C3H wild type	C3H/HeNHsd	Envigo
C3H Rag2$^{-/-}$	C3H.129S6-Rag2^{tm1Fwa}	University of Chicago
C3H CD4$^{-/-}$	C3H.129S2-Cd4a^{tm1Mak}	University of Chicago
C3H CD8$^{-/-}$	C3H.129S2-Cd8a^{tm1Mak}	University of Chicago
BALB/c	BALB/cAnNHsd	Envigo

C3H Rag2$^{-/-}$ mice were obtained from Douglas Hanahan (University of California, San Francisco, CA, USA). C3H CD8$^{-/-}$ mice were generated at The University of Chicago by crossing C3H/HeN mice with C57BL/6 CD8$^{-/-}$ mice for 20 generations. C3H CD4$^{-/-}$ mice were generated at The University of Chicago by crossing C3H/HeN mice with C57BL/6 CD4$^{-/-}$ mice for 20 generations. B6 wild type, B6 CD4$^{-/-}$ and B6 CD8$^{-/-}$ mice were used for immunization. Spleen of C3H CD8$^{-/-}$, C3H CD4$^{-/-}$ and OT-I Rag1$^{-/-}$ mice were used as T cell sources for retroviral TCR-transduction. OT-I Rag1$^{-/-}$ mice were previously described (Leisegang, Engels et al. 2016). C3H wild type mice were used for isolation of CD11b^{+} cells. BALB/c mice were used as skin donor. TCR75 mice were obtained from Anita Chong (University of Chicago, Chicago, IL, USA) and were crossbred with B6 Rag1$^{-/-}$ mice to obtain TCR75 Rag1$^{-/-}$ mice. TCR75 Rag1$^{-/-}$ mice were used as anti-BALB/c

$CD4^+$ T cell source (Honjo, Xu et al. 2004) for $CD4^+$TCR-transduction. Tumors grown in C3H $Rag2^{-/-}$ mice were used for $CD11b^+$ and $F4/80^+$ cell isolation. B6 $Rag1^{-/-}$ and C3H $Rag2^{-/-}$ mice were used for cancer cell inoculation followed by adoptive T cell transfer against established tumors. All mice were sacrificed with cervical dislocation when tumor sizes reached more than 2 cm^3 or mice appeared hunched and weak due to tumor burden.

4.2 Cell lines

6132A, 6132B, 6139B cancer cell lines were originated in UV-treated C3H/HeN, 8101 cancer cell lines were originated in UV-treated C57BL/6 mice. All cell lines were generated previously with heart-lung fibroblasts as normal tissue control (Ward, Koeppen et al. 1989, Dubey, Hendrickson et al. 1997).

Table 2. Cell lines of either C57BL/6 or C3H/HeN origin.

Cell line	Origin	Induction
8101 bulk	C57BL/6	UV-light
8101 Clone 12	C57BL/6	UV-light
MC57	C57BL/6	Methycholanthrene
6132A	C3H/HeN	UV-light
6132B	C3H/HeN	UV-light
6139B	C3H/HeN	UV-light
6132-HLF	C3H/HeN	Normal tissue

All cell lines were maintained in DMEM supplemented with 10 % FBS and 2 mM L-glutamine and cultured at 10 % CO_2 in a 37 °C dry incubator. Plat-E packaging cells (Morita, Kojima et al. 2000) used for production of retroviral supernatants, were maintained in DMEM supplemented with 10% FBS, 1 µg/mL Puromycin, 10 µg/mL Blasticidin and cultured at 5 % CO_2 in a 37 °C dry incubator. Before use, tumor cell lines were authenticated by sequencing and/or co-culture with antigen-specific T cells and by morphology. Cell lines were frozen in FBS containing 10 % DMSO. Short-time storage was done at -80 °C. Long-term storage was in a liquid nitrogen container. All cell lines were shortly passaged after thawing of the initial frozen stock to generate master cell banks. Working batches were passaged no longer than 4 weeks.

4.3 Equipment

Table 3. Equipment used.

Device	Name	Provider
Autoclave	Hinged Autoclave Steam Sterilizer	Consolidated Sterilizer Systems
Bacteria Incubator	Forma 3960 Environmental Chamber	Thermo Scientific
Bacteria Shaker	Innova 210 Platform Shaker	New Brunswick Scientific
Bacterial Hood	Vertical Laminar Flow Hood	Nuaire
Balances	E1200S	Sartorius Excellence
Bunsen Burner	Hanau Touch-O-Matic	Whip Mix
Cell Culture Hood	Bioflow Chamber Class II Type A/B3	Germfree Laboratories
Cell Sorter	BD FACS Aria II	BD Bioscience
	BD FACS Aria III	BD Bioscience
Centrifuge	5810 R	Eppendorf
	DW-41 Microcentrifuge	Qualitron
	GeneMate Minifuge	Bioexpress
	Microcentrifuge 5415 R	Eppendorf
	RC5C Plus SuperSpeed	Sorvall
	ST 8R	Sorvall
CO_2-Incubator	Automatic CO_2 Water Jacketed Incubator 1168710	Fisher Scientific
	Water Jacket CO_2 Incubator 6200	Napco Precision Instrument
Cuvettes	Quartz Spectrophotometer Cell	Thomas Scientific
Electrophoresis chamber	Horizontal Apparatus Model H5	LifeTechnologies
	Horizontal Systems	Ellard Instrumentation
Flow Cytometer	Accuri C6	BD Bioscience
	BD LSR II	BD Bioscience
Gas Analyzer	Fyrite	Bacharach

Device	Name	Provider
Glass Equipment	Beaker	Pyrex
	Duran Bottles (100 mL, 250 mL, 500 mL)	Schott
	Erlenmeyer flask	Pyrex
	Glass Pipettes (1 mL, 2 mL, 5 mL, 10 mL and 25 mL)	Bellco Glass
	Graduated Cylinder	Pyrex
Heat block	Dry Block Incubator	Fisher Scientific
Hemocytometer	Bright Line Hemocytometer	Sigma-Aldrich
Homogenizer	Polytron	Kinematica
Ice machine	Refrigerant R404A	IMI Cornelius
Lighter	Shurlite Safety Gas Lighter	Fisher Scientific
Magnet	MidiMACS separator	Miltenyi Biotec
	MiniMACS separator	Miltenyi Biotec
	QuadroMACS separator	Miltenyi Biotec
Magnetic stand	MACS multi stand	Miltenyi Biotec
Magnetic stirrer	Nuova II stir plate	Thermolyne
Microscope	Invertoscope ID 02	Zeiss
	SP5 TCS II	Leica
Microscope stage	Stage	Custom made
Microwave	Microwave	Toshiba
pH-Meter	UltraBASIC pH-Meter	Denver Instrument
Pipettes	Eppendorf Research Plus (1 µL, 10 µL, 20 µL, 100 µL, 200µL, 1000 µL)	Eppendorf
	Eppendorf Research Plus 8 channel pipette (10 µL, 100 µL, 300 µL)	Eppendorf
Pipette aid	Portable Pipet Aid	Drummond Scientific
Pipette stuffer	Bellco Pipette Plugger	Bellco Glass
Pipette Can	Stainless Steel Pipet Can	Bellco Glass
Plastic Equipment	Beakers	Nalgene
	Bottles (500 mL)	Nalgene
	Graduated Cylinder	Nalgene
Plate-reader	VersaMax microplate reader	Molecular Devices

Device	Name	Provider
Power Supply	Owl EC-105 Compact	Thermo Scientific
Printer	Digital graphic printer UP-D898MD	Sony
Real-Time PCR	ABI ViiA 7	ThermoFisher
Rodent anesthesia machine	VAD Compact	Vetamac
Shaker	Microtiter plate minishaker	Dynatech Laboratories
	Variable speed 2D Rocker	USA Scientific
Shaver	Oster Finisher Trimmer	Oster
Spectrophotometer	Biomate 3	Thermo Spectronic
Thermal cycler	GenAmp PCR System 9700	Applied Biosystems
	T100 thermal Cycler	Bio Rad
UV-Transilluminator	NucleoVision	Nucleotech
Vortex mixer	Vortex Genie 2	Scientific Industries
Water bath	Isotemp Digital 215	Fisher Scientific
Window chamber	Window Chamber	Custom made

4.4 Disposable supplies

Table 4. List of disposable supplies and their provider.

Name	Kind	Provider
Animal Lancet	Goldenrod 5 mm	Braintree Scientific inc.
Bandage	Band-Aid	Johnson & Johnson
Cell culture flasks	25 cm^2	Greiner Bio-One
	75 cm^2	Greiner Bio-One
	175 cm^2	Greiner Bio-One
Cell strainer	Nylon Mesh 40 µm	Fisher Scientific
	Nylon Mesh 70 µm	Fisher Scientific
Cover slip	Hemacytometer soda lime glass (20 x 26 x 0.4 mm)	Sigma Alderich
Cover glass	Microscope Cover Glass 12 CIR-1.5 1oz	Fisher Scientific

Name	Kind	Provider
Dish	Cell Culture Dish 60 x 15 mm	Greiner Bio-One
	Petri Dish 100 x 15 mm	VWR
	Petri Dish 100 x 20 mm Falcon	BD Bioscience
Disposable Cuvette	Semi micro cell polystyrene	Fisher Scientific
Disposable	Serological Pipettes, 1 mL	Corning
Pipettes	GeneMate Serological Pipettes, 2 mL	BioExpress
	GeneMate Serological Pipettes, 5 mL	BioExpress
	GeneMate Serological Pipettes, 10 mL	BioExpress
	Serological Pipettes, 25 mL	VWR
Filter	150 mL Vacuum Filter Bottle System, 0.22 µm Cellulose Acetate	Corning
	500 mL Bottle Top Filter, 0.2 µm Nylon	Corning
Freezing Vials	2 mL CRYO.S	Greiner Bio-One
Gauze	Xeroform Gauze	Sherwood Medica
Gloves	Industrial Grade Ntril Gloves	Condor
Heparinized Tubes	Fisherbrand Capiliary Tubes	Fisher Scientific
Laboratory Foil	Parafilm "M"	American National Can
	Supremium Aluminum Foil, Ultra-Clean	VWR
Magnetic column	MACS Separation Column MS	Miltenyi Biotec
	MACS Separation Column LS	Miltenyi Biotec
	MACS Separation Column LD	Miltenyi Biotec
Mouse Tags	Mouse Ear Tags	National Brand & Tag Company
Needles	BD PrecisionGlide Needle 25G x 5/8 (0.5 x 16 mm)	Becton-Dickinson & Co
	BD PrecisionGlide Needle 16G x 1/2 (0.5 x 16 mm)	Becton-Dickinson & Co
	Insulin Syringe, 31G, 6 mm	BD Bioscience
	Hypodermic Needles 27G x 1/2	Air-Tite Products
Pasteur Pipette	Pasteur Pipet Lime Glass 9"	VWR
Pipette tips	10 µL Pipettors	VWR
	200 µL Pipettors	VWR
	1000 µL Pipettors	VWR

Name	Kind	Provider
Pipette Tray	25 ml reservoir for 8 channel Pipette	Olympus Plastics
Plates	96-Well Cellstar F- and U-Bottom	Greiner Bio-One
	24-Well Cellstar	Greiner Bio-One
	12-Well Cellstar	Greiner Bio-One
	6-Well Cellstar	Greiner Bio-One
	Maxisorp Nunc-Immuno Plate	Thermo Scientific
	96-Well Microplate	Greiner Bio-One
Razor blades	1 - 1/2" Carbon Steel	Stanley
Sterile cotton Tip	Cotton Tipped Applicator	Puritan
Suture	4-0 Polyglycolic acid, absorbable	Oasis
	5-0 Polypropylene	Med-Vet international
Syringe filter	0.20 µm Cellulose Acetate	VWR
	0.45 µm Cellulose Acetate	VWR
Syringes	0.5 ml BD Insulin Syringes	Becton-Dickinson & Co
	1 mL BD Syringe	Becton-Dickinson & Co
	3 mL Disposable Syringe	EXELint
	5 mL Disposable Syringe	EXELint
	10 mL Fisherbrand Plastic Syringe	Fisher Scientific
	20 mL Disposable Syringe	EXELint
	30 mL BD Syringe	Becton-Dickinson & Co
Tissues	Kimwipes, Delicate Task Wipers	KimTech
Tubes	0.2 mL Thin-walled 8 PCR Tube	Thermo Scientific
	1.2 mL Fisherbrand Micro Titer Tubes	Fisher Scientific
	1.5 mL Fisherbrand MCT Graduated	Fisher Scientific
	14 mL Falcon Snap-Cap Round Bottom Polypropylene	Fisher Scientific
	15 mL Falcon Conical High-Clarity Polypropylene	Fisher Scientific
	5 mL Falcon Polystyrene Round Bottom 12 x 75 mm	Fisher Scientific
	50 mL Falcon Conical Polypropylene	Fisher Scientific
	Fisherbrand Culture Test Tube 12 x 75 mm Polystyrene	Fisher Scientific

4.5 Chemicals

Table 5. Chemicals with indicated stock concentrations and providers.

Name	Stock	Provider
1,1'-dioctadecyl-3,3,3',3'-tetramethylindodicarbocyanine, 4-chlorobenzenesulfonate salt (DiD)	2 mg/mL	Thermo Scientific
2-[4-(2-Hydroxyethyl)piperazin-1-yl]ethanesulfonic acid (HEPES)	1 M	Sigma-Aldrich
2-Amino-2-(hydroxymethyl)propane-1,3-diol (TRIS-Base)	-	Sigma-Aldrich
2-Mercapthoethanol	50 mM	Fisher Scientific
2-Propanol (Isopropanol)	-	Sigma-Aldrich
3,3′,5,5′-Tetramethylbenzidine (TMB substrate)	-	Thermo Scientific
Agar Bacto	-	Becton-Dickinson & Co
Agarose	-	J. T. Baker
Albumin from bovine serum	-	Sigma-Aldrich
Ammonium chloride (NH_4Cl)	-	Fisher Scientific
Ampicillin	100 mg/mL	Sigma-Aldrich
Blasticidin	10 mg/mL	InvivoGen
Calcium chloride ($CaCl_2$)	2.5 M	Sigma-Aldrich
Chloroform	-	Sigma-Aldrich
Chromerge	-	VWR
Diethyl dicarbonate (DEPC)	-	Sigma-Aldrich
Dimethyl sulfoxide (DMSO)	-	Sigma-Aldrich
Dulbecco's Modified Eagle Medium (DMEM)	-	Corning
Ethanoic acid (Acetic Acid)	-	J. T. Baker
Ethanol 200 Proof (EtOH)	70%	Decon Labs
Ethylenediaminetetraacetic acid disodium salt (EDTA)	0.5 M	Sigma-Aldrich
Fetal Bovine Serum for cell lines, GemCell	-	Gemini Bo-Products
Fetal Bovine Serum for T cells, Benchmark	-	Gemini Bo-Products
Gentamycin	50 mg/mL	Amresco
Hair remover lotion	-	Nair
Heparin sodium	20,000 U/mL	Pfilzer

Name	Stock	Provider
IsoThesia (Isoflurane)	-	Henry Schein
L-Glutamine	200 mM	Gibco
Luria Broth (LB)	-	Fisher Scientific
Meloxicam	100 µg/mL	University of Chicago
Non essential amino acids (NEAA)	-	Gibco
Penicillin/Streptomycin	10,000 U/mL, 10,000 µg/mL	Gibco
Potassium chloride (KCl)	-	Merck
Potassium dihydrogen phosphate (KH_2PO_4)	-	Sigma-Aldrich
Protamine sulfate	1 mg/mL	Sigma-Aldrich
Puromycin dihydrochloride	1 mg/mL	Sigma-Aldrich
Recombinant Human Interleukine-2 (IL-2)	4,000 U/mL	PeproTech
Recombinant Human Interleukine-15 (IL-15)	50 µg/mL	PeproTech
Recombinant Mouse IFN-γ	1×10^7 U/mL 1 mg/mL	Genentech
RetroNectin	1 mg/mL	Takara Bio
Roswell Park Memorial Institute medium 1640 (RPMI)	-	Corning
Sodium chloride (NaCl)	-	Fisher Scientific
Sodium hydrogen phosphate heptahydrate ($Na_2HPO_4 \times 7$ H2O)	-	Sigma-Aldrich
Sodium hydroxide (NaOH, pellets)	-	Sigma-Aldrich
Sodium Pyruvate	100 mM	Gibco
Sulfuric Acid (H_2SO_4)	-	Sigma-Aldrich
TRIS Hydrochloride	-	Sigma-Aldrich
Trizol	-	Thermo Fisher
Name	Stock	Provider
Tween	-	Sigma-Aldrich

4.6 Solutions

If not indicated otherwise, solutions were prepared in double distilled water (ddH_2O).

DEPC-ddH_2O (Enzyme-Free Water)

Double distilled water, containing 0.1 % DEPC (v/v), was stirred for 30 min at room temperature and incubated overnight before autoclaved (storage at 4 °C).

ELISA Wash Buffer

PBS (1x) was supplemented with 0.05 % Tween (v/v) and stirred for 10 min at room temperature before used (storage at room temperature).

Luria Broth (LB) Medium

25 g LB prepared powder mix (Fisher Scientific) was added into 1 L of ddH_2O and autoclaved before used for the expansion of bacterial colonies (storage at 4 °C).

LB Agar Plates

15 g Agar was added into 1 L LB medium (25 g LB powder in 1 L ddH_2O) and autoclave. As soon as the solution reached 40 °C, 100 µg/mL Ampicillin (or any other antibiotic of interest) is added and the solution is poured into petri dishes. After plates were hardened they were stored at 4 °C.

MACS Buffer

PBS (1x) is supplemented with 0.5 % albumin (Sigma), 2 mM EDTA before pH was adjusted to 7.2. The solution was filtered through a 0.22 µm filter, before degassed overnight and stored at 4 °C before used for equilibration of magnetic columns.

10x Phosphate Buffer Saline (PBS)

10x PBS was prepared by combining 1.36 M NaCl with 0.08 M Na_2HPO_4 x 7 H_2O, 0.026 M KCl and 0.015 M KH_2PO_4. The pH was adjusted to 7.4 before autoclaved and stored at 4 °C.

50x TRIS Acetate EDTA Buffer (TAE)

The 50x TAE solution contained 2 M TRIS-Base, 0.95 M acetic acid and 0.05 M EDTA with a pH of 8.0 (storage at 4 °C).

Transfection Buffer

Transfection buffer included 270 mM NaCl, 9.9 mM KOH, 3.5 mM Na_2HPO_4 and 40 mM HEPES. After stirring the pH was adjusted to 6.76, the solution was sterile filtered through a 0.22 µm filter and stored at -20 °C.

TRIS-HCl EDTA Buffer

TRIS-HCl (1M) solution contained 10 mM EDTA, was adjusted to a pH of 8.0, and filtered through a 0.22 µm filter before used (storage at room temperature).

TRIS-NH_4Cl Buffer

The solution consisted of 0.14 M NH_4Cl and 0.017 M TRIS base. The pH was adjusted to 7.2 before filtered through a 0.22 µm filter and stored at 4 °C.

Versene

Versene was prepared by adding together 170 mM NaCl, 3.3 mM KCl, 10 mM Na_2HPO_4 x $7H_2O$, 1.8 mM KH_2PO_4 and 3 mM EDTA. The pH was adjusted to 7.5, was autoclaved and stored at 4 °C before Trypsin was added.

4.7 Enzymes

Table 6. Listed enzymes and their provider.

Name	Provider
BbsI (Restriction Enzyme)	New England BioLabs
CIP (Alkaline Phosphatase, Calf Intestinal)	New England BioLabs
Collagenase D (100 mg)	Roche
DNAse I recombinant (10,000 U)	Roche
Phusion HF DNA Polymerase	New England BioLabs
RevertAid Transcriptase	Thermo Scientific
T4 Polynucleotide Kinase	New England BioLabs
T4 DNA Ligase	New England BioLabs
Go Taq DNA Polymerase	Promega
Trypsin (10x) HBSS without Ca and Mg	MP Biomedicals

4.8 Antibodies

Stock antibodies (0.2 µg/µL) summarized in table 7 were stored at 4 °C and if not other indicated in the Methods section, used as1:100 dilutions (final concentration 2 ng/µL).

Table 7. List of Antibodies used in this thesis.

Name	Clone	Provider
αCD3ε	145-2C11	University of Chicago
αFcR	2.4G2	University of Chicago
anti-mouse CD28, Ultra Leaf Purified	37.51	BioLegend
APC anti-mouse CD4	GK1.5	BioLegend
APC anti-mouse CD8	53-6.7	BioLegend
APC anti-mouse F4/80	BM8	BioLegend
APC anti-mouse/human CD11b	M1/70	BioLegend
APC anti-mouse CD146	ME-9F1	Biolegend
APC anti-mouse I-E^k	14-4-4S	Biolegend
APC Rat IgG2a κ Isotype	RTK2758	BioLegend
APC Rat IgG2b κ Isotype	MG2b-59	BioLegend
FITC anti-mouse CD3ε	145-2C11	BioLegend
FITC anti-mouse H-2Kk	36-7-5	BioLegend
FITC anti-mouse/human CD11b	M1/70	BioLegend
FITC Rat IgG2a κ Isotype	RTK2758	BioLegend
FITC Rat IgG2b κ Isotype	MG2b-57	BioLegend
PE anti-mouse F4/80	BM8	BioLegend
PE anti-mouse CD31	390	Biolegend
PE anti-mouse H-2Dk	15-5-5	BioLegend
PE anti-mouse TCR Vβ2	B20.6	BioLegend
PE anti-mouse TCR Vβ6	RR4-7	BioLegend
PE anti-mouse TCR Vβ8.3	8C1	BioLegend
PE anti-mouse TCR Vβ8.1, 8.2	KJ16-133.18	BioLegend
PE Rat IgG2a κ Isotype	RTK2758	BioLegend
PE Rat IgG2b κ Isotype	MG2b-58	BioLegend

4.9 Oligonucleotides

Lyophilized oligonucleotides indicated in table 8 were purchased from Integrated DNA Technologies (IDT), were resuspended in DEPC-ddH_2O at a 100 µM concentration and stored at –20 ° C. Oligonucleotides were further diluted to 10 µM before used in PCR. Sequences are either plasmid specific or designed for mouse genes.

Table 8. Designation and sequence of used oligonucleotides.

Category	Name	Length (in bp)	Sequence (5' – 3')
Genotyping	FOR Rag2 WT	21	ATG TCC CTG CAG ATG GTA ACA
	REV Rag2 WT	21	GCC TTT GTA TGA GCA AGT AGC
	FOR Rag2 KO	19	CCT GCC GAG AAA GTA TCC A
	REV Rag2 KO	19	ACC GTA AAG CAC GAG GAA G
	FOR CD8 Common	22	GAC CTG GTA TGT GAA GTG TTG G
	REV CD8 WT	20	ACA TCA CCG AGT TGC TGA TG
Genotyping	REV CD8 KO	20	CAT AGC GTT GGC TAC CCG TG
	FOR CD4 Common	20	CCT CTT GGT TAA TGG GGG AT
	REV CD4 WT	20	TTT TTC TGG TCC AGG GTC AC
	REV CD4 KO	19	GTG TTG GGT CGT TTG TTC G
	FOR Rag1 Common	20	CCG GAC AAG TTT TTC ATC GT
	REV Rag1 WT	20	GAG GTT CCG CTA CGA CTC TG
	REV Rag1 KO	21	TGG ATG TGG AAT GTG TGC GAG
	FOR OT-I	21	CAG CAG CAG GTG AGA CAA AGT
	REV OT-I	22	GGC TTT ATA ATT AGC TTG GTC C

Category	Name	Length (in bp)	Sequence (5' – 3')
RT-PCR	Oligo dT_{12-18}	12 - 18	TTT TTT TTT TTT TTT TTT
qPCR	FOR mp68	22	TTG GGG CTA AAA CTC AGA ATG G
	REV mp68	30	CTT CCA TAT TGC TGA GTG CTA TCA TAA C
Quencher	C-P mp68	19	VIC - TTT TGT ATC TGC TGG CAT A - MGB
	T-P mp68	19	FAM - ATT TTG TAT TTG CTG GCA T - MGB
sg RNA	FOR B2m A	25	CAC CGG CTA CTC GGC GCT TCA GTC G
	REV B2m A	25	AAA CCG ACT GAA GCG CCG AGT AGC C
	FOR B2m B	25	CAC CGA GTC GTC AGC ATG GTC CGC T
	REV B2m B	25	AAA CAG CGA GCC ATG CTG ACG ACT C
	FOR B2m C	25	CAC CGC ATG GCT CGC TCG GTG ACC C
	REV B2m C	25	AAA CGG GTC ACC GAG CGA GCC ATG C
Sequencing	FOR pMP71	20	CCC TCT CTC CAA GCT CAC TT
	REV pMP71	22	CAA ATA TGG GAA TAA ATG GCG G
Sequencing	FOR PX458	23	ACC GAA CTG AGA TAC CTA CAG CG
	REV PX458	25	ATG TAC TGC CAA GTA GGA AAG TCC C
Housekeeping Gene	FOR Gapdh	20	GCC AAA AGG GTC ATC ATC TC
	REV Gapdh	20	GCC TGC TTC ACC ACC TTC TT

4.10 Kits

Table 9. List of Kits and their providers used for this thesis.

Name	Provider
Anti-F4/80 Microbeads Ultra Pure, Mouse	Miltenyi Biotec
CD11b Microbeads Human and Mouse	Miltenyi Biotec
CD4 (L3T4) Microbeads, Mouse	Miltenyi Biotec
Invitrogen IFN gamma Mouse Uncoated ELISA Kit	Invitrogen
Legendplex Mouse Th1 Panel (5-plex)	BioLegend
Mix and Go Transformation Kit	Zymo Research
NucleoBond Xtra Maxi	Machere-Nagel

Name	Provider
QIAprep Spin Miniprep Kit (250)	Qiagen

4.11. TCR sequences

Table 10. TCR sequences from 8101 and 6132A cancer cell specific $CD8^+$ T cell clones.

$CD8^+$TCR	α-Chain	β-Chain
anti-mNav3	TRAV5D5–CAASGTGGYKVVF–TRAJ12	TRBV13–CASGAGQGPEQFF–TRBJ2
anti-8101-C	TRAV21–CILRVAQGTGSKLSF–TRAJ58	TRBV2–CASSQDRGFSNERLFF–TRBJ1
anti-6132A-A1	TRAV3D–CAVSNDSGYNKLTF–TRAJ11	TRBV19–CASTPTGIQDTQYF–TRBJ2
anti-6132A-A4	TRAV9D–CALSAINTGNYKYVF–TRAJ40	TRBV13–CASSPDWGGFAEQFF–TRBJ2
anti-6139B-A	TRAV3–CAVSNTDKVVF–TRAJ34	TRBV13–CASMLGGRFEQYF–TRBJ2

Table 11. TCR sequences from 6132A and 6139B cancer cell specific $CD4^+$ T cell hybridomas.

$CD4^+$TCR	α-Chain	β-Chain
anti-mRPL9	TRAV4–CAAGYGGSGNKLIF–TRAJ32	TRBV19–CASSIGTGGNERLFF–TRBJ1
anti-mRPL26	TRAV13–CAMVTGANTGKLTF–TRAJ52	TRBV1–CTCSAHNNQAPLF–TRBJ5

4.11 Plasmids

For retroviral TCR transduction of lymphocytes, TCR cassettes were cloned onto the pMP71 backbone (Engels, Cam et al. 2003) and were summarized in table 12. TCR-encoding vectors were provided by Prof. Dr. Matthias Leisegang.

Table 12. TCR encoded plasmids used for retroviral TCR-transduction.

Name	Encoded TCR
pMP71-A1	anti-6132A-A1
pMP71-A4	anti-6132A-A4
pMP71-C2.15	anti-6139B-A
pMP71-H6	anti-mRPL9
pMP71-12.2	anti-mRPL26
pMP71-1D9	anti-mDDX5
pMP71-U3/6	anti-mNav3

For CRISPR-Cas9 mediated gene knockout, the PX458 (Ran, Hsu et al. 2013) vector which encodes the Streptococcus pyogenes engineered Cas9 enzyme necessary for single guide mediated cutting of the targeted DNA region, was used.

Table 13. PX458 vector for CRISPR-Cas9 mediated gene knockout.

Name	Encoded Gene
pSpCas9(BB)-2A-GFP	Cas9

4.12 Software

Table 14. Software programs for data and thesis generation.

Type	Name	Provider
Citation	EndNote X7	Thomson Reuters
Data analysis	Legendplex	BioLegend
	Microsoft Excel 2015	Microsoft
	Prism 6	GraphPad
Data presentation	Adobe Acrobat DC 2019	Adobe
	Microsoft PowerPoint 2015	Microsoft
Flow cytometric analysis	FlowJo X10	FlowJo
Image acquiring	LAS-AF	Leica
Image analysis	Fiji	Open Source
Image editing	Adobe Illustrator CC 2017	Adobe

Type	Name	Provider
PCR design	Tm calculator	Thermo Scientific
PCR Images	Gel Expert 3.5	NucleoTech
Plasmid Mapping	SnapGene V2.3	SnapGene
Plate reader analysis	SoftMax Pro	Molecular Devices
Primer design	SnapGene V2.3	SnapGene
Real-Time PCR	ViiA 7 Software	ThermoFisher
Statistical Analysis	Prism 6	GraphPad
Text processing	Microsoft Word 2015	Microsoft

5. Methods

5.1 Genotyping

Confirmation of mouse strains was done by PCR. Mice were ear tagged, a 1 mm tail cut was performed and tail tissue was incubated in 500 µL 50 mM NaOH at 97 °C for 45 min to release DNA. For pH neutralization, 50 µL of 1M TRIS HCl EDTA solution were added and stored at 4 °C. DNA solution was used for strain-specific PCRs.

C3H Rag2$^{-/-}$

Amplification for the neomycin knockout cassette showed a band at 411 bp and wild type specific primers generated a band at 246 bp.

Table 15. C3H Rag2$^{-/-}$ PCR.

PCR set up per sample

Reagents	Volume (µL)
5x Go Taq buffer	5.0
25 mM $MgCl_2$	3.0
2.5 mM dNTPs	2.5
Primer: Rag 2 WT	1.0
Primer: Rag 2 KO	1.0
Taq Polymerase	0.125
DNA	1.0
ddH_2O	11.4
Total Volume	25.0

PCR program

Steps	Duration	Temperature	Cycles
1)	5 min	94 °C	1x
2)	30 s	94 °C	35x
3)	30 s	57 °C	
4)	1 min	72 °C	
5)	5 min	72 °C	1x
6)	For ever	4 °C	

C3H CD8$^{-/-}$

Amplification for the knockout cassette showed a band at 343 bp and wild type specific primers generated a band at 265 bp.

Table 16. C3H CD8$^{-/-}$ PCR.

PCR set up per sample

Reagents	Volume (µL)
5x Go Taq buffer	5.0
25 mM $MgCl_2$	3.0
2.5 mM dNTPs	2.5
Primer: Common	1.0
Primer: WT	1.0
Primer: KO	1.0
Taq Polymerase	0.125
DNA	1.0
ddH_2O	10.4
Total Volume	25.0

PCR program

Steps	Duration	Temperature	Cycles
1)	5 min	94 °C	1x
2)	20 s	94 °C	10x
3)	15 s	57 °C	
4)	10 s	72 °C	
5)	15 s	94 °C	30x
6)	15 s	60 °C	
7)	10 s	72 °C	
8)	5 min	72 °C	1x
9)	For ever	4 °C	

C3H CD4$^{-/-}$

Amplification for the knockout cassette showed a band at 225 bp and wild type specific primers generated a band at 381 bp.

Table 17. C3H CD4$^{-/-}$ PCR.

PCR set up per sample

Reagents	Volume (µL)
5x Go Taq buffer	5.0
25 mM $MgCl_2$	3.0
2.5 mM dNTPs	2.5
Primer: Common	1.0
Primer: WT	1.0
Primer: KO	1.0
Taq Polymerase	0.125
DNA	1.0
ddH_2O	10.4
Total Volume	25.0

PCR program

Steps	Duration	Temperature	Cycles
1)	5 min	94 °C	1x
2)	20 s	94 °C	10x
3)	15 s	65 °C	
4)	10 s	68 °C	
5)	15 s	94 °C	30x
6)	15 s	60 °C	
7)	10 s	72 °C	
8)	5 min	72 °C	1x
9)	For ever	4 °C	

B6 Rag1$^{-/-}$

Amplification for the knockout cassette showed a band at 530 bp and wild type specific primers generated a band at 474 bp.

Table 18. B6 Rag1$^{-/-}$ PCR.

PCR set up per sample

Reagents	Volume (µL)
5x Go Taq buffer	5.0
25 mM $MgCl_2$	3.0
2.5 mM dNTPs	2.5
Primer: Common	1.0
Primer: WT	1.0
Primer: KO	1.0
Taq Polymerase	0.125
DNA	1.0
ddH_2O	10.4
Total Volume	25.0

PCR program

Steps	Duration	Temperature	Cycles
1)	2 min	94 °C	35x
2)	30 s	58 °C	
3)	1 min	72 °C	
4)	5 min	72 °C	1x
5)	For ever	4 °C	

OT-I Rag1$^{-/-}$

Amplification of the alpha chain of the transgenic inserted OT-I TCR showed a band at 300 bp. In addition, mice were also always screen for the Rag1$^{-/-}$ gene.

Table 19. OT-I PCR.

PCR set up per sample

Reagents	Volume (µL)
5x Go Taq buffer	5.0
25 mM $MgCl_2$	3.0
2.5 mM dNTPs	2.5
For TCR-alpha	1.0
Rev TCR-alpha	1.0
Taq Polymerase	0.125
DNA	1.0
ddH_2O	11.4
Total Volume	25.0

PCR program

Steps	Duration	Temperature	Cycles
1)	5 min	94 °C	1x
2)	30 s	94 °C	35x
3)	1 min	62 °C	
4)	1 min	72 °C	
5)	5 min	72 °C	1x
6)	For ever	4 °C	

If not indicated otherwise, PCR primers and programs were provided by the Jackson Laboratory. PCR amplification was analyzed by electrophoresis using a 1.5 % agarose gel in TAE buffer with a MassRuler DNA ladder.

5.3 Immunization of mice

8101 cancer cells (1 x 10^7) were washed twice with PBS, to remove remaining FBS, before *s.c.* injection into the shaved back of B6 wild type, B6 CD4$^{-/-}$ or B6 CD8$^{-/-}$ mice. After 6 weeks, mice were boosted *s.c.* with 1 x 10^7 8101 cancer cells. Additional 6 weeks later, spleens were harvested, red blood cells were lysed with TRIS NH_4Cl and one full spleen per recipient was used for adoptive T cell transfer.

5.4 Generation of cancer fragments and adaption to *in vitro*-cultures

Mice were shaved, the skin of the tumor was removed and tumor tissue was cut out from the back of either B6 Rag1$^{-/-}$ or C3H Rag2$^{-/-}$ mice. The harvested tumor was placed into a 60 mm dish and 0.5 mL DMEM was added. The tissue was minced with a razor blade into rough pieces and further chopped with a curved scissor until an even suspension of 1 mm fragments was generated.

Fragments were put into a T-25 cell culture flask with 5 mL DMEM containing 10% FBS, 2 mM L-glutamine, 100 U/mL penicillin, 100 µg/mL streptomycin and 50 µg/mL gentamycin. After 7 days, fragments were removed and adherent cells were cultured (see under “4.2 Cell lines”).

5.5 Tumor growth and adoptive T cell transfer

In both tumor models, cancer cells (1×10^7) were injected *s.c.* into the shaved back of either B6 Rag1$^{-/-}$ (8101) or C3H Rag2$^{-/-}$ mice (6132A). Tumor volumes were measured along 3 orthogonal axes, every 2 to 3 days and were calculated as (a x b x c) ÷ 2. T cells from immunized mice or engineered to express either 8101-specific or 6132A-specific TCRs were injected *i.p.*. The number of TCR$^+$ T cells was calculated based on rate of transduction on the day of treatment prior to T cell transfer. For treatment with single TCR$^+$ T cell populations, 2×10^6 TCR-transduced CD8$^+$ or CD4$^+$ T cells were used per recipient. When combinations of multiple TCR$^+$ CD8$^+$ T cells were used or TCR$^+$ CD8$^+$ T cells were combined with TCR$^+$ CD4$^+$ T cells, the number of injected TCR$^+$ T cells of each population was 1×10^6 per recipient. Mice were randomized into different treatment groups on the day of adoptive T cell transfer and euthanized when tumor sizes reached more than 2 cm^3 or appeared hunched and weak due to tumor burden.

5.6 Peripheral blood preparation

Peripheral blood was taken by buccal bleeding with a 5 mm animal lancet. Mice were grabbed firmly and punctured on the cheek, at the branching point of the external jugular vein into the facial vein and submandibular vein. Blood (100 µL) was collected into 1.5 mL tubes containing 50 µL heparin (80 U/mL).

Preparation for T cell analysis

Red blood cells were lysed with 1 mL TRIS NH_4Cl. After 10 min incubation at room temperature, cells were spun down at 9,000x g for 30 s. Supernatants were removed and cell pellet was resuspended in PBS containing αFcR block antibody. After incubation for 10 min at 4 °C, cells were washed twice with 150 µL PBS and used for subsequent T cell staining and flow cytometric analysis.

Preparation of blood plasma

Cells were spun down at 9,000x g for 30 s, supernatants (150 µL) were transferred into a 1.5 mL tube and analyzed for IFN-γ by flow cytometry. Samples were stored at -20 °C. Blood was collected at day of adoptive T cell transfer and every 3rd day for a total of 21 days.

5.7 Isolation of $CD11b^+$ and $F4/80^+$ cells

Fragments of 6132A tumors grown in C3H $Rag2^{-/-}$ mice were generated and single cell suspensions were made by enzymatic digestion (Spiotto, Rowley et al. 2004). Collagenase D (2 mg/mL) and DNAse I (100 U/mL) were added to 5 mL tumor fragments in RPMI and incubated on a table shaker at 30 rpm for 30 min at 37 °C. Subsequently, Trypsin was added (1 mg/mL) and the suspension was incubated for 15 min (table shaker, 30 rpm, 37 °C). The digested suspension was filtered over a 70 µm cell strainer, washed with 10 mL RPMI and then filtered over a 45 µm cell strainer and washed again with 10 mL RPMI. The suspension was spun down at 350x g for 10 min and counted (red blood cells were lysed with 5 mL TRIS NH_4Cl and incubated for 3 min, then washed with 30 mL RPMI before counting). Up to 1 x 10^8 cells were used for either $CD11b^+$ or $F4/80^+$ cell isolation. Cells were incubated with 10 µL magnetic beads, resuspended in 90 µL MACS buffer (both volumes adjusted per 1 x 10^7 cells) and incubated for 20 min at 4 °C. Afterwards 5 mL MACS buffer were added and cells were centrifuged for 10 min at 350x g. A LS column was equilibrated with 4 mL MACS buffer before cells suspended in 1 mL MACS buffer were carefully add onto the LS column without bubble formation. The column was washed once with 5 mL MACS buffer, then taken out of the magnet, placed onto a 15 mL tube and flushed with 5 mL MACS buffer using the stamp. Isolated cells were counted and purity was confirmed by flow cytometry before used *in vitro*.

5.8 Isolation of $CD4^+$ T cells

$CD4^+$ T cells were isolated from 8101-immune B6 wild type spleen cells by magnetic cell sorting before used for adoptive T cell transfer. Mice were sacrificed, sprayed with 70 % EtOH and skinned. Spleens were removed from the left flank and squashed with the stamp of a 5 mL syringe through a 45 µm strainer, in a 60 mm dish containing 5 mL RPMI. The cell suspension was transferred into a 50 mL tube. The cell strainer was washed with 10 mL RPMI and also transferred into the same tube. After centrifugation (10 min, 350x g), red blood cells were lysed for 3 min with 5 mL TRIS NH_4Cl and then washed with RPMI (30 mL, centrifuged 10 min, 350x g). The cell pellet was incubated with 10 µL (10^7) magnetic beads, resuspended in 90 µL MACS buffer (both volumes adjusted per 1 x 10^7 cells), for 20 min at 4 °C. Afterwards, cells were washed with 5 mL MACS buffer. A LS column was equilibrated with 4 mL MACS buffer and cells suspended in 1 mL MACS buffer were carefully add onto the LS column without the bubble formation. The column was washed once with 5 mL MACS buffer, then taken out of the magnet, placed onto a 15 mL tube and flushed with 5 mL MACS buffer using the stamp. Isolated cells were counted, purity was confirmed by flow cytometry and $CD4^+$ T cells were immediately used for adoptive T cell transfer.

5.9 CRISPR-Cas9-mediated gene knockout

The 6132A *B2m*$^{-/-}$ cell line was generated using CRISPR-Cas9 mediated gene knockout. Single guide (sg) RNAs targeting exon 1 of the murine *B2m* gene were designed with the design tool from the Broad Institute (Doench, Fusi et al. 2016). Corresponding sense and antisense DNA oligomers were compared to earlier publications (Das, Eisel et al. 2017), annealed and cloned over an BbsI side into PX458 as described (Ran, Hsu et al. 2013). The sg RNA 5' CATGGCTCGCTCGGTGACCC – 3' was successfully used to generate the 6132A *B2m*$^{-/-}$ cell line. Parental 6132A cancer cells were transferred into one well of a 6-well plate (1 x 10^5) in 3 mL DMEM containing 10 % FBS. The next day, cells were transfected with calcium phosphate (2.5 mM $CaCl_2$ with 10 µg PX458-B2m plasmid and 50% transfection buffer) and incubated for 6 h before supernatant was renewed. After 42 h, GFP expressing cells were sorted by flow cytometry. Recovered cells were sorted for H-2D^k and H-2K^k MHC class I negative populations and cloned afterwards to establish a pure MHC class I-negative cell line.

5.10 Retroviral transduction of T cells

T cells were engineered to express TCRs via retroviral transduction as described (Engels, Engelhard et al. 2013). Plat-E packaging cells were transfected with the plasmids pMP71-anti-mDDX5, -anti-mNav3, -anti-6132A-A1, -anti-6132A-A4, -anti-6139B-A, -anti-mRPL9 or -anti-mRPL26 by calcium phosphate precipitation. Plat-E were seeded into 6-well plates (3 x 10^5 cells per well) in 3 mL DMEM containing 10 % FBS per well. The next day, the plasmid transfection solution was added (300 µL per well, containing 10 µg corresponding plasmid, 2.5 mM CaCl and 50 % transfection buffer) and incubated for 6 h. The supernatant was renewed and another 42 h later the virus supernatant was harvested. The day before spleen cells were harvested, a 24-well plate had been coated over night at 4 °C with 500 µL PBS containing 1.4 µg/mL αCD3 and 0.2 µg/mL αCD28 per well. Spleens from mice were removed from the left flank and squashed with the stamp of a 5 mL syringe through a 45 µm strainer, in a 60 mm dish containing 5 mL RPMI. The cell suspension was transferred into a 50 mL tube. The strainer was washed with 10 mL RPMI and transferred into the same tube. After centrifugation (10 min, 350x g), red blood cells were lysed for 3 min with 5 mL TRIS NH_4Cl. Cells were washed with RPMI (30 mL, centrifuged for 10 min at 350x g) and counted. The αCD3/αCD28 solution was removed from the coated 24-well plate and 1 mL of spleen cells at a concentration of 3 x 10^6 cells per mL in complete medium (RPMI, 10 % FBS, 2 mM L-glutamine, 1 mM sodium pyruvate, 0.1 mM non-essential amino acids, 100 U/mL penicillin, 100 µg/mL, 50 µM 2-mercaptoethanol and 50 µg/mL gentamycin), supplemented with 40 U/mL recombinant human IL-2 was added into one well. On the next day,

0.5 mL of corresponding virus supernatant, filtrated through a 0.45 µm syringe filter, containing 8 µg/mL protamine sulfate, was added per 24-well and cells were spinoculated (800 x g, 90 min, 32 °C). Overnight at 4 °C, a 12-well plate was coated with 0.5 mL per well RetroNectin at a 12.5 µg/mL concentration. The following day, RetroNectin was removed and the coated 12-well was centrifuged (3000 x g, 90 min, 4 °C) with 1.5 mL per well virus supernatant, filtered through a 0.45 µm syringe filter. Afterwards, virus supernatants were removed and 5 x 10^6 of $CD8^+$ T cells in 2.5 mL complete medium containing 50 ng/mL recombinant human IL-15 or 5 x 10^6 of $CD4^+$ T cells in 2.5 mL complete medium with 40 U/mL IL-2, harvested from the 24-well plate were added and spinoculated (800 x g, 90 min, 32° C). After 48 h, transduction rate was estimated by flow cytometry and T cells were used for adoptive transfer. TCR-engineered $CD8^+$ T cells were maintained for 12 days in complete medium with 17 ng/mL IL-15 before used for *in vitro* assays. TCR-engineered $CD4^+$ T cells were maintained 4 days in complete medium with 40 U/mL IL-2 before used in *in vitro* analysis respectively.

5.11 T cell stimulation

To analyze antigen presentation by cancer and stromal cells, T cells were cocultured for 24 h in 96-well plates with 200 µL medium (RPMI, 10 % FBS, 2 mM L-glutamine, 1 mM sodium pyruvate, 0.1 mM non-essential amino acids, 100 U/mL penicillin, 100 µg/mL, 50 µM 2-mercaptoethanol and 50 µg/mL gentamycin) per well with their specific targets as described before (Engels, Engelhard et al. 2013). $CD8^+$ or $CD4^+$ T cells (5 x 10^4) were added to 1 x 10^5 cancer cells or stromal cells. For TCR-independent stimulation a mixture of plate-coded 8 µg/mL αCD3 monoclonal antibody (mAb) with 2 µg/mL αCD28 mAb were used. Antigen in form of cancer cell lysate loaded on $CD11b^+$ cells isolated from spleen of C3H/HeN cells were performed as previously described (Monach, Meredith et al. 1995, Philip, Schietinger et al. 2010). 6132A or 6139B cancer cells (1 x 10^7 cells/mL in RPMI) were lysed by three cycles of freezing in liquid nitrogen and thawing in a 37 °C water bath and immediately used for digestion and antigen-presentation by $CD11b^+$ cells (1 x 10^5 cancer cell equivalents were added to 1 x 10^5 $CD11b^+$ cells). After 24 h, supernatants were harvested and tested for IFN-γ values by ELISA.

5.12 Enzyme-linked immunosorbent assay (ELISA)

Sandwich ELISA was performed following the manufactures protocol. Immunosorbent 96-well plates were coated over night at 4°C with 50 µL per well of IFN-γ capture antibody used at a 1:1000 dilution in coating buffer. Supernatants were removed and plate was washed three times with 150 µL wash buffer (PBS containing 0.05 % Tween) per well. The plate was blocked with

100 µL ELISA diluent (1 x PBS containing 10 % FBS) per well for 1 h at room temperature. Plates used for co-cultures were spin down (3,000 rpm for 3 min) and 170 µL per well supernatant was transferred into non-sterile, U-bottom 96-well plates and used either immediately or was stored at -20 °C. After blocking, immunosorbent plates were washed three times and 50 µL co-culture supernatant was added per well. IFN-γ standard was prepared in ELISA diluent starting at 2 ng/mL followed by 2-folded dilutions until 31 pg/mL was reached (30 pg/mL represents the detection limit of the used ELISA kit). Plates were incubated over night at 4 °C before washed five times and 50 µL per well of ✔-IFN-γ detection antibody in ELISA diluent as a 1:1000 dilution was added. After incubation for 1 h at room temperature, the plate was washed three times, 50 µL per well of a 1:250 dilution of horseradish peroxidase (HRP)-conjugated αFc antibody was added and the plate was incubated for additional 30 min at room temperature. The plate was washed five times and 50 µL per well of 3,3',5,5'-tetramethylbenzidine (TMB) substrate was added. Colorimetric reaction was observed for 5 min and 25 µL per well 2N H_2SO_4 solution was used to terminate the reaction and absorbance at 450 nm was recorded.

5.14 RNA isolation and reverse transcriptase PCR (RT-PCR)

RNA was isolated using Trizol. Cells were seeded into one well of a 6-well plate. When confluent, cells were washed with 0.5 mL cold PBS, lysed with 1 mL cold Trizol, transferred into a 1.5 mL tube and vortexed thoroughly. After 5 min incubation at room temperature, the tube was centrifuged at 12,000 rpm for 10 min and supernatant (~ 900 µL) was transferred into a new 1.5 ml tube. Chloroform was added (200 µL), vortexed vigorously and incubated for 3 min at room temperature. After 15 min centrifugation at 12,000 rpm (4 °C), the top aqueous layer (~ 500 µL) was transferred into a new 1.5 mL tube. After addition of Isopropanol (500 µL), the tube was inverted three times and incubated for 10 min at room temperature. Centrifugation for 10 min at 12,000 rpm at 4 °C yielded a gel-like RNA pellet. The supernatant was removed, 1 mL 75 % EtOH was added, vortexed and centrifuged for 5 min at 7,500 rpm at 4 °C. The EtOH was removed and the pellet had been air-dried for 30 min at room temperature before it was resuspended in 40 µL RNAse free DEPC-water. After storage over night at 4 °C, the concentration was determined by OD_{260}/OD_{280} absorption. For generation of cDNA, 5 µg RNA was used together with 1 µL $oligo_{18}$ dT primer and brought up with DEPC-water to a final volume of 14 µL. The solution was heated for 5 min at 65 °C and cooled on ice for 2 min. Two µL of 10 mM deoxynucleoside triphosphates (dNTPs) and 4 µL of 5x reaction buffer were then added. The solution had been heated for 2 min at 42 °C before 1 µL reverse transcriptase was added. After 60 min at 42 °C for 60 min, the reaction was terminated at 70 °C for 10 min. The quality of cDNA (200 ng/µL) was determined by

PCR amplification of the housekeeping gene glyceraldehyde 3-phopsphate dehydrogenase (Gapdh) generating a band at 450 bp analyzed by electrophoresis using a 1.0 % agarose gel in TAE.

Table 20. PCR for mouse Gapdh verification.

PCR set up per sample

Reagents	Volume (µL)
5x Buffer GC	5.0
2.5 mM dNTPs	2.5
For Gapdh	1.0
Rev Gapdh	1.0
Phusion Polymerase	0.25
cDNA	1.0
ddH_2O	14.3
Total Volume	25.0

PCR program

Steps	Duration	Temperature	Cycles
1)	2 min	98 °C	1x
2)	30 s	98 °C	30x
3)	30 s	61 °C	
4)	30 s	72 °C	
5)	10 min	72 °C	1x
6)	For ever	4 °C	

5.15 Allele-specific quantitative PCR (qPCR) analysis

Dr. Kazuma Kiyotani at The University of Chicago, now at the Cancer Precision Medicine Center in Tokyo (Japan), designed mDDX5 allele-specific quantitative primers to amplify the mutant region of DDX5 and conducted the qPCR. Two different fluorescent TaqMan probes, VIC and FAM, specific to wild-type and mutated alleles were used. Real-time qPCR was carried out on ABI ViiA 7 system. With the data provided by Dr. Kazuma Kiyotani, the mRNA expression levels were normalized to murine Gapdh (assay Mm99999915_g1) and relative fold change in expression was calculated using the $\Delta\Delta C_T$ method (Livak and Schmittgen 2001).

5.16 Flow cytometry

Flow cytometry was used to determine successful TCR-transduction of either $CD4^+$ or $CD8^+$ T cells, presence of T cells in peripheral blood, cytokine analysis in blood plasma, purity of isolated cells from tumor and spleen and analysis of MHC I loss on cancer cells.

TCR-transduction rate

TCR-transduction rate of lymphocytes was determined by staining of the TCR specific Vβ-chain. Lymphocytes from the same spleen, which were not TCR-transduced, were used as background control. TCR-transduced and background control lymphocytes were suspended and 200 µL were transferred into one well of a U-bottom 96-well plate. Cells were spun down (3 min, 3,000 rpm), supernatant was removed and cells were stained in 50 µL PBS containing antibodies against CD8 or CD4 and against the TCR specific Vβ-chain (see section 4.8 Antibodies). After incubation at 4 °C for 20 min, cells were washed twice with 150 µL PBS before analyzed by flow cytometry.

T cell analysis in peripheral blood

T cell persistence after adoptive T cell transfer was analyzed in peripheral blood. Red blood cells were lysed by adding 1 mL TRIS NH_4Cl, for 10 min at room temperature. Cells were spin down for 30 s at 10,000 rpm, supernatants were removed and cells were resuspended in 50 µL PBS containing αFcR block. After 10 min incubation at 4 °C, cells were washed once with 150 µL PBS (centrifuged at 3 min, 3,000 rpm) and then stained in 50 µL PBS containing antibodies against CD8 or CD4 and against the TCR specific Vβ-chain. After incubation at 4 °C for 20 min, cells were washed twice with 150 µL PBS before analyzed by flow cytometry.

Cytokine analysis from blood plasma and tumor tissue

Cytokine from blood plasma samples was analyzed using LEGENDplex (Biolegend). Samples were not diluted and prepared in a U-bottom 96-well plate. Standard was prepared as a 4-fold dilution, starting at 8,000 pg/mL. Every well contained 25 µL of each reagent: matrix B, standard or sample, assay buffer, cytokine beads and biotin-detection antibodies. The plate shook on a horizontal shaker at 600 rpm for 2 h at room temperature, protected from light. Afterwards, 25 µL streptavidin-PE was added and the plate was incubated for additional 30 min at room temperature (horizontal shaker at 600 rpm, protected from light). The plate was spun down at 1,000x g for 5 min and supernatants (120 µL) were removed using a multichannel pipette. The plate was washed once with 200 µL wash buffer per well (centrifuged for 5 min, 1,000x g), wells were transferred into 1.2 mL micro titer tubes in 200 µL wash buffer and used for analysis by flow cytometry.

Purity of isolated $CD11b^+$, $F4/80^+$ cells and $CD4^+$ T cells

During cell sorting with magnetic beads, 200 µL of cell suspension before and after cell isolation was analyzed for cell enrichment. Cells were spun down for 3 min at 3,000 rpm, were then resuspended in 50 µL PBS containing αFcR block and incubated for 10 min at 4 °C. Afterwards,

cells were washed once with 150 µL PBS before stained for 20 min at 4°C with antibodies against either CD11b, F4/80 or CD4 in 50 µL PBS. Cells were washed twice with 150 µL PBS and analyzed by flow cytometry.

MHC stain

In vitro cultured cells were harvested and 5 x 10^5 cells were stained for 20 min at 4°C in 50 µL PBS containing antibodies against either H2-D^k or H2-K^k. Subsequently, cells were washed twice with 150 µL PBS and analyzed by flow cytometry for MHC class I and II expression. Isotype antibodies were used as background stain.

Analysis of dead endothelial cells

Single cell suspensions from tumor tissue were spun down for 3 min at 3,000 rpm, were then resuspended in 50 µL PBS containing αFcR block and incubated for 10 min at 4 °C. Afterwards, cells were washed once with 150 µL PBS before stained for 20 min at 4°C with antibodies against CD31 and CD146 in 50 µL PBS. Cells were washed twice with 150 µL PBS. Samples were treated with 1:5000 Sytox Blue to differentiate live from dead cells shortly before analysis by flow cytometry.

5.17 Generation and isolation of TCR genes

T cell clones specific for 6132A (Ward, Koeppen et al. 1989, Monach, Meredith et al. 1995), 6139B (Ward, Koeppen et al. 1989, Beck-Engeser, Monach et al. 2001) and 8101 (Dubey, Hendrickson et al. 1997) have been described. TCR sequences from T cell clones were obtained by 5' – RACE-PCR (Life Technologies, Carlsbad, CA, USA) following manufactures protocol, codon optimized (GeneArt, Thermo Fisher Scientific, Waltham, MA, USA) and integrated into the retroviral vector pMP71 using NotI and EcoRI flanked restriction sides as described (Engels, Chervin et al. 2012). The $CD8^+$TCR anti-mDDX5 has been described before (Leisegang, Engels et al. 2016). TCR sequences are detailed in Material section 4. All TCR-encoding pMP71-vectors were provided by Prof. Dr. Matthias Leisegang (Charité - Universitätsmedizin Berlin, Germany).

5.18 Molecular cloning with PX458

The plasmid PX458 encodes the streptococcus pyogenes engineered Cas9 enzyme, needed for CRISPR-Cas9 mediated gene knockout. Gene knockout is likely when exon 1 is targeted (Ran, Hsu et al. 2013)) with 25 bp long, single guide RNAs (sg RNA (Doench, Fusi et al. 2016)). For efficiency, three different sg RNA were designed and flanked by BbsI restriction side ends.

Forward and reverse oligonucleotides were ordered, annealed and phosphorylated using polynucleotide kinase (PNK). Forward and reverse oligonucleotides (1 µL each) were combined with 2 µL PNK, 2 µL adenosine triphosphate (ATP, 10 mM) and 13 µL ddH_2O (20 µL total reaction volume). Annealing program starts with (i) incubation at 37 °C for 30 min, (ii) heating at 75 °C for 10 min, (iii) termination of the reaction for 5 min at 95 °C and cooling to 25 °C at 5 °C intervals per minute. PX458 was digested with BbsI for 1 h at 37 °C, purified from a 1 % agarose gel (9,000 bp band, open plasmid) and then dephosphorylated for 1 h at 37 °C, using alkaline phosphatase (CIP) before purification over a DNA column. The annealed and phosphorylated oligonucleotides were ligated with the opened and dephosphorylated PX458 over night at a 1:1 molecular ratio using Ligase enzyme. Competent bacteria were transformed, colonies expanded and after plasmid isolation insertion of the sg RNA was determined by sequencing.

5.19 Generation of competent bacteria

Competent bacteria were generated with the mix and go transformation kit (Zymo Research). Frozen competent bacteria were scraped with a tip and shook overnight (250 rpm) at 37 °C in 2 mL LB medium under sterile conditions without antibiotics. Then 150 µL were transferred into 50 mL LB medium and shook at 250 rpm (37 °C) until a OD_{600} of 0.2 – 0.5 was reached. Bacteria had been cooled on ice for 10 min before spun down at 4 °C in a 50 mL tube at 3,000 rpm. Supernatant was removed and bacteria were resuspended in 5 mL pre-cooled wash buffer. Bacteria were kept on ice for 10 min and centrifuged (10 min, 3,000 rpm, 4 °C), while sterile 1.5 mL tubes were precooled in a dry ice and EtOH solution. Bacteria were resuspended in 2.5 mL competent buffer and 100 µL were transferred into each tube. Competent bacteria were confirmed by transformation and stocks were stored at -80 °C.

5.20 Transformation of bacteria

Competent bacteria were thawed on ice and 50 ng plasmid were added. After 20 min incubation, bacteria underwent head shock (42 °C, 30 s) and were then cooled 2 min on ice. Bacteria were moved into a 15 mL snap cap tube with 900 µL LB medium and shook at 250 rpm for 60 min (37 °C) before 100 µL were placed onto ampicillin LB plates which incubated over night at 37 °C.

5.21 Plasmid isolation

For one round of TCR-transduction up to 20 µg plasmid were used and high concentrated plasmid stocks (~ 2.0 µg/µL) were made. After bacteria transformation, plasmid mini preparations were done to confirm plasmid sequence before using it for plasmid MAXI preparation.

Mini plasmid preparation

Bacterial colonies were picked with a sterile tip, transferred into a 15 mL snap cap tube containing 2 mL LB medium with 200 µg ampicillin and shook at 250 rpm (37 °C) overnight. Bacteria were transferred into a 1.5 mL tube and spin down at 6,000 rpm for 1 min. Supernatant were removed and plasmid was harvested using the QIAprep Spin Miniprep Kit (Qiagen). Bacteria pellet were resuspended in 250 µL resuspension buffer. Then 250 µL lysis buffer was added, tubes were inverted 2 – 3 times, then 350 µL neutralization buffer was added and tubes were inverted until white precipitation was formed. Tubes were spin down for 10 min at 13,000 rpm, supernatants were transferred onto spin columns and centrifuged for 1 min (13,000 rpm). The flow through was discarded and columns were washed with 750 µL wash buffer (centrifuged for 1 min, 13,000 rpm). Flow through was discarded and columns were dried (1 min centrifugation at 13,000 rpm). Afterwards, the column was placed into a 1.5 mL tube, 35 µL DEPC-ddH_2O was added and columns were incubated for 1 min at room temperature before eluted by centrifugation (1 min, 13,000 rpm). Plasmid was confirmed by sequencing using primers specific for the pMP71 plasmid backbone, all TCRs are encoded on.

Maxi plasmid preparation

Bacteria (500 µL) were transferred into a 1 L Erlenmeyer beaker with 350 mL LB containing 350 µg ampicillin. The bacteria suspension shook over night at 250 rpm (37 °C). Bacteria were transferred into a 500 mL wide mouth Nalgene bottle and spun down for 15 min at 6,000 rpm (4 °C). Supernatants were removed and plasmid was isolated with the NucleoBond Xtra Maxi kit (Macherey-Nagel). Bacteria were resuspended in 12 mL resuspension buffer, transferred into a 50 mL tube, 12 mL lysis buffer were added and solution was incubated on a vertical shaker at 16 rpm for 5 min at room temperature. Afterwards, 12 mL neutralization buffer were added and tubes were inverted until white precipitation was formed before tubes were centrifuged at 4°C for 15 min at 5,000x g. Filters and columns were equilibrated with 25 mL equilibration buffer. Lysed bacteria were transferred onto the filter and went through the column by gravity flow. Filter was washed with 15 mL equilibration buffer, removed and then the column was washed with 25 mL wash buffer. Afterwards, the column was placed onto a 50 mL tube and 15 mL elution buffer was added. Plasmid was precipitated with 10.5 mL isopropanol and tubes were inverted 4 – 5 times, followed by centrifugation at 4 °C for 1 h at 5,000x g. Plasmid pellet was washed with 4 mL 70% EtOH (centrifuged at 4 °C, 10 min, 5,000x g), then air-dried for 20 min at room temperature and resuspended in 250 µL DEPC-ddH_2O. Plasmid was verified by sequencing and concentration was measured by photometry (260 nm).

5.22 Full thickness skin graft

After cervical dislocation of the donor mouse (BALB/cAnN), skin along the dorsal surface was shaved and wiped clean with gauze soaked in 70% ethanol. Around 2 cm^2 sized pieces of the dorsal skin were dissected with blunt scissors. The donor skin dissections were then placed into a petri dish with ice-cold PBS and the underlying fat and connective tissue were scraped away with a new clean single-edged razor blade. Recipients (B6 $Rag^{-/-}$ or C3H $Rag^{-/-}$) were anesthetized using isofluorane inhalation (1-3% delivered in 100% oxygen). Hair was shaved from the dorsum and flanks and the shaved skin was wiped clean with gauze soaked in 70% ethanol. Then, an approximately 2 cm^2 sized full thickness skin dissection from the recipient's dorsum was removed with blunt scissors while preserving the underlying musculus carnosus layer. The graft bed was then covered with the piece of donor skin, positioned so that the hair direction was opposite of the recipient's hair in order to make it easy to distinguish the two types of skin once the graft has healed. Donor skin was secured by suturing (4-0 Polyglycolic acid, absorbable suture) the edge of the graft to the cut edge of the recipient skin, starting with the four corners. For proper healing of the graft, a 2 cm^2 piece of gauze was placed over the graft and held in place by two bandages. Bandages were removed seven days after skin grafting and inspected daily to monitor the graft rejection process. Ten to fourteen days after the skin graft surgery, cancer cells were injected *s.c.* on the opposite flank. Grafts were recorded as rejected when 80% or more of the graft became non-viable.

5.23 Window chamber implantation

C3H $Rag^{-/-}$ were anaesthetized by isoflurane inhalation (1-3% delivered in 100% oxygen). The entire back was first shaved and then remaining hair was removed with remover lotion and Kimwipes. Afterwards the mouse was washed with PBS and rubbed dry to prevent hypothermia. The front plate was used to draw the window position on the back of the mouse and a circle was cut out of the skin. The skin around the hole was separated from muscle tissue with a PBS soaked sterile cotton tip. Suture (5-0 polypropylene) was taken to prepare a loop on either side of the top hole. The top was held by the loops and needles (16G x ½, 0.5 x 16 mm) were inserted to create wholes around the window area needed for insertion of the plate. The plate was prepared with three screws and space holders and oriented such that the sharp, curved end of the back plate faced away from the mouse before inserted into the holes. The front plate was added and fastened with one nut on every screw and the top and bottom part of the plate was sutured. The window area was moistened with PBS and 2,5 x 10^5 6132A-cerulean cancer cells in 100 µL PBS were injected between the fascia and the dermis of the rear skin layer inside the window area with a

bend insulin syringe (31G, 6 mm) on three to four different spots (25 µL per spot). At the end the microscope cover glass was added and 200 µL painkiller (meloxicam) were injected *s.c.*

5.24 Longitudinal confocal imaging

The method of longitudinal confocal microscopy was already described (Schietinger, Arina et al. 2013). For longitudinal *in vivo* imaging mice were anesthetized and positioned on a custom-made stage adaptor. The three screws that are used to hold the window frame also fixed the mouse onto the stage adaptor always in the same position and the window was secured by two mechanical clamps. A motorized microscope XY scanning stage and Leica LAS-AF software allowed recording individual 3-dimensional positions per field-of-view and returning to them later with high precision (stated accuracy ± 3µm; reproducibility < 1.0 µm). Around the microscope was build a custom fit, clear full incubation jacket with temperature control for increased thermal stability and prevention of hypothermia. Blood vessels were used as “landmarks” and could be located within 50 µm on the same day and within 100 µm on the next day. Data were acquired using a Leica SP5 II TCS tandem scanner two-photon spectral confocal microscope (long-working distance 20x/NA 0.45 and 4x/NA 0.16 dry lenses, Olympus). To determine the fraction of area occupied by vessels or cerulean fluorescent cancer cells, acquired images were analyzed using Fiji software (Laboratory for Optical and Computational Instrumentation; University of Wisconsin-Madison, WI). Tumor blood flow was visualized by retro orbital injection of DiD-labeled red blood cells.

5.25 Labelling of red blood cells

Around 100 µL peripheral blood was taken from C3H $Rag^{-/-}$ mice and the blood was washed once with 1 mL PBS (spun down at 5,000 rpm for 5 min). The cell pellet was resuspended in 2 mL DMEM containing 5 % FBS before 20 µL of DiD solution was added (2 mg/mL in 100 % EtOH). Cells were incubated for 30 min at 37 °C on a horizontal shaker and then washed three times with 5 mL DMEM containing 5% FBS. In the end, cells were filtered through a sterile 70 µm cell strainer and injected as 200 µL PBS suspension.

5.26 MHC upregulation by IFN-γ

Cancer cells (1 x 10^5) were transferred into a T25 cell culture flask in 5 mL DMEM + 5 % FBS. On the next day, 25 ng/mL (250 U/mL) recombinant murine IFN-γ (Gray and Goeddel 1983) were add and cells were incubated for 48 h. Then cells were washed once with 0.5 mL 1x PBS, trypsinized

and harvested in 5 mL 1x PBS before used for analysis of MHC expression by flow cytometry. Cells cultured with IFN-γ were used as control.

5.27 Tumor tissue analysis

At day six, seven and eight after adoptive T cell transfer, tumors were isolated and analyzed for IFN-γ and TNF concentrations for dead endothelial cell populations by flow cytometry.

Preparation for cytokine analysis

About 100 mg tumor tissue was transferred with 1 mL 1x PBS into a 15 mL snap cap tube and homogenized for 2 min on ice using a Polytron slowly turning up to full speed (intensity 10). Afterwards, the sample was spun down at 13,000x g for 5 min and supernatants were transferred into a 1.5 mL tube and stored at -20 °C before used for determination of cytokines by flow cytometry using Legendplex.

Preparation for endothelial cell analysis

Tumor fragments were generated and single cell suspensions were made as described in “5.7 Isolation of $CD11b^+$ and $F4/80^+$ cells”. Subsequently, about 1 x 10^7 cells were used for analysis of dead endothelial ($CD31^+$ and $CD146^+$) by flow cytometry.

6. Results

6.1 Tumors grown from a cancer cell clone escape CD8$^+$TCR monotherapy.

In order to test whether tumors with a homogenous mutant neoantigen expression pattern can be eradicated with a single CD8$^+$TCR, B6 Rag$^{-/-}$ mice were injected *s.c.* with the 8101 derived Clone 12 and adoptive transfer of anti mDDX5 CD8$^+$ T cells was performed 30 days later. Of the 11 mice treated, five did not delay tumor outgrowth while initial tumor destruction followed by relapse was observed in six mice (**Figure 11A**). Three escape variants were reisolated and tested for their ability to stimulate mDDX5-specific T cells (**Figure 11B**). Compared to the original 8101 Clone 12, isolate #1 and #2 stimulated IFN-γ release from T cells at reduced levels while isolate #3 no longer stimulated T cells. Consistent with these findings, isolate #1 and #2 had reduced and isolate #3 had lost mDDX5 mRNA expression which was determined by mDDX5-specific qPCR.

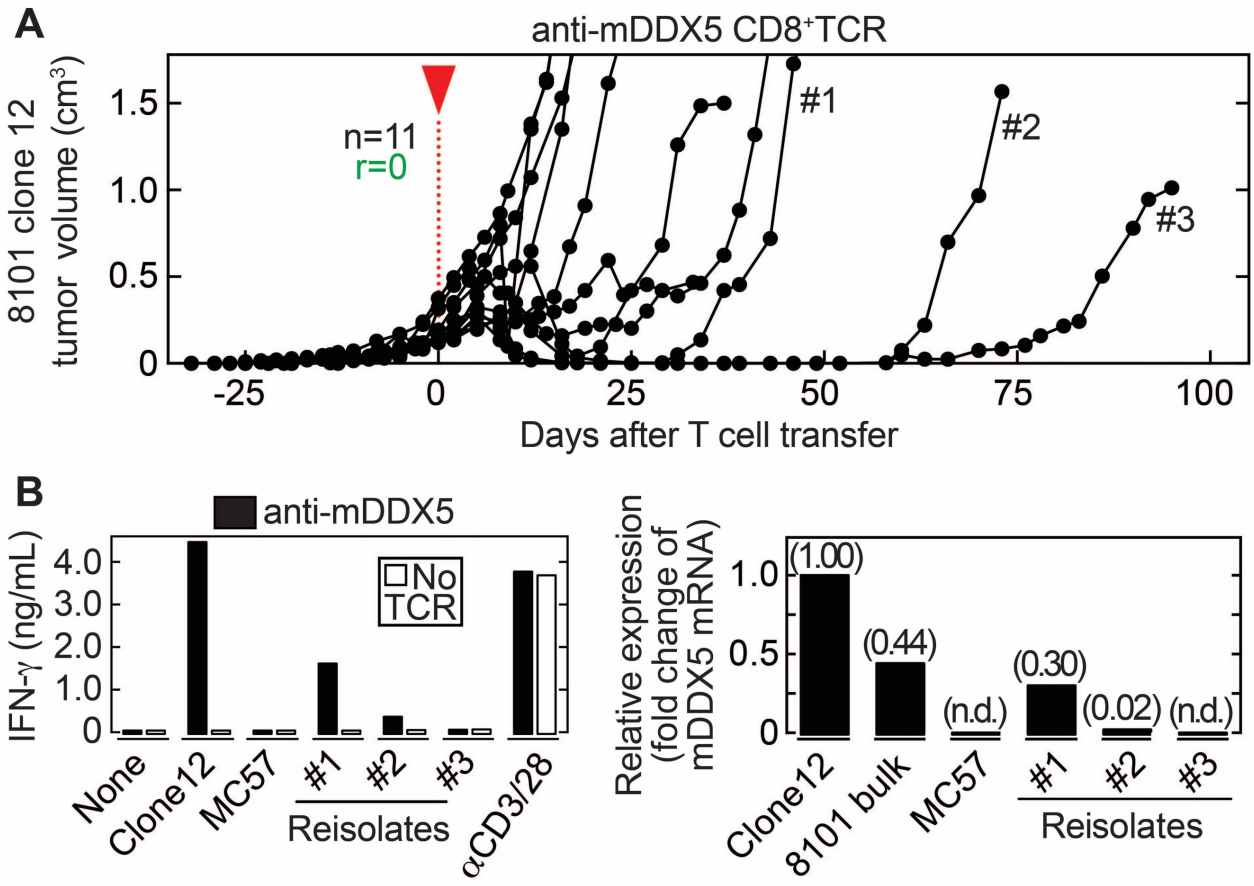

Figure 11. Variants occur when a tumor derived from an 8101 clone is treated with the mDDX5-specific CD8$^+$TCR. (A) C57BL/6 Rag$^{-/-}$ mice bearing established 8101 clone 12 tumors were treated with anti-mDDX5 CD8$^+$TCR-transduced T cells 30 days after cancer cell inoculation as

indicated by the red arrow head (n = 11). Spleen cells from OT-I Rag$^{-/-}$ mice were used as CD8$^+$ T cell source. Average tumor sizes were 196 mm^3 ± 94 mm^3 SD at day of T cell transfer. Three indicated relapsed tumors were reisolated (#1, #2 and #3) and readapted *in vitro*. Indicated are total number of mice (n) of which mice rejected (r) their tumor after adoptive T cell transfer. Shown are data from three independent experiments. **(B)** I*n vitro* analysis of the three reisolates together with the original 8101 Clone 12 and MC57 cancer cells. **Left:** Cancer cells and anti-mDDX5 T cells were cocultured for 24 h and supernatants were analyzed for IFN-γ concentrations by ELISA. No stimulation and TCR independent αCD3/αCD28 stimulation were used as controls. Data are means of duplicates and one representative of two independent experiments is shown. **Right:** RNA was isolated and reverse transcribed. Relative expression (fold change) was calculated using $\Delta\Delta C_T$ method after mDDX5-specific qPCR was conducted (n.d. – not detectable).

6.2 Relapse of a cancer cell clone occurs even when CD8$^+$TCRs target two independent, autochthonous mutant neoantigens.

Since targeting mDDX5 did not led to tumor eradication it was investigated whether targeting another, independent autochthonous mutant neoantigen (mNav3) would achieve tumor elimination. Long-established tumors derived from Clone 12 were treated with anti-mNav3-transduced CD8$^+$ T cells in B6 Rag$^{-/-}$ mice about 25 days after cancer cell injection (**Figure 12**). Similar to what had been observed after the anti-mDDX5 treatment, most mice did not show any anti-tumor effect and had to be sacrificed within 25 days after T cell transfer.

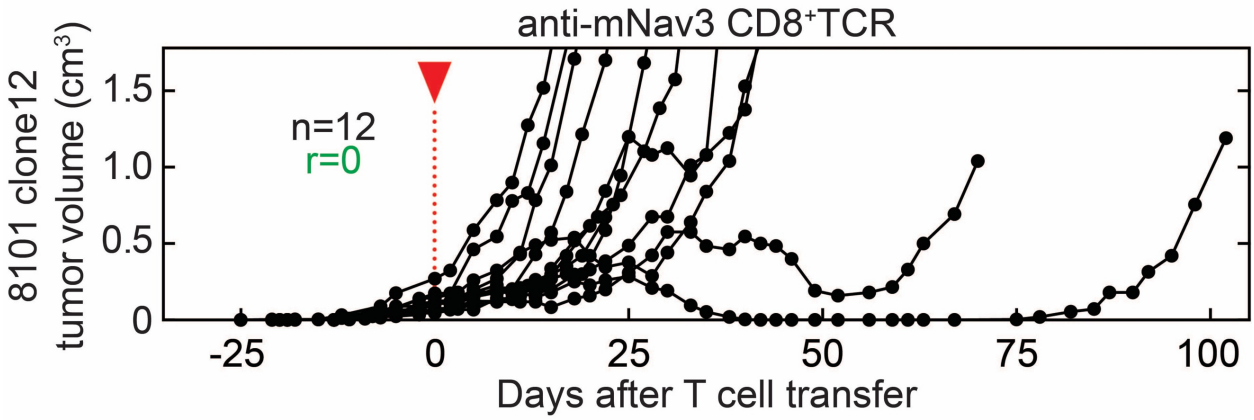

Figure 12. Relapse also occurs when tumors derived from an 8101 clone are treated with the mNav3-specific CD8$^+$TCR. C57BL/6 Rag$^{-/-}$ mice (n = 12) bearing established 8101 Clone 12 tumors were treated with ant-mNav3 CD8$^+$TCR-transduced T cells 25 days after cancer cell inoculation as indicated by the red arrow head. Spleen cells from OT-I Rag$^{-/-}$ mice were used as CD8$^+$ T cell source. Average tumor sizes were 118 mm^3 ± 60 mm^3 SD at day of T cell transfer. Indicated are total mice (n) of which mice rejected (r) their tumor after adoptive T cell transfer. Shown are data from two independent experiments.

Only two mice showed initial tumor destruction, followed by relapse. Targeting two independent mutant neoantigens would be expected to reduce the chance of escape and greatly enhance the likelihood of successful tumor eradication. To test this notion, tumors that had been developed from 8101 Clone 12 were treated 25 days after cancer cell inoculation with a combination of anti-mDDX5- and anti-mNav3-transduced $CD8^+$ T cells (**Figure 13**). Indeed, eight mice treated showed initial tumor destruction and 50 % of mice (n = 4) never relapsed. Nevertheless, tumors relapsed in the other half of the mice demonstrating that even targeting two independent mutant neoantigens against a homogenous cancer cell population is still not sufficient to prevent relapse consistently in all mice.

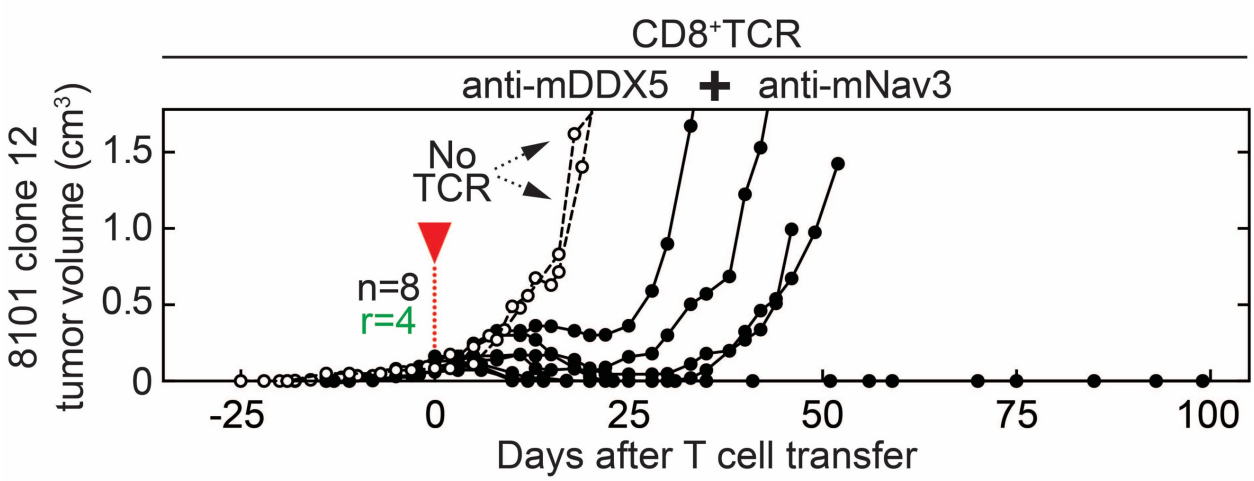

Figure 13. Tumors developed from Clone 12 escape even when $CD8^+$TCR therapy targets two independent mutant neoantigens. C57BL/6 $Rag^{-/-}$ mice bearing established 8101 Clone 12 tumors were treated with $CD8^+$TCR-transduced T cells 25 days after cancer cell inoculation as indicated by the red arrow head. Spleen cells from OT-I $Rag^{-/-}$ mice were used as $CD8^+$ T cell source. Average tumor sizes were 94 mm^3 ± 36 mm^3 SD at day of T cell transfer. Indicated are total mice (n) of which mice rejected (r) their tumor after adoptive T cell transfer. Shown are data from two independent experiments. Mice were treated with a combination of anti-mDDX5 together with anti-mNav3 $CD8^+$TCRs (n = 8). Untreated mice are shown as controls (n = 2).

6.3 Polyclonal spleen cells from $CD4^{-/-}$ mice that had rejected viable cancer cells fail to eradicate tumors in most of the mice.

Targeting more than two independent mutant neoantigens by $CD8^+$ T cells might be needed to eradicate cancers. Therefore, the effect of a polyclonal $CD8^+$ T cell response by which multiple, independent mutant neoantigens could be targeted was tested. Thus, C57BL/6 $CD4^{-/-}$ mice were injected *s.c.* with 1 x 10^7 cancer cells of the original 8101 bulk culture. These viable cancer cells

were rejected which is consistent with a T cell response against multiple, independent antigens. About six weeks after cancer cell injection, mice were challenged with another dose of 1 x 10^7 viable cancer cells of the 8101 bulk cell line. The cancer cells were rejected again and mice were therefore considered to be immune against 8101. Six weeks after cancer cell challenge, the spleen cells of one spleen equivalent from these mice were used for adoptive transfer to treat established 8101 bulk tumors in B6 $Rag^{-/-}$ mice. However, only one mouse rejected the tumor while four mice died of progressing tumors within 25 days after T cell transfer started (**Figure 14**). These data suggest that successful treatment against established tumors with $CD8^+$ T cells alone might be very difficult to achieve, even when the immune $CD8^+$ T cells are polyclonal.

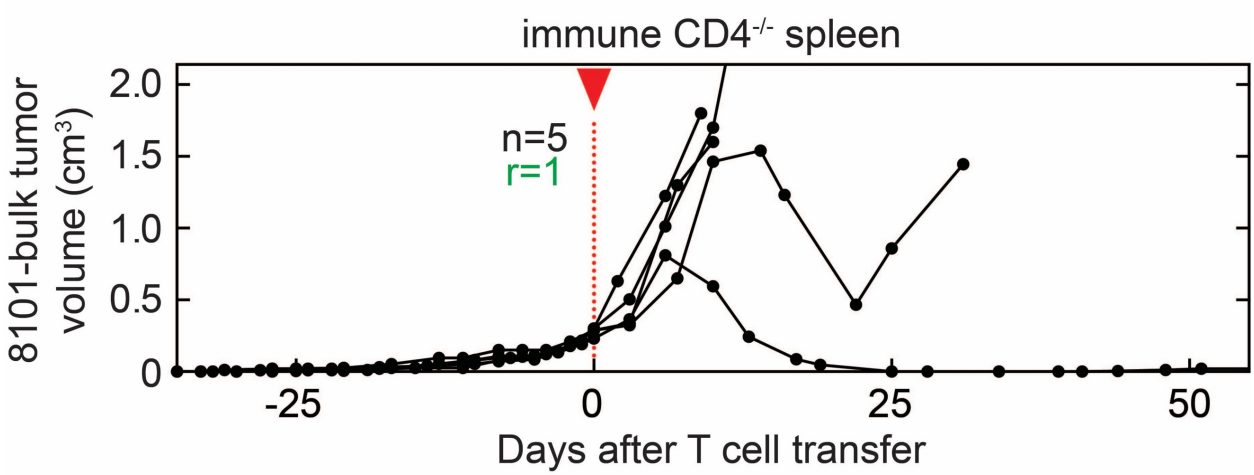

Figure 14. Polyclonal spleen cells from $CD4^{-/-}$ mice fail to eradicate established tumors. 8101 tumor-bearing C57BL/6 $Rag^{-/-}$ mice were treated with ATT 30 days after cancer cell inoculation as indicated by the red arrow head. Average tumor sizes were 281 mm^3 ± 29 mm^3 SD at day of ATT and are summarized from three independent experiments. Indicated are total numbers of mice (n) and how many mice rejected the tumor after T cell transfer (r). C57BL/6 $CD4^{-/-}$ mice that had rejected a challenge of *s.c.* injected viable 8101 cancer cells were considered immune before the cells of the spleen were used for adoptive transfer (n = 5).

6.4 Tumor eradication by adoptive transfer of spleen cells from wild type mice that had rejected a *s.c.* challenge with viable cancer cells.

The inefficiency of $CD8^+$ T cells in rejecting established 8101 tumors could be due to the missing help by $CD4^+$ T cells that might be needed for $CD8^+$ T cell function. Therefore, the effects of spleen cells from C57BL/6 wild type mice was tested. Mice rejected a viable 8101 cancer cell injection *s.c.* (1 x 10^7 cancer cells) and were challenged six weeks later with another dose of 1 x 10^7 viable

8101 cancer cells that were rejected too. As in the previous experimental setting, mice were therefore considered to be immune against 8101 and the spleen cells consisting of one spleen equivalent were used for adoptive transfer in 8101 tumor bearing B6 Rag$^{-/-}$ mice. Indeed, adoptive transfer of these spleen cells eradicated the 8101 tumors in all mice even some very large long-established once. No signs of relapse were observed in any of the five treated B6 Rag$^{-/-}$ mice for over 100 days after T cell transfer (**Figure 15**) which is consistent with the notion that CD4^{+} T cells might be needed for CD8^{+} T cells to eradicate the cancer.

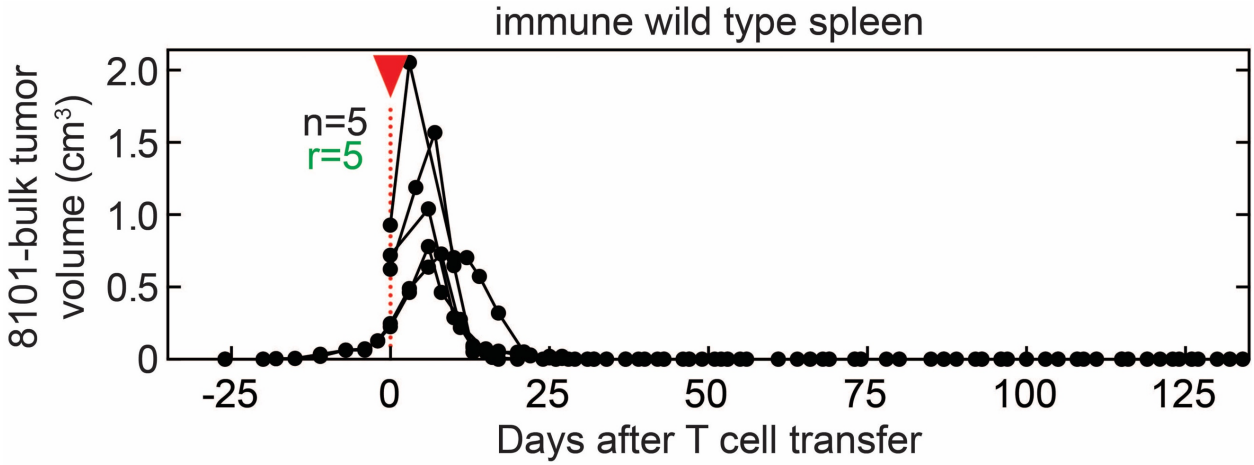

Figure 15. Polyclonal spleen cells from wild type mice eradicate established tumors. 8101 tumor-bearing C57BL/6 Rag$^{-/-}$ mice were treated with ATT 30 days after cancer cell inoculation as indicated by the red arrow head. Average tumor sizes were 549 mm³ ± 306 mm^3 SD at day of ATT and are summarized from three independent experiments. Indicated are total numbers of mice (n) and how many mice rejected the tumor after T cell transfer (r). C57BL/6 wild type mice that had rejected a challenge of *s.c.* injected viable 8101 cancer cells were considered immune before the cells of the spleen were used for adoptive transfer (n = 5).

6.6 One CD8^{+}TCR is sufficient for tumor eradication when combined with a cancer-directed polyclonal CD4^{+} T cell response.

In order to analyze whether a polyclonal CD8^{+} T cell response was required for tumor eradication only anti-mDDX5-transduced T cells were combined with polyclonal CD4^{+} T cells. These T cells target just one MHC class I restricted mutant neoantigen. The source for the polyclonal CD4^{+} T cells were C57BL/6 mice that rejected an injection of 1 x 10^7 viable 8101 cancer cells and were challenged six weeks later with another dose of 1 x 10^7 viable 8101 cancer cells that were rejected as well.

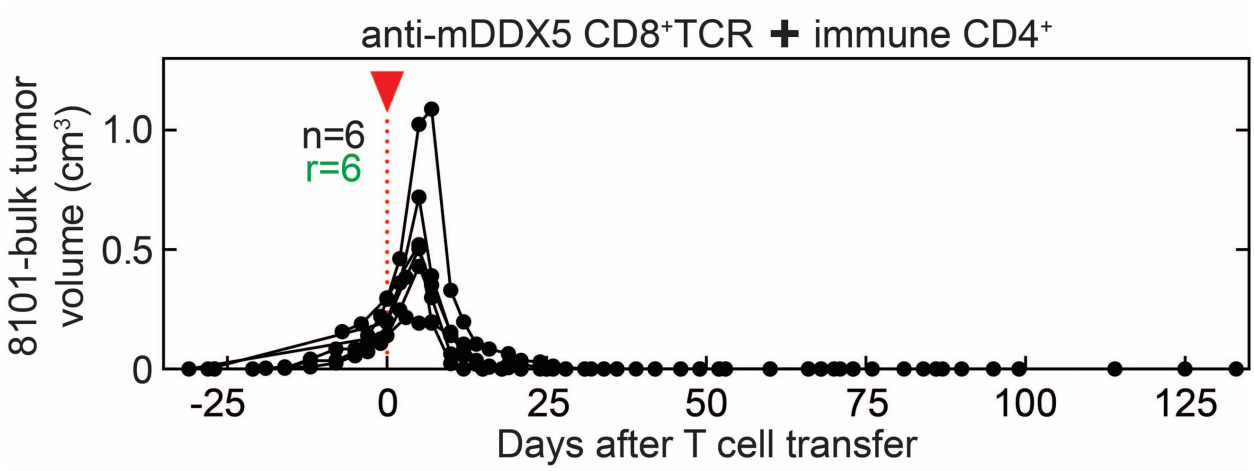

Figure 16. Cotransfer of polyclonal, caner-directed CD4$^+$ T cells together with a single CD8$^+$TCR leads to tumor eradication. 8101 tumor-bearing C57BL/6 Rag$^{-/-}$ mice were treated with ATT 30 days after cancer cell inoculation as indicated by the red arrow head. Average tumor sizes were 211 mm³ ± 70 mm^3 SD at day of ATT and are summarized from three independent experiments. Indicated are total numbers of mice (n) and how many mice rejected the tumor after T cell transfer (r). Spleen cells from OT-I Rag$^{-/-}$ mice transduced with the anti-mDDX5 CD8$^+$TCR were combined with CD4$^+$ T cells isolated with magnetic beads from the spleen of C57BL/6 wild type that had rejected a challenge of *s.c.* injected viable 8101 cancer cells and were considered immune before used (n = 6).

From the spleens of these mice, polyclonal CD4$^+$ T cells were isolated by magnetic beads (99 % purity) and combined with anti-mDDX5-transduced T cells before used for adoptive transfer in 8101 tumor bearing B6 Rag$^{-/-}$ mice. Even under those conditions, combination therapy of one CD8$^+$TCR with polyclonal CD4$^+$ T cells was sufficient to accomplish tumor eradication (**Figure 16**). T cell therapy was as effective as using polyclonal, unseparated spleen cells from immunized C57BL/6 mice (**Figure 15**) because again all treated mice stayed tumor free for over 100 days after T cell transfer and had no signs of relapse.

6.5 Polyclonal spleen cells from CD8$^{-/-}$ mice that had rejected viable cancer cells cause tumor destruction and long-term growth arrest without eradication of the tumor.

To control experiments shown in **Figure 15** and **Figure 16,** it was determined whether CD4$^+$ T cells can cause 8101 tumor elimination on their own. Therefore, C57BL/6 CD8$^{-/-}$ mice were used. These mice were able to reject 1 x 10^7 *s.c.* injected viable 8101 cancer cells and were even protected against another challenge of 1 x 10^7 viable 8101 cancer cells six weeks later suggesting that CD8$^+$ T cells are not required for prevention of 8101 cancer cell outgrowth.

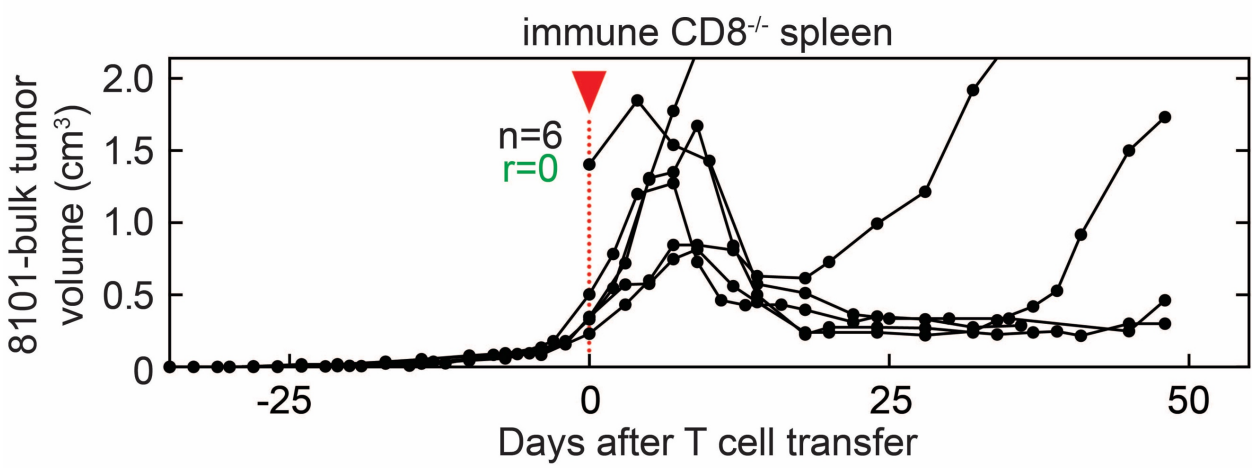

Figure 17. Polyclonal spleen cells from CD8$^{-/-}$ mice cause tumor destruction and growth arrest without eradication. 8101 tumor-bearing C57BL/6 Rag$^{-/-}$ mice were treated with ATT 30 days after cancer cell inoculation as indicated by the red arrow head. Average tumor sizes were 527 mm³ ± 438 mm^3 SD at day of ATT and are summarized from three independent experiments. Indicated are total numbers of mice (n) and how many mice rejected the tumor after T cell transfer (r). C57BL/6 CD8$^{-/-}$ mice that had rejected a challenge of *s.c.* injected viable 8101 cancer cells were considered immune before the cells of the spleen were used for adoptive transfer (n = 6).

Six weeks after the second 8101 cancer cell challenge, the spleen cells from one spleen equivalent were used for adoptive transfer in 8101 tumor bearing B6 Rag$^{-/-}$ mice. Surprisingly, seven to ten days after transfer tumor destruction was observed in five out of six mice treated (**Figure 17**). Furthermore, three out of six mice showed a tumor growth arrest where the tumor became stabilized at a much smaller tumor size for up 50 days after T cell transfer. However, none of the treated mice achieved tumor eradication inferring that CD8$^+$ T cells might be needed for eradication of established tumors.

6.7 One CD4$^+$TCR is sufficient for tumor destruction and growth arrest.

The above data suggest that established tumors could be destroyed and brought into growth arrest by presumably polyclonal CD4$^+$ T cells from mice that have rejected a *s.c.* challenge with live cancer cells. It was not resolved whether multiple MHC class II-restricted mutant neoantigens have to be targeted to get a tumor-destructive CD4$^+$ T cell effect. Therefore, the tumor response of anti-mRPL9 CD4$^+$ T cells targeting a single mutant neoantigen in the 6132A tumor model were investigated. Spleen cells from C3H CD8$^{-/-}$ mice were used as T cell source and were transduced with the anti-mRPL9 CD4$^+$TCR before adoptively transferred.

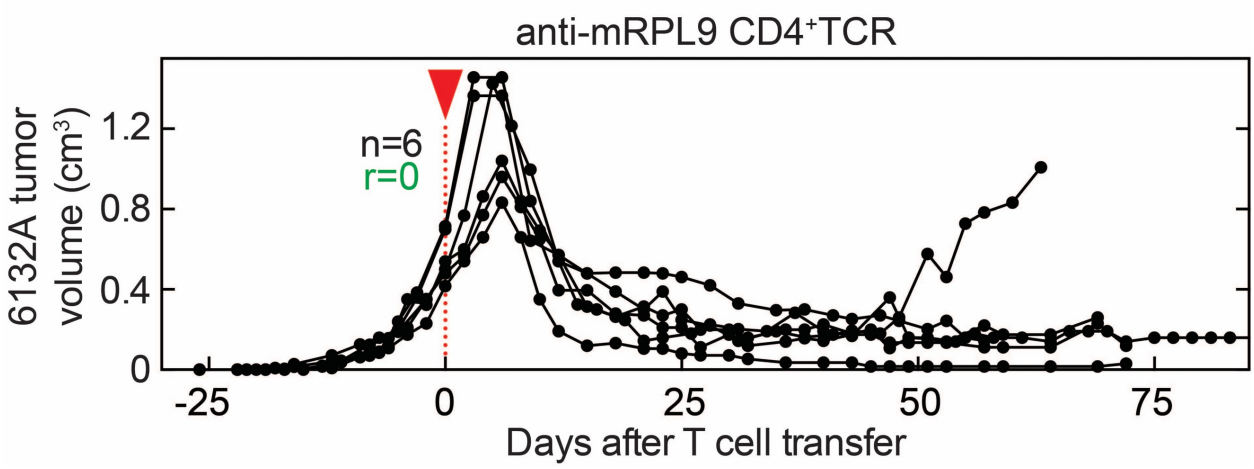

Figure 18. One CD4$^+$TCR is sufficient for tumor destruction and causes growth arrest. Spleen cells from C3H CD8$^{-/-}$ mice were used as CD4$^+$ T cell source for anti-mRPL9 CD4$^+$TCR-transduction. 6132A tumor-bearing C3H Rag$^{-/-}$ mice were treated with TCR-transduced T cells 25 days after cancer cell injection as indicated by the red arrow head. Average tumor sizes were 558 mm³ ± 122 mm^3 SD at day of ATT. Indicated are total numbers of mice (n = 6) and how many mice rejected the tumor after T cell transfer (r = 0) and are summarized from three independent experiments.

Indeed, when 6132A tumor bearing C3H Rag$^{-/-}$ mice were treated with anti-mRPL9-transduced CD4$^+$ T cells 25 days after cancer cell inoculation tumors shrunk in all mice between day seven and ten (**Figure 18**). Subsequently, tumors were kept at a much smaller tumor volume in all mice and in five out of six mice the growth arrest was monitored for even more than 50 days after T cell transfer. The growth arrest of 6132A tumors without eradication showed high similarities to the observations in the 8101 tumor model (**Figure 17**) and was achieved with targeting just one MHC class II restricted mutant neoantigen.

6.8 CD4$^+$ T cells specific for mRPL9 recognize tumor-stroma derived CD11b$^+$ cells but not cancer cells directly.

Subsequently, it was analyzed which compartment of the 6132A tumor is recognized by CD4$^+$ T cells. Spleen cells of C3H CD8$^{-/-}$ mice were engineered to express the anti-mRPL9-TCR and cocultured with either cancer cell lines or with CD11b$^+$ cells. Interestingly, anti-mRPL9 T cells did not release IFN-γ when stimulated with 6132A cancer cells nor when stimulated with other C3H cell lines (**Figure 19A**).

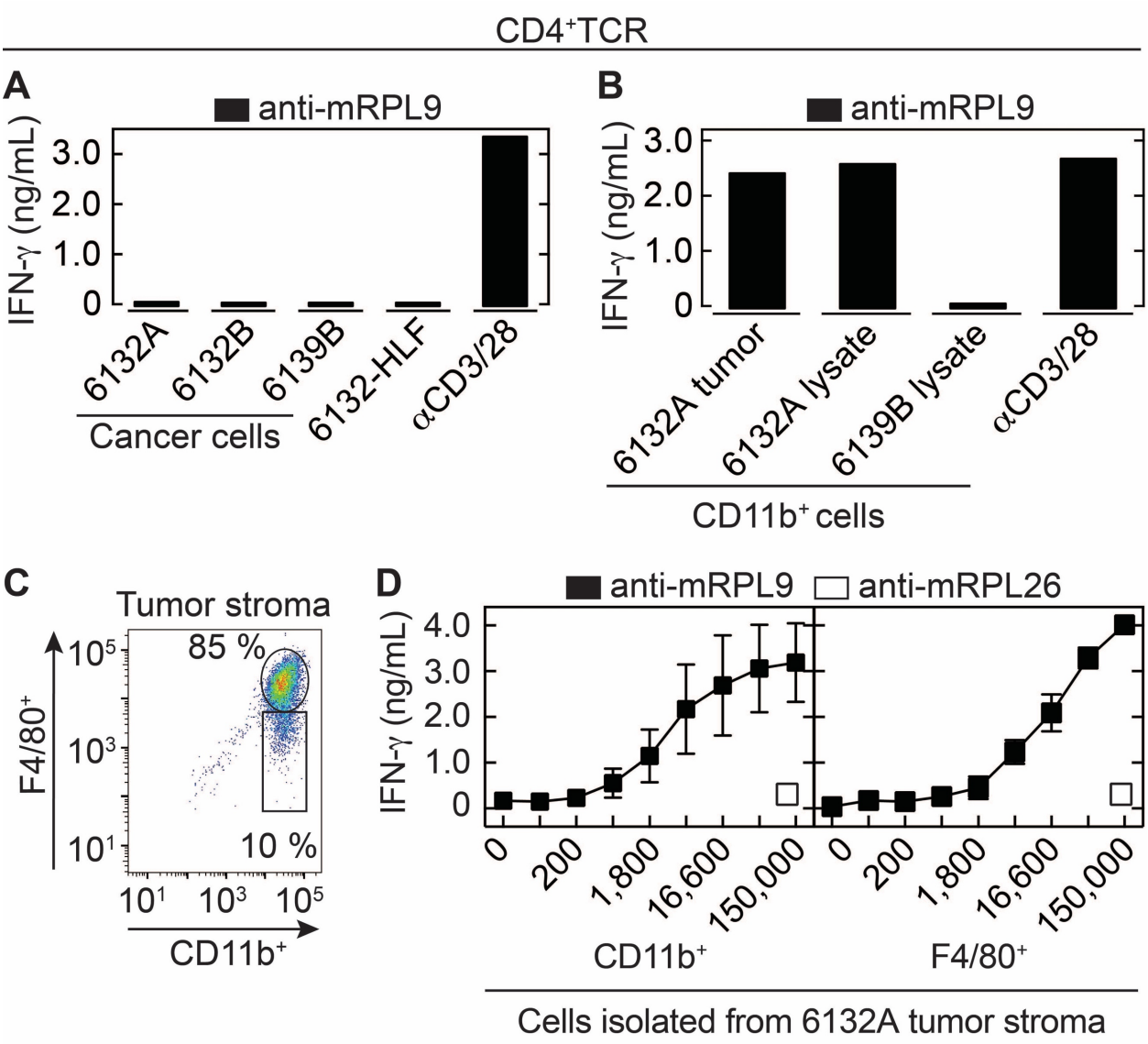

Figure 19. mRPL9-specific CD4$^+$ T cells recognize tumor stroma but not cancer cells directly. Spleen cells from C3H CD8$^{-/-}$ mice were used as source of CD4$^+$ T cells and were transduced with the anti-mRPL9 CD4$^+$TCR. T cells were cocultured for 24 h and supernatants were analyzed for IFN-γ concentrations by ELISA. **(A)** Neither the 6132A cancer cell line naturally expressing mRPL9 nor any of the various *in vitro* cultured cancer cell lines and heart-lung fibroblasts (HLF), generated as autologous tissue control, used as stimulators were recognized. Data are means of duplicates and shown is one representative out of 3 independent experiments. **(B)** In contrast, CD11b$^+$ cells isolated from 6132A tumors grown in C3H Rag$^{-/-}$ mice were recognized. In addition, CD11b$^+$ cells isolated from the spleen of tumor-free C3H/HeN mice cultured with 6132A cancer cell lysates but not with 6139B cancer cell lysates were also recognized. For TCR-independent T cell stimulation αCD3/αCD28 was used. Data are means of duplicates and shown is one representative out of 3 independent experiments. **(D)** Proportion of F4/80$^+$ cells of bulk CD11b$^+$ cells isolated from a 6132A tumor analyzed by flow cytometry. **(D)** CD11b$^+$ and F4/80$^+$ stroma cells isolated from 6132A tumors grown in C3H Rag$^{-/-}$ mice were recognized similarly. Open boxes represent the level of IFN-γ released by CD4$^+$ T cells that were transduced with a CD4$^+$TCR against the mutant ribosomal protein L26 (anti-mRPL26) as controls. Data are summarized from three independent experiments and are means ± SD.

Instead, stromal CD11b$^+$ cells isolated from 6132A tumors grown in C3H Rag$^{-/-}$ mice were able to stimulate T cells to release IFN-γ (**Figure 19B**). In addition, CD11b$^+$ cells isolated from spleen of tumor-free C3H wild-type mice when cultured with 6132A cancer cell lysates stimulated mRPL9-specific CD4$^+$ T cells to release IFN-γ while no stimulation was observed by CD11b$^+$ cells cultured with 6139B cancer cell lysates (**Figure 19B**). DC's represent a very small proportion of the CD11b$^+$ cell population but are powerful stimulators of primary immune responses. Therefore, it was also analyzed whether DCs as part of the CD11b$^+$ cell population are the only stimulator of anti-mRPL9 T cells. Thus, F4/80$^+$ cells that describe tumor-associated macrophages (TAMs) and represent around 85 % of CD11b$^+$ cells (**Figure 19C**) isolated from 6132A tumors were isolated and used for stimulation of anti-mRPL9 CD4$^+$ T cells to release IFN-γ. To compare relative stimulatory efficiency of tumor-derived F4/80$^+$ cells with tumor-derived CD11b$^+$ cells, 3-fold dilutions of both cell populations were conducted (**Figure 19D**). Interestingly, F4/80$^+$ and CD11b$^+$ cells stimulate similarly because the EC_{50} value to induce 50 % of the maximum possible IFN-γ release response was around 5,000 cells for both cell types. This comparison shows that stimulation of CD4$^+$ T cells does not depend only on the presence of DCs in the tumor microenvironment because the F4/80$^+$ marker is not expressed by DC's. In order to examine whether CD4$^+$ T cell stimulation was not only TCR dependent but also specific for the mRPL9 peptide, T cells transduced with the mRPL26 specific CD4$^+$TCR were cocultured with high numbers (150,000) of tumor-derived F4/80$^+$ and CD11b$^+$ cells. **Figure 19D** (open squares) shows that only very small amounts of IFN-γ were released. Together, these data indicate that an effective, mutant-neoantigen specific anti-tumor response by CD4$^+$ T cells depends on recognition of cells of the tumor stroma which take up and process mutant neoantigens. Thus, effective tumor destruction by CD4$^+$ T cells may not require direct cancer cell recognition.

6.9 CD4$^+$ T cell cause death of endothelial cells and regression of tumor vasculature.

Since anti-mRPL9 CD4$^+$ T cells do not recognize 6132A cancer cells directly but tumor stroma, the *in vivo* effects that cause tumor destruction were investigated. It was postulated that cytokines might have a high intratumoral concentration shortly before tumors start to shrink and that this could be one reason for tumor destruction. From the tumor growth kinetics shown in **Figure 18**, it was known that tumors start to shrink around seven to ten days after adoptive T cell transfer.

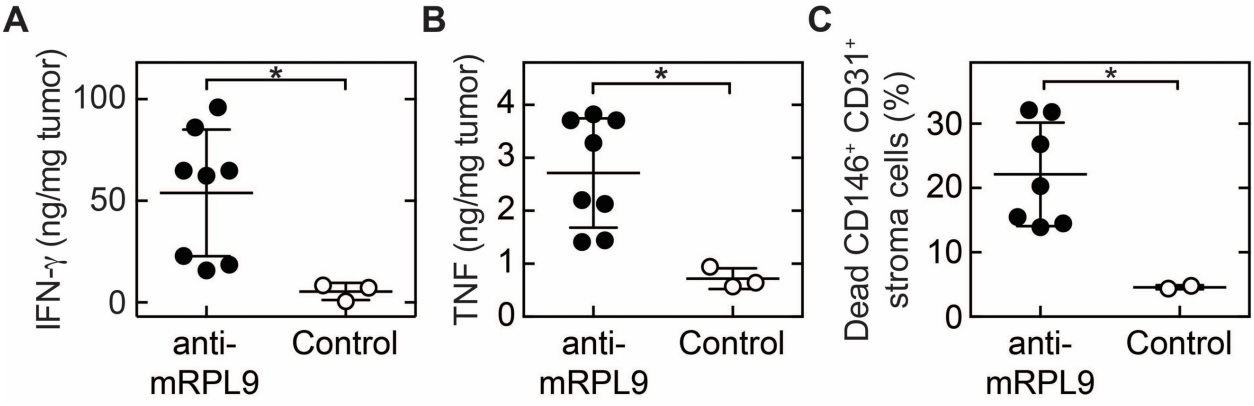

Figure 20. CD4$^+$ T cells release high amounts of IFN-γ and TNF and cause death of endothelial cells. (A – C) 6132A tumor bearing mice were treated 25 days after cancer cell injection with anti-mRPL9 CD4$^+$ T cells. Tumor tissue was analyzed on day six, seven and eight after T cell transfer. Control tumors received either no T cell transfer (n = 1) or anti-mRPL26 CD4$^+$ T cells (n = 2) and were analyzed eight days after ATT. **(A)** IFN-γ and **(B)** TNF concentrations were analyzed by flow cytometry from n = 8 mice and are means ± SD from two independent experiments. **(C)** Single cell suspension from isolated tumors were analyzed for dead CD146 and CD31 double positive cell populations (n = 6). Results are means ± SD from two independent experiments. The significance between the two groups was determined by a two-tailed Student's t-test with $*P \leq 0.05$.

Therefore, 6132A tumor bearing Rag$^{-/-}$ mice that were treated 25 days after cancer cell injection with anti-mRPL9 T cells were sacrificed six, seven and eight days after T cell transfer and tumors were analyzed for cytokine concentrations (IFN-γ and TNF) and dead cells of the stroma (**Figure 20**). As controls, 6132A tumor-bearing Rag$^{-/-}$ mice received either no treatment or were treated with anti-mRPL26-transduced T cells and tumors were analyzed eight days after T cell transfer. Tumors from anti-mRPL9 treated mice had IFN-γ values that were on average 50x times higher compared to the control tumors (**Figure 20A**), whereas TNF values were on average 2.8x higher (**Figure 20B**). During analysis of cells of the tumor stroma, it was found that a significant part of the CD146 and CD31 double-positive cell population was dead (on average about 22 %) in anti-mRPL9 CD4$^+$ T cell-treated tumors compared to the controls (**Figure 20C**). The CD146 and CD31 double-positive cells represent endothelial cells that built the lumen of blood and lymphatic vessels. Therefore, it was investigated whether death of endothelial cells correlates to regression of tumor vasculature and the function and the appearance of tumor vasculature following adoptive T cell transfer was examined. Thus, beginning at day four after anti-mRPL9 CD4$^+$ T cell transfer, 6132A tumor bearing C3H Rag$^{-/-}$ mice were injected with DiD-labelled erythrocytes and were followed up by longitudinal confocal microscopy imaging. Tumor areas were randomly chosen before T cell transfer started and vascularity was followed up for one week.

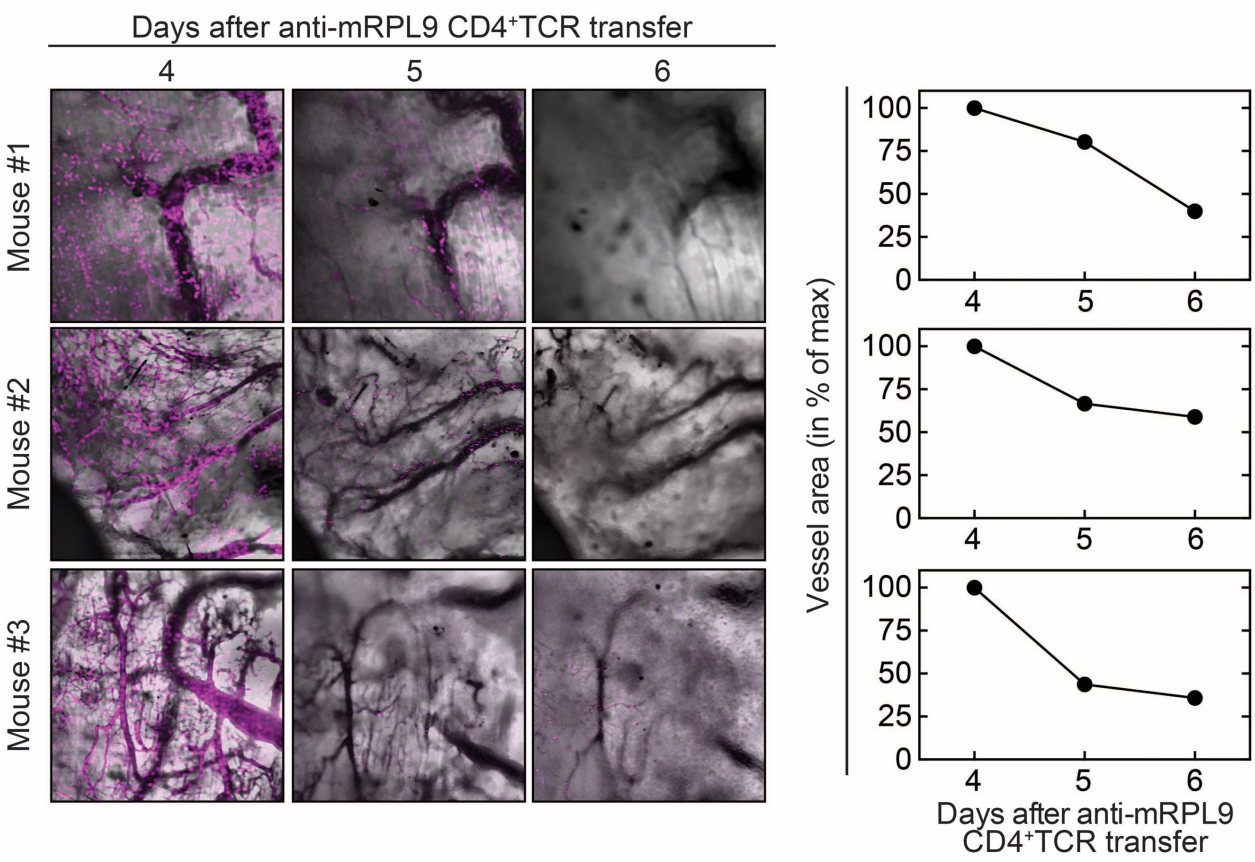

Figure 21. Regression of tumor vasculature by CD4$^+$ T cells. Longitudinal confocal microscopy imaging of tumor vessel reduction in 6132A tumor bearing C3H Rag$^{-/-}$ mice five days after anti-mRPL9 CD4$^+$ T cell treatment (n = 3). Part of the image area (in pixels) that was covered by vessels (black) was set to 100 % vessel area one day before vessel regression was observed and the following days were assigned as percentage of maximum vessel area coverage. To analyze vessel function, mice were injected retro orbital with DiD-labelled (magenta) erythrocytes four days after T cell transfer. Image analysis was performed using Fiji.

Indeed, major effects on tumor vasculature (shown in black) was observed at day five and six after T cell transfer in three mice. **Figure 21** shows that no effects on tumor vasculature and function were noticeable during the first four days following T cell transfer, but within additional two days a major reduction of blood flow and reduction of vessel area was observed. Reduced DiD signal on day five and no DiD signal on day six after T cell transfer was examined. The area covered by vessels regressed on average by 50 % on day 6 compared to day 4 after T cell transfer.

6.10 MHC class II expression on cancer cells is not induced by IFN-γ *in vitro*.

Cytokines such as IFN-γ are able to induce and upregulate MHC class I and II expression in cancer cells which suggests that cancer cells could also be recognized directly by mRPL9-specific T cells. Therefore, it was investigated whether 6132A cancer cells that are exposed to IFN-γ *in vitro* upregulate expression of the mRPL9-restricted MHC class II molecule I-E^k. Cultures of 6132A cancer cells were exposed to IFN-γ for 48 h before expression of surface MHC class I and II was analyzed by flow cytometry (**Figure 22**). The detected signal indicated as mean fluorescence intensity (MFI) increased ten-fold for staining of the MHC class I molecule H-$2K^k$ and 24-fold for staining of the H-$2D^k$ molecule after exposure to IFN-γ. In contrast, neither a signal above background could be detected from the I-E^k MHC class II stain compared to the isotype control nor an increase in signal was observed after IFN-γ exposure on 6132A cancer cells. By comparison, $CD11b^+$ cells from peripheral blood of C3H $Rag^{-/-}$ mice were stained positive for all analyzed MHC class I and II haplotypes.

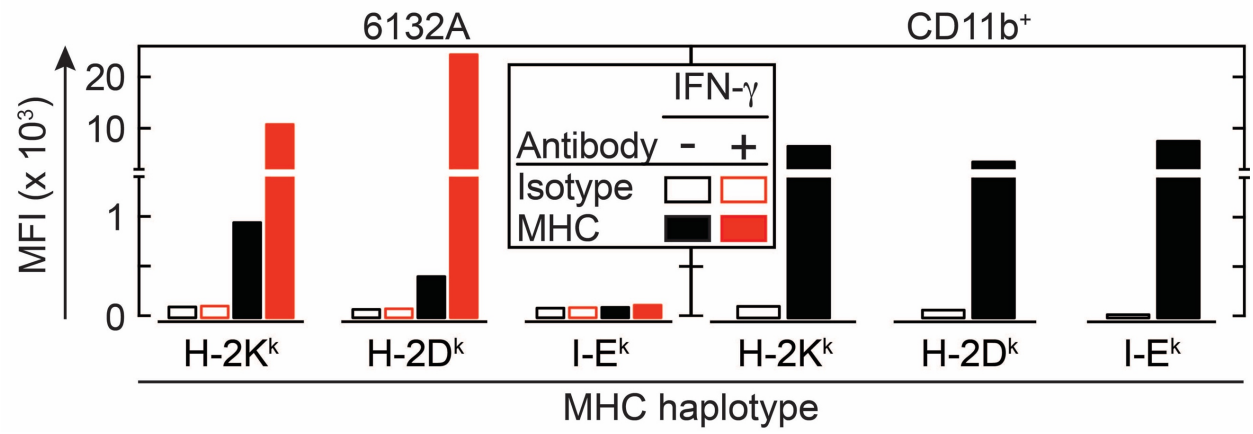

Figure 22. 6132A cancer cells do not upregulate MHC class II expression after exposure to IFN-γ *in vitro*. 6132A cancer cells were cultured for 48 h with or without 25 ng/mL IFN-γ (250 U/mL) before MHC class I and II molecules were stained and analyzed by flow cytometry. In addition, peripheral blood from C3H $Rag^{-/-}$ mice was taken and $CD11b^+$ cells were also stained and analyzed for MHC class I and II molecules. Isotype antibodies were used as background stain controls.

6.11 Stroma recognition of the $CD4^+$TCR T cell is required for tumor destruction.

It could be argued that *in vivo* other mechanisms than IFN-γ are present that can induce MHC class II upregulation in cancer cells. Thus, it is unknown whether tumor destructive effects by

mRPL9-specific T cells depend on stroma recognition. For that reason, 6132A cancer cells were injected *s.c.* into B6 Rag$^{-/-}$ mice. The stroma from B6 mice does not express the MHC class II haplotype I-E^{k} and can therefore not be recognized by mRPL9-specific T cells whereas 6132A cancer cells possess the gene to express the correct MHC class II haplotype I-E^{k}. If direct recognition of 6132A cancer cells *in vivo* is sufficient to cause tumor destruction by mRPL9-specific T cells, then the same tumor growth kinetics as shown in C3H Rag$^{-/-}$ mice (**Figure 18**) would be observed in B6 Rag$^{-/-}$ mice. Furthermore, in order to prove that the CD4^{+} T cells used for adoptive transfer were functional upon recognition of the correct MHC class II haplotype, a system that includes a positive control and that shows the hypothesized outcome that CD4^{+} T cells are stroma dependent was developed (**Figure 23**). Spleens of TCR75-transgeneic mice that express an MHC class II I-A^{b} dependent anti-BALB/c CD4^{+}TCR were used for anti-mRPL9 CD4^{+}TCR transduction (see Introduction section 3.4.3 Research Approach for more detailed information). In addition, mice received a full thickness BALB/c skin graft on one flank and 6132A cancer cells on the other.

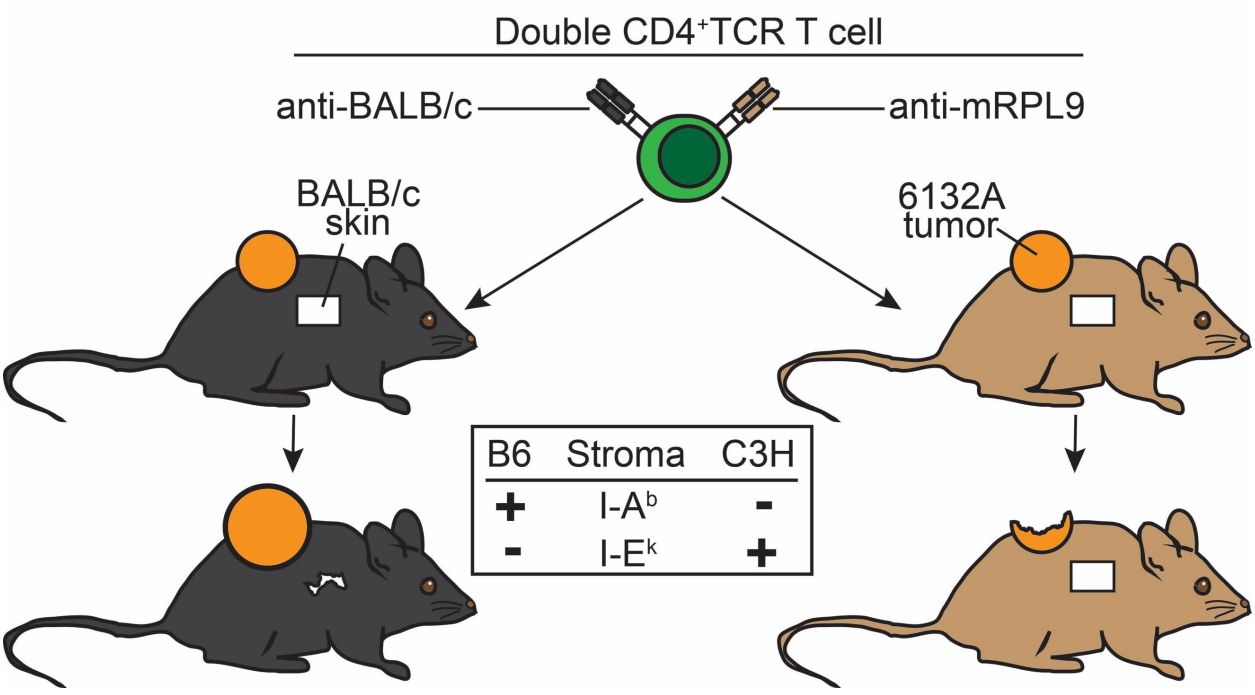

Figure 23. Experimental design to prove that activation of CD4^{+} T cells is stroma dependent. Mice receive a BALB/c full thickness skin graft in addition to 6132A cancer cells. Spleens of TCR75-transgenic B6 mice will be transduced with the anti-mRPL9 CD4^{+}TCR before used for adoptive T cell transfer. B6 mice possess the correct stroma for the anti-BALB/c CD4^{+}TCR which leads to skin graft rejection. C3H mice possess the correct stroma for the anit-mRPL9 CD4^{+}TCR which causes tumor destruction.

In one situation, 6132A tumor-bearing B6 Rag$^{-/-}$ mice that also have a BALB/c skin receive a T cell population that expresses both an anti-BALB/c and an anti-mRPL9 CD4^{+}TCR, the BALB/c skin will be rejected but the 6132A tumor grows out. In the control situation, where 6132A tumor bearing C3H Rag$^{-/-}$ mice that also harbor a BALB/c skin graft are used, the same T cell population will cause 6132A tumor destruction while the BALB/c skin will not be rejected. Indeed, 6132A tumor-bearing and BALB/c skin grafted B6 Rag$^{-/-}$ mice that were treated with T cells that express both anti-BALB/c and anti-mRPL9 CD4^{+}TCRs reject the BALB/c skin graft around 17 days after T cell transfer (**Figure 24**). Shown is the healthy BALB/c skin at day of adoptive T cell transfer that becomes red and necrotic over time until it eventually falls off leaving only a scar behind. At the same time, all three mice tested developed large 6132A tumors and had to be sacrificed due to high tumor burden. None of the mice ever showed visible or measurable effects of tumor destruction even though the used T cells expressed the anti-mRPL9 CD4^{+}TCR and were functionally *in vivo* because the BALB/c skin graft was rejected. As expected in the control experiment, the 6132A tumor-bearing and BALB/c skin grafted C3H Rag$^{-/-}$ mouse, which was also treated with T cells that express both anti-BALB/c and anti-mRPL9 CD4^{+}TCRs, did not reject the BALB/c skin graft (**Figure 25**).

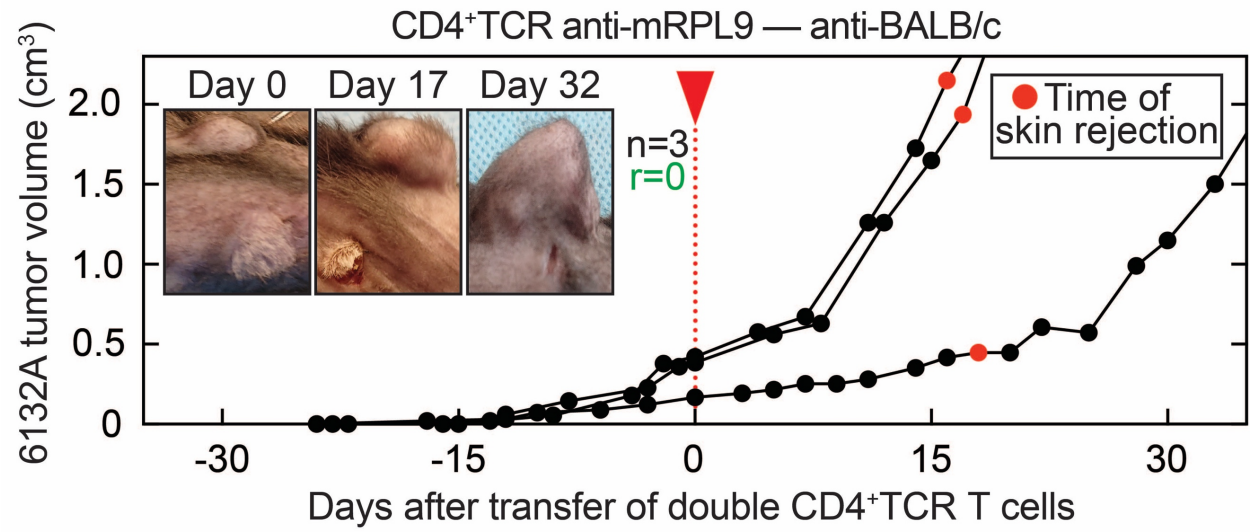

Figure 24. CD4^{+} T cells are stroma dependent and therefore cause BALB/c skin graft rejection and no tumor destruction in B6 mice. B6 Rag$^{-/-}$ mice received a full thickness BALB/c skin on one flank and were injected *s.c.* with 6132A cancer cells on the other flank. Mice (n = 3) are summarized from three independent experiments and received adoptive T cell transfer around 25 days after cancer cell injection as indicated by the red arrow head. Average tumor sizes were 324 mm³ ± 136 mm^3 SD at day of adoptive T cell transfer. Spleen cells from TCR75-transgenic mice used as anti-BALB/c CD4^{+} T cell source were transduced with the anti-mRPL9 CD4^{+}TCR before adoptively transferred. Red dots indicate the day on that more than 80 % of the BALB/c skin graft was rejected. The course of skin graft rejection is also exemplified by the pictures from one mouse.

Instead, the 6132A tumor was destroyed and kept in a tumor growth arrest comparable to experiments shown in **Figure 18**. The tumor became large and ulcerated before collapsing and leaving a viable tumor rim with a necrotic center behind while the BALB/c skin stayed intact the whole follow up period. This time, no skin graft rejection was observed even though the used T cells expressed the anti-BALB/c $CD4^+$TCR and were functionally *in vivo* because tumor destruction occurred. In summary, these experiments show that $CD4^+$ T cells act stroma dependent because the BALB/c skin is only rejected in the B6 stroma background and tumor destruction only appeared in the C3H stroma background. Furthermore, it demonstrates that stroma recognition by mRPL9-specific $CD4^+$ T cells is essential for destruction of 6132A tumors because recognition of 6132A cancer cells alone, that might be MHC class II positive *in vivo*, was not sufficient (**Figure 24**) to cause the same tumor destructive effect compared to the situation when the correct stroma can also be recognized (**Figure 25**).

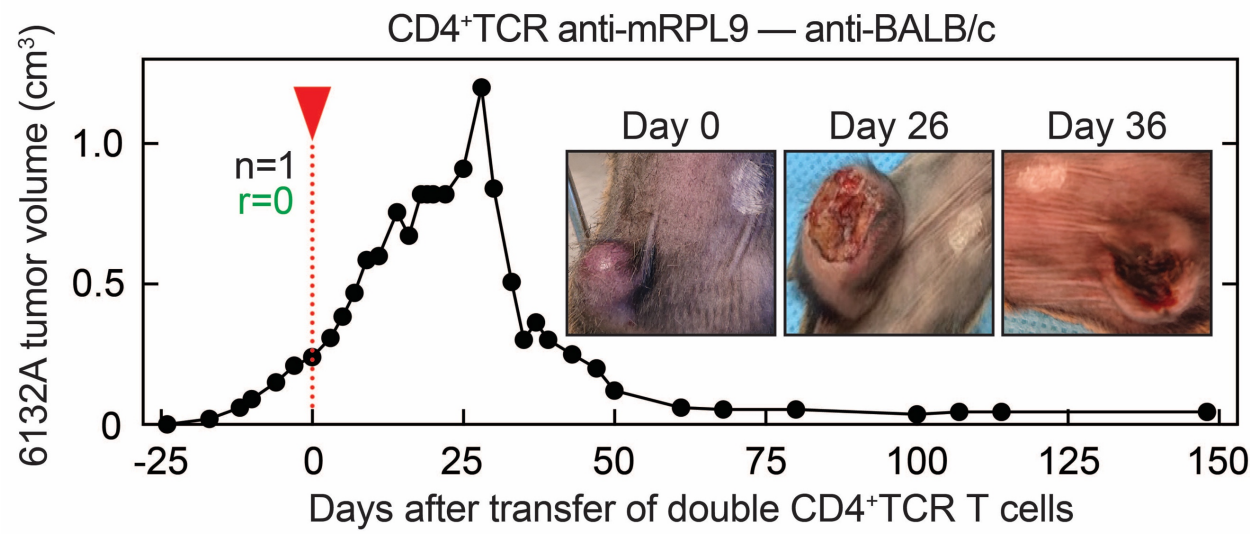

Figure 25. $CD4^+$ T cells are stroma dependent and therefore cause tumor destruction and no BALB/c skin graft rejection in C3H mice. The C3H $Rag^{-/-}$ mouse received a full thickness BALB/c skin on one flank and were injected s.c. with 6132A cancer cells on the other flank. The mouse (n = 1) received adoptive T cell transfer 25 days after cancer cell injection as indicated by the red arrow head. Tumor size was 240 mm^3 at day of adoptive T cell transfer. Spleen cells from TCR75-transgenic mice used as anti-BALB/c $CD4^+$ T cell source were transduced with the anti-mRPL9 $CD4^+$TCR before adoptively transferred. The course of tumor destruction is also exemplified by pictures that also indicate integrity of the BALB/c skin.

6.12 CD4$^+$ T cells persist long term *in vivo* during tumor growth arrest.

Since 6132A tumors persist at a small size for months after destruction by CD4$^+$ T cells, it was investigated whether CD4$^+$ T cells are detectable during this whole time. Thus, peripheral blood was taken from 6132A tumor bearing C3H Rag$^{-/-}$ mice either 40 to 50 days or 70 to 80 days after anti-mRPL9 T cell transfer and analyzed by flow cytometry for CD4$^+$, Vβ6$^+$ cell populations that mainly represent the anti-mRPL9 CD4$^+$ T cell population. In all tested mice, it was possible to find the mRPL9-specific CD4$^+$ T cell population even when more than two months had passed after adoptive T cell transfer (**Figure 26**).

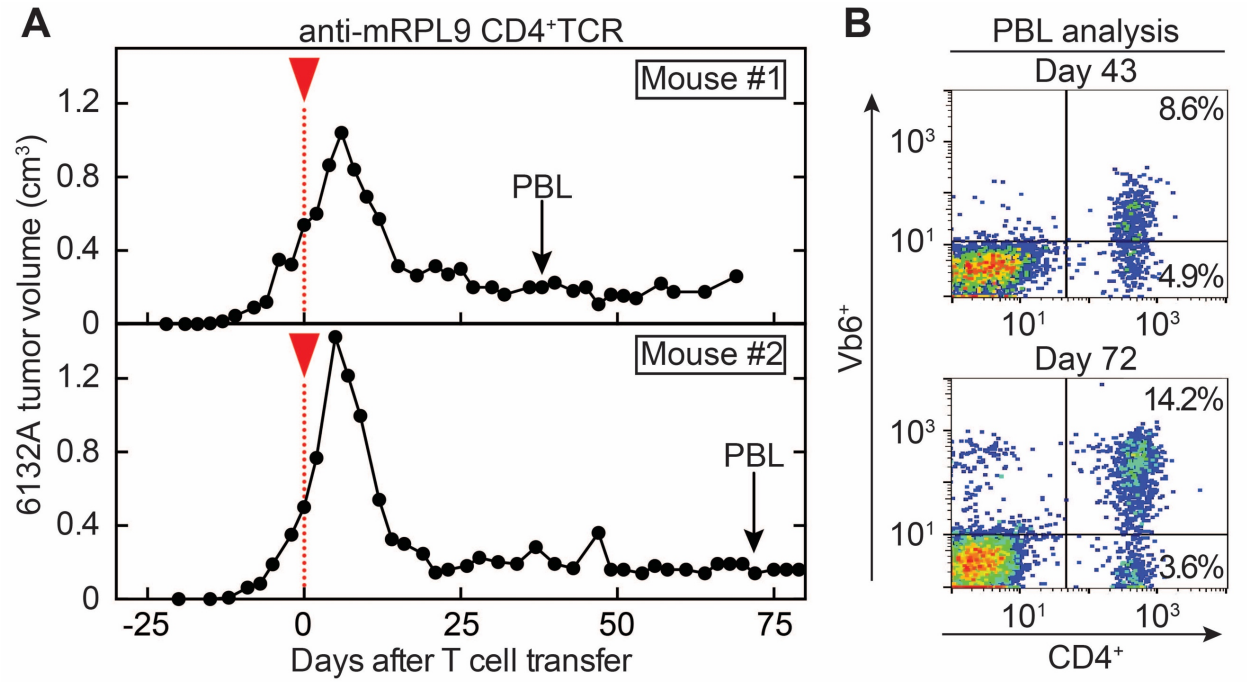

Figure 26. During the stable disease stage of the cancer that follows the destruction of solid 6132A tumors, mRPL9-specific CD4$^+$ T cells are detectable in blood months after adoptive T cell transfer. (A) The points of PBL samplings in relation to the growth kinetics and stage of the cancer in the two mice analyzed for anti-mRPL9 CD4$^+$TCR expression in panel B. Spleen cells from C3H CD8$^{-/-}$ mice were used as CD4$^+$ T cell source for anti-mRPL9 CD4$^+$TCR-transduction. 6132A tumor-bearing C3H Rag$^{-/-}$ mice were treated with TCR-transduced T cells 25 days after cancer cell injection as indicated by the red arrow head. Shown are mice which are also included in Figure 18. **(B)** Flow cytometric detection of anti-mRPL9-transduced T cell population in PBL of mice during stable disease. The upper and lower panels show a detectable population of CD4$^+$ and Vβ6$^+$ cells gated on lymphocytes above the background population of 5 % that is part of the polyclonal spleen cell population from CD8$^{-/-}$ mice. Day 43 (upper panel) shows a representative result from three mice analyzed. On average 11 % were found to be CD4$^+$ and Vβ6$^+$ cells in the PBL samples. On a later time point (lower panel), PBLs were again analyzed for CD4$^+$ and Vβ6$^+$ cells. One mouse was analyzed at day 72 (example shown) and a second mouse was analyzed at day 85 (20 % CD4$^+$ and Vβ6$^+$ cells). Even months after T cell transfer, on average 16 % of PBLs were still CD4$^+$ and Vβ6$^+$ cells.

These findings support that $CD4^+$ T cells participate in the tumor growth-arrest and remain measurable as long as mutant neoantigen persists in the host.

6.13 A $CD8^+$TCR that recognizes both cancer cells and tumor stroma can still be mostly ineffective against established tumors.

It could be argued that the inability of $CD8^+$TCRs to eradicate established solid tumors is unique to the 8101 tumor model and that effects seen by the mRPL9-specific $CD4^+$TCR are not needed in the 6132A model to achieve tumor eradication if 6132A-specific $CD8^+$TCRs are being used. Therefore, the recognition patterns and the *in vivo* effects of the two $CD8^+$TCRs, anti-6132A-A1 and anti-6132A-A4, were investigated in the 6132A tumor model. When spleens from C3H $CD4^{-/-}$ mice were transduced with either of the two $CD8^+$TCRs, they released IFN γ specifically after stimulation with 6132A cancer cells (**Figure 27A**) but not when stimulated with the cancer cell lines 6132B, a cancer cell line which was generated from a second UV-induced tumor on the back of the same 6132 mouse, or 6139B, another syngeneic UV-induced tumor from a different mouse. Furthermore, Heart Lung-Fibroblasts (HLF) generated from the same 6132 mouse as autologous tissue control were also not recognized suggesting that the $CD8^+$TCRs anti-6132A-A1 and anti-6132A-A4 are uniquely specific for the 6132A cancer. Interestingly, $CD11b^+$ cells isolated from 6132A tumors grown in C3H $Rag^{-/-}$ mice also stimulated both $CD8^+$TCRs to release IFN-γ (**Figure 27B)**. However, $CD11b^+$ cells isolated from spleen of tumor-free C3H wild-type mice cultured with 6132A or 6139B cancer cell lysates did not stimulate either of the two $CD8^+$TCRs. As had been done for the $CD4^+$TCR, it was analyzed whether a $CD11b^+$ cell population lacking DCs could also stimulate $CD8^+$TCR-transduced T cells. Thus, $F4/80^+$ cells (TAMs) were isolated from 6132A tumors and stimulatory capacity was compared to tumor-derived $CD11b^+$ cells when 3-fold dilutions were conducted to stimulate anti-6132A-A1 and anti-6132A-A4 T cells to release IFN-γ (**Figure 27C**). As observed for stimulation of $CD4^+$TCR-transduced T cells by stromal cells, $F4/80^+$ cells stimulate as well as unseparated $CD11b^+$ cells. The EC_{50} value to induce 50 % of the maximum possible IFN-γ release response was similar for both cell types (comparison of **Figure 27C** and **Figure 19D**). However, the maximum IFN-γ release response from $CD8^+$TCRs (2 ng/mL IFN-γ, **Figure 27C**) was only half as high as the maximum IFN-γ release response of the $CD4^+$TCR (4 ng/mL IFN-γ, **Figure19D**).

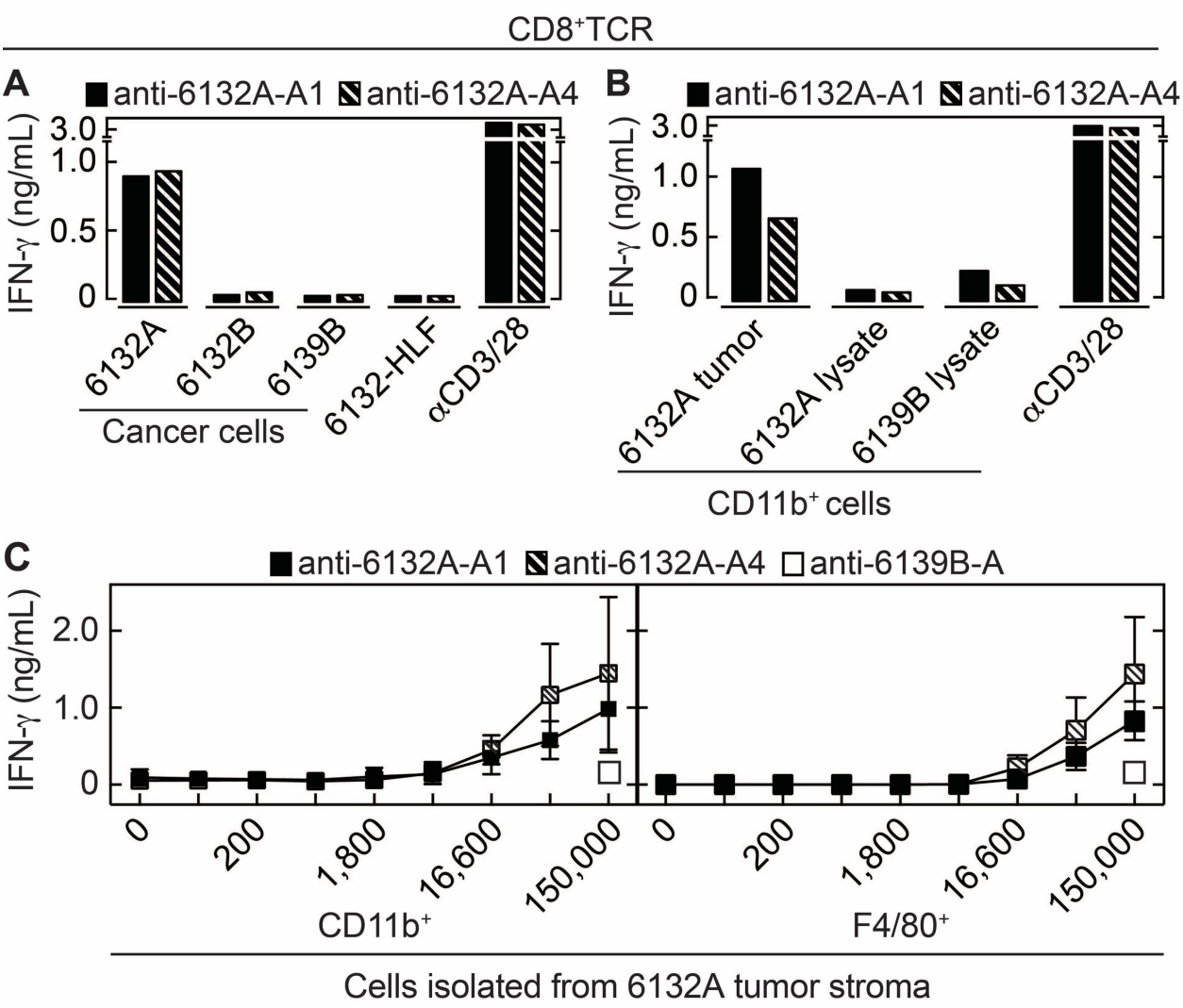

Figure 27. CD8$^+$TCRs recognize both 6132A cancer cells and tumor-stroma cells *in vitro*. Spleen cells from C3H CD4$^{-/-}$ mice were used as CD8$^+$ T cell source and were TCR-transduced before being cocultured for 24 h with indicated targets. Supernatants were analyzed for IFN-γ concentrations by ELISA. For TCR-independent T cell stimulation αCD3/αCD28 was used. Data are means of duplicates and shown is one representative out of 3 independent experiments. **(A)** 6132A-specific CD8$^+$TCR-transduced T cells only recognized 6132A cancer cells but not unrelated cancer cells from independent tumors or HLF generated from the mouse of 6132A origin. **(B)** Only CD11b$^+$ cells isolated from 6132A tumors grown in C3H Rag$^{-/-}$ mice but not from spleen of C3H/HeN wild type mice loaded with cancer cell lysates were recognized. **(C)** Gradually, 3-fold diluted CD11b$^+$ and F4/80$^+$ stroma cells isolated from 6132A tumors grown in C3H Rag$^{-/-}$ mice were recognized similar. Data are summarized from three independent experiments and are means ± SD. Open boxes represent CD8$^+$ T cells that were engineered with a CD8$^+$TCR against 6139B (anti-6139B-A) and show TCR dependent T cell stimulation.

In addition, about ten times more tumor stromal cells were needed to induce similar amounts of IFN-γ (50,000 stromal cells induced a similar IFN-γ response for the CD8$^+$TCR compared to 5,000 stromal cells for the CD4$^+$TCR). T cell stimulation was TCR dependent because T cells

transduced with the anti-6139B-A CD8$^+$TCR cocultured with high numbers of tumor-derived F4/80$^+$ and CD11b$^+$ cells produced IFN-γ concentrations that were comparable to background IFN-γ release from anti-6132A-A1 and anti-6132A-A4 T cells. Together, these data show that the two CD8$^+$TCRs (anti-6132A-A1 and anti-6132A-A4) recognize both cancer cells and tumor-stroma directly. Despite of their ability to recognize both tumor compartments, in contrast to the CD4$^+$TCR, CD8$^+$TCR-transduced T cells had only modest tumor destructive effects *in vivo* (**Figure 28**).

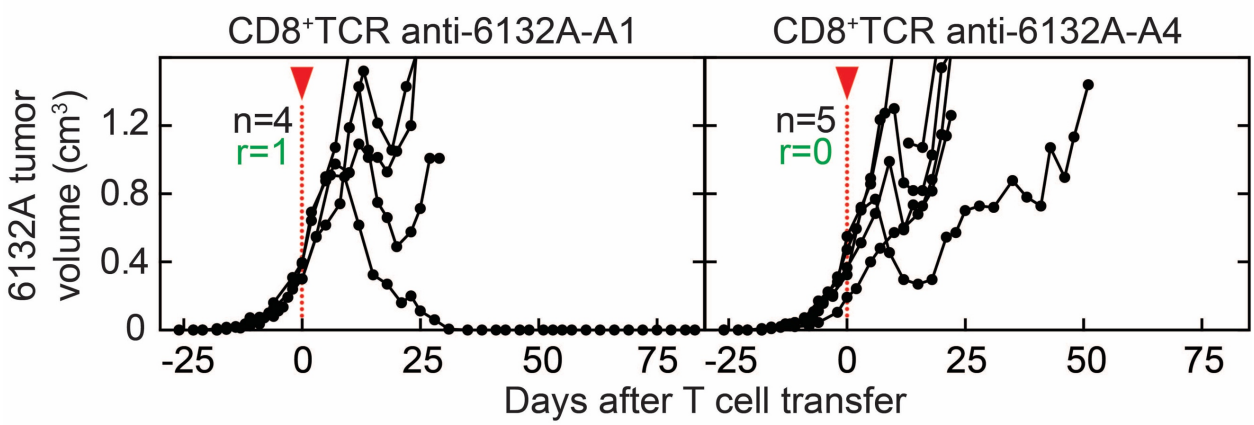

Figure 28. Cancer-specific CD8$^+$TCRs mostly fail to reject established 6132A tumors. Spleen cells from C3H CD4$^{-/-}$ mice were CD8$^+$TCR-transduced before 6132A tumor-bearing C3H Rag$^{-/-}$ mice were treated 25 days after cancer cell injection as indicated by the red arrow head. Average tumor sizes were 347 mm³ ± 46 mm^3 SD at day of ATT and are summarized from three independent experiments. Indicated are total numbers of mice (n) and how many mice rejected the tumor after T cell transfer (r). CD8$^+$ T cells expressing either the CD8$^+$TCR anti-6132A-A1 (**left**, n = 4) or the anti-6132A-A4 CD8$^+$TCR (**right**, n = 5) were used.

C3H Rag$^{-/-}$ mice that had long and established 6132A tumors showed some tumor shrinkage around 15 to 20 days after T cell transfer but eventually died of progressing tumors around 25 days after treatment had started. Nevertheless, one out of four mice treated with the anti-6132A-A1 CD8$^+$TCR rejected the tumor and one out of five mice treated with the anti-6132A-A4 CD8$^+$TCR showed delayed tumor outgrowth. This tumor was readapted in culture and analyzed whether it was still able to stimulate CD8$^+$TCR-T cells. **Figure 29A** shows that the adapted escape cell line was still able to stimulate anti-6132A-A1 T cells to release IFN-γ but no longer stimulated anti-6132A-A4 T cells that had been used for the adoptive T cell transfer. Furthermore, the escape when analyzed for expression of MHC class I molecules by flow cytometry showed a reduced signal for H2-K^k molecule and was negative for H2-D^k molecule expression compared to the original 6132A cancer cell line (**Figure 29B**).

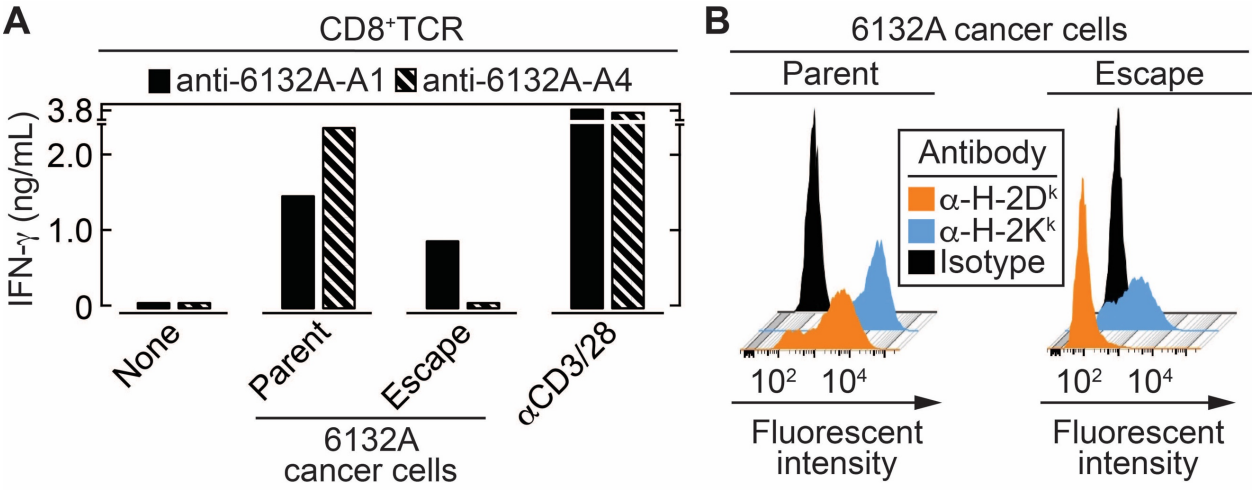

Figure 29. Analysis of a tumor that had delayed outgrowth after anti-6132A-A4 CD8$^+$TCR therapy. (A) Spleen cells from C3H CD4$^{-/-}$ mice were TCR-transduced and were cocultured for 24 h with the parental 6132A and the escape cancer cell line. Supernatants were analyzed for IFN-γ concentrations by ELISA. For TCR-independent T cell stimulation αCD3 and αCD28 were used. Data are means of duplicates and shown is one representative out of 3 independent experiments. **(B)** MHC class I staining of the parental 6132A cancer cell line and the tumor that had escaped anti-6132A-A4 CD8$^+$TCR therapy. This escape tumor appears to be a variant which lacks H-2D^k expression.

Together, both CD8$^+$TCRs targeting independently restricted, cancer-specific antigens had only limited anti-tumor efficiency *in vivo* consistent with what had been observed in the 8101 tumor model.

6.14 One ineffective CD8$^+$TCR when combined with one CD4$^+$TCR still suffices for tumor eradication.

Data above showed that the CD4$^+$TCR and the CD8$^+$TCRs used in the 6132A tumor model have similar effects to the CD4$^+$ T cells and the CD8$^+$TCRs used in the 8101 model. Cancer eradication was achieved in the 8101 model after one CD8$^+$TCR was combined with a polyclonal, 8101-directed CD4$^+$ T cell population. Therefore, it was analyzed whether tumor eradication in the 6132A tumor model could also be achieved by combining just one CD4$^+$TCR with one CD8$^+$TCR. Indeed, the combination of spleen cells from C3H CD8$^{-/-}$ mice transduced with the anti-mRPL9 CD4$^+$TCR and spleen cells from C3H CD4$^{-/-}$ mice transduced with either of the CD8$^+$TCRs (anti-6132A-A1 or anti-6132A A4) used for T cell transfer was able to achieve tumor eradication in 6132A tumor-bearing C3H Rag$^{-/-}$ mice (**Figure 30A**). When treatment started, tumors were large and long-established (size of about 450 mm^3).

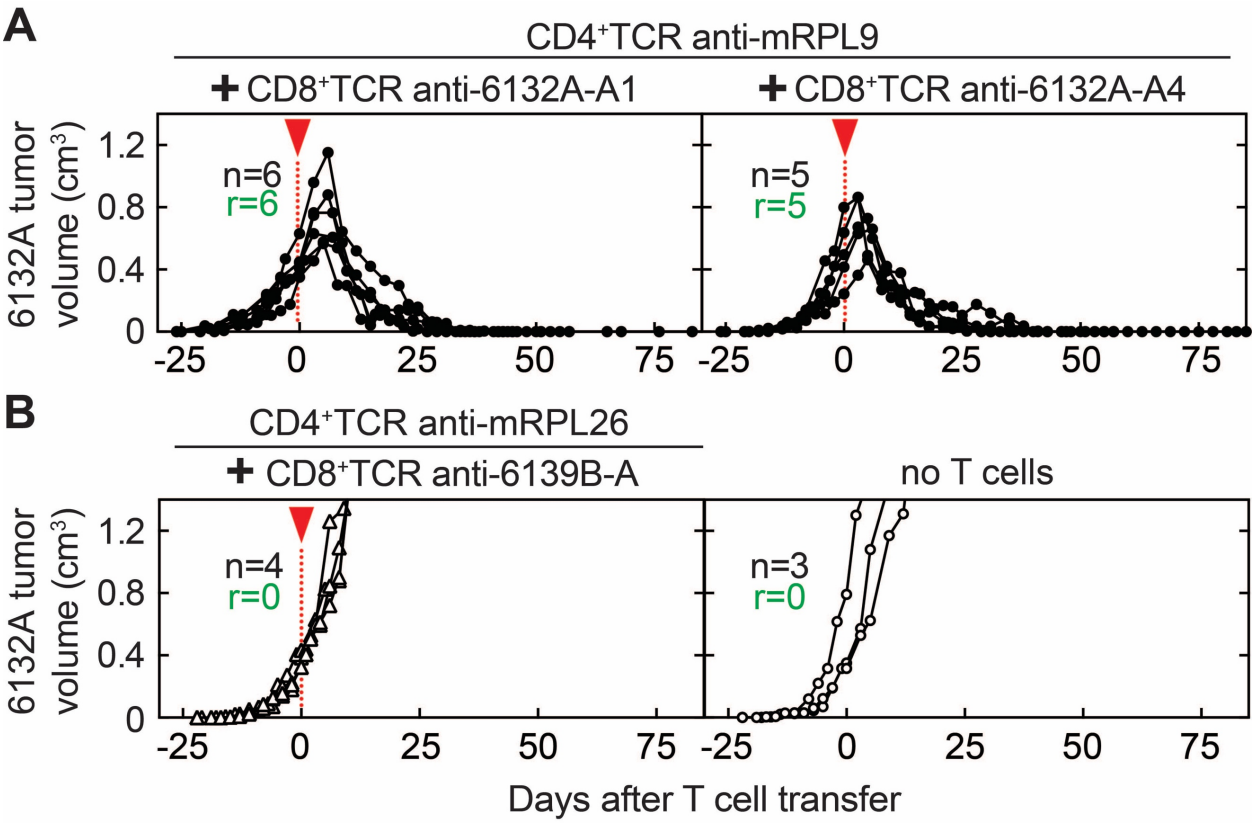

Figure 30. One CD4$^+$TCR and one CD8$^+$TCR are essential and sufficient for tumor eradication. **(A - B)** 6132A tumor-bearing C3H Rag$^{-/-}$ mice were treated with CD4$^+$TCR- and CD8$^+$TCR-transduced T cells 25 days after cancer cell injection as indicated by the red arrow head. C3H CD4$^{-/-}$ and C3H CD8$^{-/-}$ mice were used as CD8$^+$ and CD4$^+$ T cell sources. Average tumor sizes were 450 mm³ ± 154 mm^3 SD at day of ATT and are summarized from three independent experiments. Indicated are total numbers of mice (n) and how many mice rejected the tumor after T cell transfer (r). **(A)** For ATT a combination of anti-mRPL9 CD4$^+$ T cells together with CD8$^+$ T cells (which either expressed anti-6132A-A1 (**left**, n = 6) or anti-6132A-A4 (**right**, n = 5)) was used. **(B)** Mice treated with a combination of CD8$^+$ and CD4$^+$ T cells which were TCR-transduced with TCRs of unrelated specificity (**left**, n = 4) had the same outcome as untreated mice (**right**, n = 3). The CD8$^+$ T cell expressed the CD8$^+$TCR anti-6139B-A which is specific for the cancer cell line 6139B and the CD4$^+$ T cells expressed the CD4$^+$TCR anti-mRPL26 which recognizes the histidine to tyrosine mutation at position 96 of the ribosomal protein L26.

Seven days later, tumors began to shrink and all treated mice seemingly eradicated their tumors within 30 days after T cell transfer. No signs of relapse were observed in the more than two months long follow up time period and all mice stayed tumor-free. To prove that tumor destruction depended on the 6132A-specificity of the used TCRs, anti-mRPL26-transduced CD4$^+$ T cells were combined with anti-6139B-A-transduced CD8$^+$ T cells for treatment of 6132A tumors in C3H Rag$^{-/-}$ mice at a size and duration of growth similar to what had been used to treat 6132A tumors with 6132A-specific TCRs (**Figure 30B**). This combination of a CD4$^+$TCR and a CD8$^+$TCR both specific for the 6139B tumor showed no anti-tumor effects. Thus, growth of these tumors

continued unabated similar to what was observed in untreated control mice that needed to be sacrificed 40 days after injection of 6132A cancer cells.

6.15 $CD4^+$ T cells are the main IFN-γ producer *in vivo*.

Comparing the average release of IFN-γ by $CD4^+$TCR T cells (**Figure 19)** with that released by $CD8^+$TCR T cells (**Figure 27**), it seems as $CD4^+$TCR T cells release two to three times more IFN-γ compared to $CD8^+$TCR T cells at least *in vitro*. Therefore, the IFN-γ response found in blood plasma was compared between the three possible treatments $CD4^+$TCR only, $CD8^+$TCR only and $CD4^+$TCR combined with $CD8^+$TCR (**Figure 31**). Blood samples were taken from 6132A tumor-bearing C3H $Rag^{-/-}$ mice every three days after T cell transfer for three weeks and evaluated for IFN-γ values by flow cytometry. When mice received only anti-mRPL9 $CD4^+$ T cells, the IFN-γ value peaked six days after T cell transfer. At this time point, levels of IFN-γ were about 40x higher than the IFN-γ levels at the end of the follow up period.

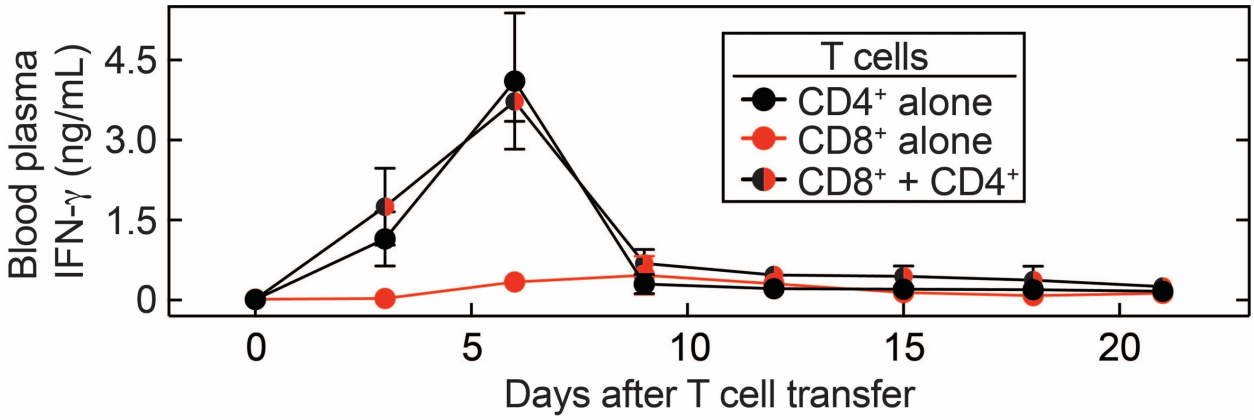

Figure 31. $CD4^+$ T cells are the main IFN-γ producer *in vivo*. Spleens from C3H $CD4^{-/-}$ and C3H $CD8^{-/-}$ mice were used for TCR-transduction before 6132A tumor bearing mice received adoptive T cell transfer 25 days after *s.c.* cancer cell injection. Blood samples were collected by buccal bleeding every 3 days beginning at start of ATT. Blood plasma was prepared and IFN-γ concentrations were determined by FACS. Analyzed were mice which received either $CD8^+$TCR only (total n = 3, anti-6132A-A1 n = 2, anti-6132A-A4 n = 1), $CD4^+$TCR only (anti-mRPL9 n = 4) or a combination of $CD8^+$TCR with $CD4^+$TCR (total n = 3, anti-6132A-A1 with anti-mRPL9 n = 2, anti-6132A-A4 with anti-mRPL9 n = 1). Data are means of duplicates ± SD and are summarized from two independent experiments.

Surprisingly, only small amounts of IFN-γ could be detected in blood plasma throughout the whole follow up period when mice were treated only with $CD8^+$TCRs, either anti-6132A-A1 or anti-6132A-A4. The highest average value of IFN-γ was found at day nine after T cell transfer and was only two to three times higher than the background IFN-γ amounts before treatment started (day 0). Furthermore, when mice were treated with the combination of a $CD4^+$TCR and a $CD8^+$TCR, the analyzed IFN-γ levels were similar to these found after treatment with $CD4^+$TCR only. Thus, values peaked at day six after T cell transfer and were again about 40x higher than IFN-γ values observed in samples from other time points. These results suggest that $CD4^+$ T cells are also the main IFN-γ source *in vivo* which is consistent with results shown already in **Figure 19** and **Figure 27**. In addition, it also indicates that the success of the combination therapy does not originate from enhanced IFN-γ production.

6.16 Direct cancer cell recognition by the $CD8^+$TCR is required for tumor elimination.

Since $CD8^+$TCR T cells seemed not to be a major contributor to IFN-γ production, the role of $CD8^+$TCR T cells was investigated in greater detail. In the used model, the main advantage of $CD8^+$TCR-transduced T cells could be that only they are able to recognize cancer cells directly and thus could potentially find remaining cancer cells that were still alive after initial tumor destruction by the $CD4^+$TCR T cells. Therefore, it was determined whether direct cancer cell recognition was required for tumor elimination. An MHC class I-negative 6132A cancer cell line was generated by knocking out the beta-2-microglobulin gene using CRISPR/Cas technology. The established 6132A cell line no longer stained positive for the MHC class I molecules $H\text{-}2D^k$ and $H\text{-}2K^k$ by flow cytometry compared to the original 6132A cancer cell line (**Figure 32A**) and was designated 6132A $B2m^{-/-}$. This cancer cell line also no longer stimulated anti-6132A-A1 $CD8^+$TCR-transduced T cells to release IFN-γ *in vitro* (**Figure 32B**). To prove that knocking out the beta-2-microglobulin gene did not alter antigen expression, it was analyzed whether the tumor stroma of tumors formed by 6132A $B2m^{-/-}$ cancer cells was still able to cross-present the cognate antigen that is recognized by the anti-6132A-A1 $CD8^+$TCR. Thus, $CD11b^+$ cells from tumors that either developed from the original 6132A cancer cell line or from the 6132A $B2m^{-/-}$ variant were used for T cell stimulation. **Figure 32C** shows that both groups of $CD11b^+$ cell were able to stimulate specific T cells to release IFN-γ in comparable amounts thereby proving that the cognate antigen was still released into the tumor microenvironment by the 6132A $B2m^{-/-}$ cancer cells.

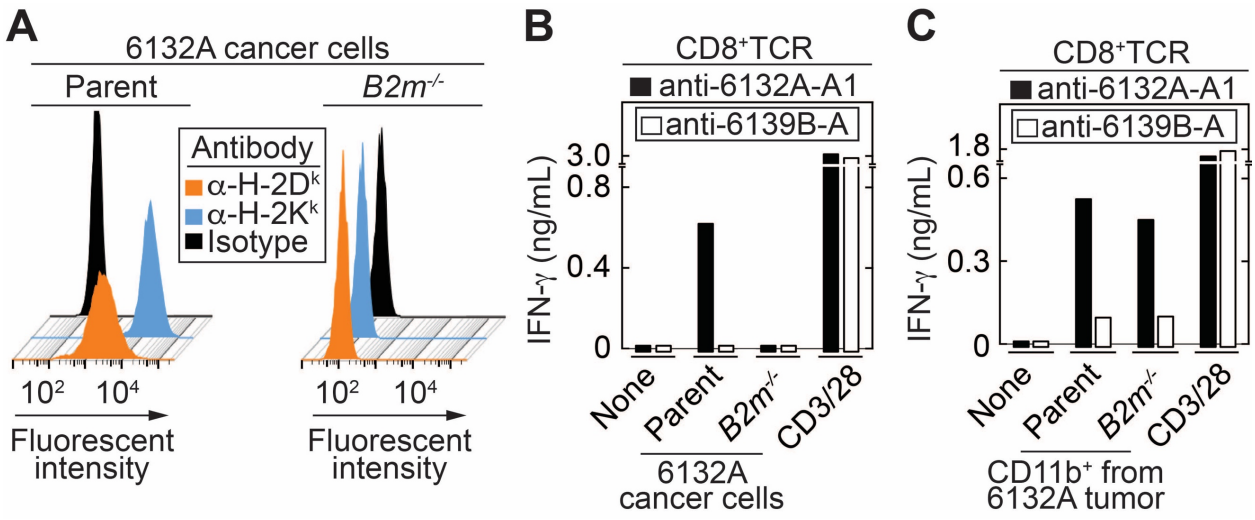

Figure 32. 6132A cancer cells lacking the beta-2-microglobulin gene no longer stimulate T cells directly but the cognate antigen is still being cross-presented on CD11b$^+$ tumor stroma cells. **(A)** Lack of MHC class I H-2D^k and H-2K^k surface expression in the 6132A beta-2-microglobulin knockout cell line (B2m$^{-/-}$) generated by CRISPR-Cas9. **(B – C)** Spleen cells from C3H CD4$^{-/-}$ mice were CD8$^+$TCR-transduced (anti-6132A-A1) and cocultured for 24 h. Supernatants were analyzed for IFN-γ concentrations by ELISA. CD8$^+$TCR-transduced T cells against the cancer cell line 6139B (anti-6139B-A) were used as negative control. T cells cultured alone or stimulated with αCD3/αCD28 antibodies were used as TCR-independent controls. Data are means of duplicates ± SD and one representative out of 3 independent experiments is shown. **(B)** *In vitro* cultured 6132A but not 6132A B2m$^{-/-}$ cancer cells were able to stimulate anti-6132A-A1 CD8$^+$TCR-transduced T cells. **(C)** Both CD11b$^+$ cells isolated from either 6132A or 6132A B2m$^{-/-}$ tumors grown in C3H Rag$^{-/-}$ mice were able to stimulate anti-6132A-A1 CD8$^+$TCR-transduced T cells.

The above results indicate that the 6132A B2m$^{-/-}$ cell line was no longer directly recognized by CD8$^+$TCR T cells but still expressed the cognate antigen that was being cross-presented on cells of the tumor stroma. It could therefore be analyzed whether tumor stroma recognition could suffice for tumor elimination when CD4$^+$TCR and CD8$^+$TCR T cells were used together for adoptive T cell transfer. However, **Figure 33** shows that 6132A B2m$^{-/-}$ tumors were not eradicated in C3H Rag$^{-/-}$ mice treated with the combination of anti-mRPL9 CD4$^+$TCR-transduced T cells and anti-6132A-A1 CD8$^+$TCR-transduced T cells. Nevertheless, tumors were destroyed in all six mice between seven to ten days after T cell transfer and this was followed by a long-term tumor growth arrest for up to 50 days. None of the mice eliminated their tumors even though both types of TCRs were present. These findings were similar to what had been observed after treatment with anti-mRPL9 T cells only (**Figure 18**) and suggest that CD8$^+$ T cells are required to directly find and kill residual persisting cancer cells remaining in the tumors after destruction of the bulk of the tumor tissue.

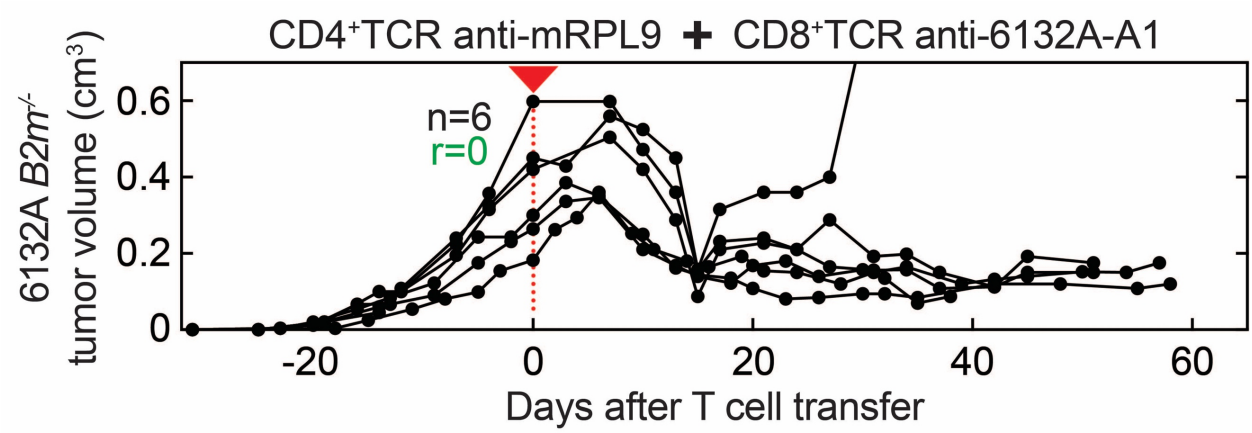

Figure 33. Failure of the CD8$^+$TCR T cells to eradicate 6132A tumors in collaboration with the CD4$^+$TCR T cells when the CD8$^+$TCR T cells can no longer recognize the cancer cells directly. 6132A B2m$^{-/-}$ tumor-bearing C3H Rag$^{-/-}$ mice were treated around 25 days after tumor injection as indicated by the red arrow head. Average tumor sizes were 369 mm^3 ± 150 mm^3 SD at day of ATT. CD8$^+$TCR anti-6132A-A1-transduced CD8$^+$ T cells together with CD4$^+$TCR anti-mRPL9-transduced CD4$^+$ T cells were used for treatment (n = 6). Spleen from C3H CD4$^{-/-}$ and C3H CD8$^{-/-}$ mice were used as T cell source. Indicated are the total numbers of mice (n) and mice which rejected (r) the tumor after T cell treatment. Results are summarized from three independent experiments.

7. Discussion

In this thesis, it was explored how unmanipulated large and long established solid tumors can be eradicated by adoptive T cell therapy. Just two different cancer-specific TCR clonotypes were required and the cancers expressed targeted mutant-neoantigens at “natural, unmanipulated levels”. One TCR, isolated from $CD4^+$ T cells, needed to recognize the tumor stroma while the other one, isolated from $CD8^+$ T cells, needed to recognize the cancer cells directly. A single $CD8^+$TCR or a combination of two different $CD8^+$TCR clonotypes that targeted MHC class I restricted mutant neoantigens was insufficient even though solid tumors were treated that arose from a cancer cell clone to reduce tumor heterogeneity. The $CD4^+$TCR caused tumor destruction followed by long-term growth arrest but was not able to eradicate cancers. It is suggested that the tumor destruction caused by the $CD4^+$TCR depends on stroma recognition and is due to high interstitial IFN-γ and TNF levels that cause tumor vasculature to regress. Tumor eradication was achieved when one $CD4^+$TCR was combined with one $CD8^+$TCR but only when cancer cells expressed MHC class I molecules. Tumors from cancer cells that were deficient in MHC class I surface expression were destroyed and kept at a small size as observed with $CD4^+$TCR therapy even when the $CD8^+$TCR had also been used for the treatment. These findings are in consistence with a model in which four cell types, a cancer cell, a professional APC, $CD8^+$ and $CD4^+$ T cell, interact to eradicate large-established solid tumors.

7.1 Preclinical tumor models

The choice of *in vivo* models used in this thesis to test the efficiency of therapeutic approaches tried to overcome three major problems concisely present in previous tumor mouse models. First, cancer cell lines used were never immunoselected by serial transplantation in normal immunocompetent mice. Such selection may occur even after a single transplantation into a naïve fully immunocompetent host (Ward, Koeppen et al. 1990, Dubey, Hendrickson et al. 1997, Matsushita, Vesely et al. 2012). Thus, the composition of the tumors treated in this thesis probably more closely mirror original primary tumors as they developed in the original host. Second, only long-established tumors were treated to overcome the artifact that transplanted, *s.c.* injected cancer cells create necrosis and an acute inflammation causing cancer cell death. Such early palpable lesions do not resemble the tumor tissue in patients requiring therapy (Schreiber, Rowley et al. 2006). These artifacts vanish after about 10 to 14 days after which the developing tumor acquires histopathological characteristics observed in primary tumor tissue of patients (Schreiber, Rowley et al. 2006). Therefore, treatment success was analyzed in systems which simulated the

situation in a cancer patient as closely as possible. Third, cancers were targeted that expressed autochthonous mutant neoantigens at unmanipulated levels. Previous investigations in preclinical models have demonstrated that adoptive T cell transfer can be highly effective with just one mutant neoantigen-specific $CD8^+$TCR against large and established solid tumors in mice (Leisegang, Engels et al. 2016, Leisegang, Kammertoens et al. 2016). However, in these and other studies (Alspach, Lussier et al. 2019) the cancer cell lines needed to be engineered to express the mutant neoantigen at high levels to allow tumor eradication. Cancer relapse occurred when the autochthonous unmanipulated mutant neoantigen was targeted on the original cancer cell population (Leisegang, Engels et al. 2016). Unmanipulated cancers that relapse after adoptive T cell transfer are more representative of the situation in cancer patients (Mackensen, Meidenbauer et al. 2006, Rosenberg, Yang et al. 2011) and were therefore investigated in this thesis.

The two tumor models (8101 and 6132A) were induced by intermittent exposure to UVB-light on the back of normal mice. Sequencing analyses of both tumors showed several thousand somatic mutations and even after RNA-sequencing a multitude of potential mutant neoantigens prevailed that could be targeted by TCR gene therapy (1,207 mutant neoantigens for 8101 (Leisegang, Engels et al. 2016) and 1,687 mutant neoantigens for 6132A). These seemingly high numbers also occur in mutagen-induced human cancers such as lung carcinomas and melanomas but most human cancers exhibit only 10 to 200 mutant neoantigens at the day of diagnosis (Alexandrov, Nik-Zainal et al. 2013, Lawrence, Stojanov et al. 2013, Vogelstein, Papadopoulos et al. 2013, Schumacher and Schreiber 2015). It could be argued that it is more likely to find a successful pair of one $CD4^+$TCR and one $CD8^+$TCR for therapy in tumors with high mutational burden. This notion would be consistent with the observation that inhibitor checkpoint therapy has a higher success rate in these cases (Goodman, Kato et al. 2017, Yarchoan, Hopkins et al. 2017). However, studies along different cancer types have shown that mutant neoantigen specific TCRs can also be identified even in cancers with low mutational burden (Veatch, Lee et al. 2018, Yossef, Tran et al. 2018, Zacharakis, Chinnasamy et al. 2018, Leko, McDuffie et al. 2019).

7.2 Tumor escape from $CD8^+$TCR therapy

In a recent study, it was shown that one $CD8^+$TCR is sufficient to prevent outgrowth of a cancer cell clone (8101 Clone 12) expressing homogenously the targeted autochthonous mutant neoantigen mDDX5 (Schreiber, Karrison et al. 2020). However, due to the inflammatory artifact caused by the cancer cell inoculation prevention of outgrowth of injected cancer cells may be

much easier to achieve than therapy of established cancers. Clone 12 was therefore also used in this thesis. When mDDX5 was targeted by anti-mDDX5-transduced T cells on established 8101 Clone 12 tumors, tumors escaped therapy even though the mDDX5 neoantigen was seemingly expressed homogenously. This was not a result of the mutant peptide binding with a low affinity since mDDX5 binds with sub-nano molar affinity to MHC class I (Schreiber, Arina et al. 2012). In addition, wild type DDX5 functions as a coactivator of p53 (Bates, Nicol et al. 2005). Also mDDX5 plays an important role in tumor development (Yang, Lin et al. 2005) because it was found that DDX5 is important for different transcriptional activators (Fuller-Pace 2013). Taken together, mDDX5 plays an important role in cell proliferation, has a high MHC binding affinity and should therefore be an ideal target for adoptive T cell transfer. Yet, tumors escaped therapy by mDDX5 downregulation and progression seems to be independent of mDDX5 function. In a recent study, it was found that downregulation of DDX5 activates the mTOR and MDM2 pathways (Kokolo and Bach-Elias 2017). Through the activation of MDM2, p53 gets degraded (Haupt, Maya et al. 1997) and due to activation of mTOR cell proliferation pathways are increased (Aoki, Blazek et al. 2001, Vogt 2001). Thus, there appears to be multiple mechanisms whereby the 8101 Clone 12 tumor can circumvent the disadvantage of mDDX5 downregulation and escape.

Many different immune escape pathways have been studied. The mechanism behind escape of a cancer cell clone might be non-heritable intraclonal heterogeneity (Taupier, Kearney et al. 1983) that represents a phenotypic equilibrium within a cancer cell population. More recently, these transitions have been modeled (Gupta, Fillmore et al. 2011) and referred to as non-genetic cancer cell plasticity (Pisco and Huang 2015). This mechanism is well studied in the development of multiple myeloma (Walker, Wardell et al. 2012, Walker, Wardell et al. 2014) and one of the reasons why relapse is common in multiple myeloma treatment (Brioli, Melchor et al. 2014). In multiple myeloma, global DNA methylation is an ongoing process and clones switch between different states (Walker, Wardell et al. 2011). This phenomenon was also reported as a drug-resistance mechanism in melanoma against BRAF inhibitors which is initially reversible (Sharma, Lee et al. 2010, Sun, Wang et al. 2014) and thus non-heritable. However, with continued drug exposure the epigenetic changes become non-reversible and heritable (Shaffer, Dunagin et al. 2017). Consistent with this notion, the 8101 Clone 12 reisolates from tumors that relapsed early still had some sensitivity to the anti-mDDX5 $CD8^+$TCR while the reisolate from a tumor that relapsed later was no longer recognized. Nevertheless, other mechanisms of immune escape could be additional reasons why mDDX5 expression is lost. One possibility could be antigenic drift (Bai, Liu et al. 2003). There, additional mutations in the recognized epitope could occur which would reduce the ability of specific T cells to effectively recognize their target and also disable

detection by mutant-specific qPCR due to primer mispairing. Another possibility could be antigenic loss on the genomic level (Bai, Liu et al. 2006) due to insertions or deletions causing frame shifts in front of the targeted epitope. The genomic DNA of the 8101 Clone 12 escape tumors has not been sequenced and thus genomic antigen loss cannot be excluded.

Since adoptive T cell therapy with mDDX5-specific $CD8^+$ T cells was not sufficient for tumor eradication, the effects of targeting mNav3 were tested. Using this mutant neoantigen seemed even more promising because it was found also on mDDX5 negative 8101 clones which grow in immunocompetent normal mice and have therefore a progressor phenotype (Dubey, Hendrickson et al. 1997). The wild type Nav3 protein is a cytoskeleton navigator and, when it becomes dysfunctional, tumor invasion is enhanced (Maliniemi, Carlsson et al. 2011, Carlsson, Krohn et al. 2013, Cohen-Dvashi, Ben-Chetrit et al. 2015). This biological effect might be a reason why the mNav3 is conserved between regressor and progressor phenotypes and tumors without its mutant form could have a growth disadvantage. However, even the combination of anti-mNav3 and anti-mDDX5 TCR-transduced T cells did not succeed in eradication of 8101 Clone 12 tumors. At this point, it had not been proven that the mNav3 neoantigen, like mDDX5 (Leisegang, Engels et al. 2016), is a rejection antigen under ideal circumstances. Therefore, 8101 would need to be engineered to express high amounts of the mNav3 epitope to show that high amounts could be sufficient to eradicate established solid tumors. Another reason for fail could be that the predicted pMHC affinity of mNav3 to $H\text{-}2D^b$ is 156 nM, which might be too high to expect tumor eradication when targeted by $CD8^+$ T cells (Engels, Engelhard et al. 2013). Therefore, it could be argued that mNav3 is not an as ideal target for adoptive T cell transfer as mDDX5 and targeting a different mutant neoantigen in combination with mDDX5 might still suffice to eliminate unmanipulated established 8101 tumors. Another reason for relapse could be ineffective mNav3 and mDDX5 cross-presentation on 8101 tumor stroma. It was shown that high amounts of cross-presented antigen on tumor stroma were needed to prevent the escape of antigen-loss variants when exclusively $CD8^+$ T cells were used for adoptive T cell transfer (Spiotto, Yu et al. 2002, Spiotto, Rowley et al. 2004). Since by comparison only little cross-presentation of mDDX5 was observed in 8101 tumors it could be one of the discussed reasons why treatment of unmanipulated 8101 tumors with anti-mDDX5 $CD8^+$TCR-transduced T cells alone was not sufficient (Leisegang, Engels et al. 2016).

Antigen-loss variants were regularly found only in the 8101 but not in the 6132A tumor model. Therefore, it could be argued that $CD8^+$TCR therapy against 8101 was effective but insufficient while failing against 6132A. Only one MHC class I loss variant could be reisolated in the 6132A model. Other tumors showed signs of minor tumor destruction during the observed

time period and the reisolated tumors were still recognized by the anti-6132A-A1 or -A4 $CD8^+$TCRs. It could be that due to high tumor burden mice were sacrificed too early before it was possible to observe a prolonged tumor destructive effect. In addition, $CD8^+$TCR T cells could have been more effective when only T cells would have been used for adoptive transfer that expressed the TCR at very high amounts (e.g. selected by mean fluorescent intensity of the TCR-transduced Vα- or Vβ-chain). Another reason could be that the $CD8^+$ T cell clones, from which the anti-6132A-A1 and -A4 $CD8^+$TCRs were isolated from, were not able to lyse the majority of 6132A cancer cells even at very high effector-to-target ratios in a chromium release assay (Ward, Koeppen et al. 1989), which could be due to activation properties associated with the T cell clone or with the $CD8^+$TCR itself. Since the molecular origins of the targeted cancer-specific antigens are unknown, it can only be speculated that these antigens might be either essential for tumor growth and are therefore not lost or that their expressed amount is too low for effective $CD8^+$ T cell activation *in vivo.* Either way, determining the type of recognized antigen is an important future goal that might help to understand why $CD8^+$TCR therapy fails in 6132A. In general, two ways can be considered for antigen determination. One approach uses so called “tandem minigene libraries” (Lu, Yao et al. 2014) to introduce mutant neoantigens into APCs. These APCs are then screened with T cells and the minigene of the APC which stimulates T cells to secrete IFN-γ will be analyzed further to narrow down the specific recognized mutation. Improvements of this general approach have been published, that promise a higher throughput screening (Lu, Zheng et al. 2018, Kula, Dezfulian et al. 2019, Sharma, Rive et al. 2019). A different, earlier approach analyzes peptides eluted directly from the MHC class I cleft. This approach was used to determine the mDDX5 antigen (Dubey, Hendrickson et al. 1997) and was also used to characterize H-$2K^k$ restricted self-peptides in C3H mice (Brown, Wooters et al. 1994).

7.3 Destruction of the tumor microenvironment by $CD4^+$TCRs

The tumor microenvironment is considered to be immune-suppressive (Binnewies, Roberts et al. 2018) and tumor promoting (Seung, Rowley et al. 1995). It is known to enhance cancer cell resistance to radiation and chemotherapy and limits the drug access (Valkenburg, de Groot et al. 2018). Therefore, different approaches have been developed to target the tumor microenvironment directly to improve cancer therapies (Bouzin and Feron 2007, Erkan, Hausmann et al. 2012, Mao, Keller et al. 2013, Binnewies, Roberts et al. 2018, Valkenburg, de Groot et al. 2018). The most promising studies used immunotherapy approaches by activation of $CD8^+$ T cells with DNA-vaccines against the fibroblast activation protein (FAP) (Loeffler, Kruger et al. 2006) or against the legumain protein (asparagine endopeptidase, AEP) (Luo, Zhou et al.

2006) to kill tumor-associated fibroblasts and macrophages. Furthermore, it was shown that $CD8^+$ T cells selectively targeting antigen cross-presented by tumor stroma can also arrest tumor growth (Zhang, Zhang et al. 2008). These experiments involved cancer cells that over-expressed the model xenoantigen SIYRYYGL where the cancer cells lacked the MHC class I needed for direct recognition by the anti-SIY 2CTCR-transgenic T cells. The possibility, that MHC class II expressing stromal cells can be targeted by $CD4^+$ T cells recognizing an autochthonous mutant neoantigen expressed at unmanipulated levels has not yet been exploited. These T cells caused tumor-destruction followed by long-term growth arrest in the 6132A tumor model. Similar observations were made in the 8101 tumor model in this thesis even though 8101 tumors have previously been shown to have an immune-suppressive microenvironment (Arina, Schreiber et al. 2014). Targeting MHC class II restricted mutant neoantigens might have the advantage over MHC class I restricted mutant neoantigens that the class II presentation pathway is more efficient (Inaba, Turley et al. 1998) than the MHC class I cross-presentation pathway because the latter is prone to fail (Gil-Torregrosa, Lennon-Dumenil et al. 2004, Otahal, Hutchinson et al. 2005).

Antigen recognition on cells of the tumor stroma by $CD4^+$ T cells led to high amounts of secreted IFN-γ *in vitro*. High amounts of IFN-γ were also found in blood plasma and tumor tissue during the course of treatment. Furthermore, it was demonstrated by longitudinal *in vivo* imaging that IFN-γ production correlated with regression of vessels and loss of endothelial cells in tumors and causes ischemic necrosis consistent with previous results that had proven a coagulative role of IFN-γ in these events (Kammertoens, Friese et al. 2017). In this publication, it was unknown if the artificially high induced IFN-γ values can be reached by targeting unmanipulated mutant neoantigens which was proven in this thesis. It was also reported that IFN-γ is a key player in tumor stroma destruction and acts on both bone marrow- and non-bone marrow-derived cells (Zhang, Karrison et al. 2008). The importance of IFN-γ in tumor destruction is widely accepted but thus far, research has focused on $CD8^+$ T cells as main IFN-γ source (Barth, Mule et al. 1991, Ibe, Qin et al. 2001) or only showed indirect that IFN-γ and the IFN-γ receptor on stroma is important for prevention of tumor outgrowth by $CD4^+$ T cells (Mumberg, Monach et al. 1999, Qin and Blankenstein 2000). As shown in this thesis, high IFN-γ values that can induce tumor vessel reduction depend on release from $CD4^+$ T cells while the contribution from $CD8^+$ T cells is small. In all studies the synergy between IFN-γ and TNF secretion in tumor destruction has been analyzed and concluded that both cytokines are major players for successful tumor stroma destruction. The $CD4^+$ T cells used in this dissertation also secreted high amounts of TNF but whether TNF is needed in combination with IFN-γ for tumor destruction in the 6132A tumor model

needs to be further investigated. Nonetheless, the use of $CD4^+$ T cells for tumor stroma recognition followed by IFN-γ and TNF secretion as main effectors adds a new concept for immunotherapy.

A partial destruction of a cancer followed by growth control of the cancer persisting at a smaller size has also been achieved in a patient after adoptive transfer of tumor-infiltrating T cell population of $CD4^+$ T cells recognizing a mutant neoantigen (Tran, Turcotte et al. 2014). Similarly, after transfer of bulk TIL populations dominant mutant-specific $CD4^+$ T cell responses were found during durable regression (Veatch, Lee et al. 2018, Zacharakis, Chinnasamy et al. 2018). Analysis of the TIL response revealed that mutation-specific $CD4^+$ T cells can be found more frequently in patients than mutation-specific $CD8^+$ T cell responses (Linnemann, van Buuren et al. 2015, Yossef, Tran et al. 2018, Leko, McDuffie et al. 2019). In human patients (Tran, Turcotte et al. 2014, Veatch, Lee et al. 2018, Zacharakis, Chinnasamy et al. 2018) and in the experimental model used in this dissertation, persistence of mutation-specific $CD4^+$ T cells was demonstrated. This is consistent with clinical and experimental observations that exhaustion signatures are usually associated with $CD8^+$ T cells and thus checkpoint inhibitor strategies effect mainly the $CD8^+$ T cell response (Wei, Levine et al. 2017, Sade-Feldman, Yizhak et al. 2018, Yost, Satpathy et al. 2019). Furthermore, an advantage of mutant neoantigen-specific $CD4^+$ T cells could be that they cannot select for variants with reduced levels or loss of antigen expression because only stromal cells are recognized directly. In the state of long-term growth arrest, antigen positive cancer cells will grow and load the stroma up to a point where $CD4^+$ T cells are activated again. The secretion of IFN-γ and TNF will destroy the surrounding supportive stroma tissue and affect antigen-positive and negative-cancer cells similarly resulting in the reduction of tumor volume and growth arrest. Apparently, only very small antigen amounts are needed for stable pMHC class II complex formation (Demotz, Grey et al. 1990, Harding and Unanue 1990) and only 0.03 % of all pMHC class II complexes on a cell surfaces are needed to activate a specific $CD4^+$ T cell response. Due to lipid raft arrangements multiple MHC class II molecules associate together on the cell surface (Khandelwal and Roche 2010) and thus lower the needed amount of MHC class II molecules and antigen for successful $CD4^+$ T cell stimulation (Anderson, Hiltbold et al. 2000). In addition to this mechanism, it was also shown that a single pMHC class II molecule can be sufficient to trigger $CD4^+$ T cell activation and cytokine secretion (Huang, Brameshuber et al. 2013). Therefore, even if targeted antigen expression is reduced, small antigen amounts might still suffice for successful stroma loading and activation of $CD4^+$ T cells. This was however not experimentally tested using reduced amounts of mRPL9 antigen.

7.4 Targeting mutant ribosomal proteins

The need of $CD4^+$ T cells for successful immunotherapy is becoming increasingly recognized (Kreiter, Vormehr et al. 2015) and so are efforts to improve the prediction of MHC class II restricted mutant neoantigens (Abelin, Harjanto et al. 2019). Targeting mutant ribosomal proteins maybe ideal targets for cancer therapy by $CD4^+$ T cells as many or all of them are essential for growth of any cell including cancers (Beck-Engeser, Monach et al. 2001, Amsterdam, Sadler et al. 2004). Disorders related to ribosomal protein dysfunction are named “ribosomopathies” and all of them are associated with high risk of tumor development (Narla and Ebert 2010). Ribosomal proteins are sentinels of protein biosynthesis and many of them are linked to the activation of the p53 pathway (Lohrum, Ludwig et al. 2003). This function is conserved even in prokaryotic organisms (Shoji, Dambacher et al. 2011). Since biosynthesis of proteins *in vitro* can proceed without the presence of any ribosomal protein yet they are essential *in vivo* even in archaebacterial, their main importance is likely related to regulatory functions in transcription and translation (Sonenberg 1993). A common issue with ribosomal proteins is that they are often haploinsufficient (one allele is not able to produce sufficient amounts of ribosomal protein) (Panic, Tamarut et al. 2006, Dutt, Narla et al. 2011, Fortier, MacRae et al. 2015) and loss of one allele causes therefore activation of p53 and cell death. Interestingly, cancers with one allele mutated can show either loss of the second allele or can have a different mutation in the second allele (Beck-Engeser, Monach et al. 2001). Both events are especially common also in human cancers when they harbor an additional p53 mutation (Ajore, Raiser et al. 2017, Fancello, Kampen et al. 2017) to prevent apoptosis. Due to this connection, loss of the mutated allele which would lead to antigen loss variants is very unlikely since the mutant allele is required for cancer cell growth and survival, as demonstrated for mRPL9 in the 6132A tumor model (Beck-Engeser, Monach et al. 2001). For these reasons mutant ribosomal proteins gain more attention and RPL5, RPL11, RPL23 and RPS5 have been described as targets for cancer therapy (Lawrence, Stojanov et al. 2013, Lawrence, Stojanov et al. 2014).

7.5 Indirect and direct targeting of cancer cells by $CD4^+$ T cells

The 6132A tumor model lacks expression of MHC class II molecules (Mumberg, Monach et al. 1999) which was confirmed *in vitro* in this thesis and is also the case in most human cancers. Therefore, no direct cancer cell recognition by $CD4^+$ T cells *in vivo* should be possible. However, the field continuous to argue that MHC class II expression can be induced in cancer cells *in vivo* by IFN-γ or other mediators. Furthermore, in some cases it is difficult to differentiate MHC class II positive stroma cells and cancer cells in histologic samples (Oldford, Robb et al. 2004) or by flow

cytometry (Durrant, Ballantyne et al. 1987) from background that is usually subjective and thus separation can be difficult. Also there are conclusive examples that cancer cells negative for MHC class II *in vitro* become positive *in vivo* (Arina, Karrison et al. 2017). It was shown in this thesis that stroma recognition by $CD4^+$ T cells is essential for tumor destruction. In order to also prove that stroma recognition was also sufficient to cause tumor destruction a MHC class II knockout (reviewed elsewhere (Das, Eisel et al. 2017)) of $I\text{-}E^k$ in 6132A needs to be used. If recognition of tumor stroma by $CD4^+$ T cells is sufficient for tumor destruction, $CD4^+$ T cells in future experiments would show the same effects on 6132A $I\text{-}E^k$ knockout derived tumors as on tumors derived from the original 6132A cell line. In the case of melanoma, some studies showed prevention of outgrowth of MHC class II positive cancer cells by $CD4^+$ T cells (Muranski, Boni et al. 2008, Quezada, Simpson et al. 2010). For patients with MHC class II positive melanoma, it could be of interest to focus the therapeutic approach on $CD4^+$ T cells only. To further explore the power of direct cancer cell recognition by $CD4^+$ T cells in models other than melanoma, the 6132A cancer cell line could be modified to express MHC class II $I\text{-}E^k$ molecules. It would be interesting to determine whether under such circumstances 6132A tumors could be eradicated by $CD4^+$ T cells alone. Nevertheless, adoptive transfer of $CD4^+$ T cells has been shown to eradicate disseminated Friend virus-induce erythroleukemia even though these cancer cells were found to be MHC class II negative (Greenberg, Kern et al. 1985). Importantly, $CD8^+$ T cells were not required for eradication of the leukemia but the participation of $CD8^+$ T cells may be needed in eradication of solid tumors. As shown in this thesis with B2m-negative cancer cells, even when both $CD4^+$ and $CD8^+$ T cells were used for adoptive transfer, direct cancer cell recognition by $CD8^+$ T cells was essential for eradication of established tumors unlike what had been observed in a model that prevented the outgrowth of inoculated cancer cells (Schietinger, Philip et al. 2010).

7.6 Four-cell type interaction and the eradication of solid tumors

There is an increasing recognition that the need of both $CD4^+$ and $CD8^+$ T cells is essential to prevent the outgrowth of inoculated cancer cells (Bos and Sherman 2010, Schietinger, Philip et al. 2010, Kreiter, Vormehr et al. 2015, Alspach, Lussier et al. 2019). In addition, it also becomes evident that both recognized antigens need to be expressed on the same cancer cell for enhanced CD4-CD8 T cell interaction at the effector phase, at the tumor site (Bos and Sherman 2010, Schietinger, Philip et al. 2010, Alspach, Lussier et al. 2019). The help that $CD4^+$ T cells provide in lymph nodes during $CD8^+$ T cell priming (Kumamoto, Mattei et al. 2011, Olson, McDermott et al. 2012, Ahrends, Spanjaard et al. 2017) may not be sufficient to effectively treat and eradicate

solid tumors, once they are established and express mutant neoantigens at “natural” unmanipulated levels.

It is uncertain how much “help” $CD8^+$ T cells need from the APC and/or from the $CD4^+$ T cell (Wang, Norbury et al. 2001). Pathways which allow for direct cell-to-cell interactions between $CD4^+$ T cells, APC and $CD8^+$ T cell have been reported (Schoenberger, Toes et al. 1998, Feau, Garcia et al. 2012) but the dynamics of interactions between these three cell types have remained unclear (Mitchison and O'Malley 1987, Ahmed, Wang et al. 2012).

This dissertation outlines the hypothesis that the cancer cell-eradicating capacity of $CD8^+$ T cells depends on a four cell-type interaction. The APC in the tumor stroma is loaded with MHC class I- and II-restricted mutant neoantigens by adjacent cancer cells and are recognized by $CD8^+$ and $CD4^+$ T cells (illustrated in **Figure 1**, Summary section). By expressing both, the class I-restricted and class II-restricted mutant neoantigen on a single APC, the APC enables the required CD4-CD8 interaction *in vivo*. This is also the case in the three cell-type model (Mitchison and O'Malley 1987). However, there are differences in the four cell-type model proposed here. The APC does not necessarily have to be a DC. As described in this thesis, $F4/80^+$ cells that are specifically defined as macrophages (Austyn and Gordon 1981) also seem to suffice for the four cell-type interaction because $F4/80^+$ cells were as well recognized as unseparated $CD11b^+$ populations in the 6132A tumor model. It is proposed that once the $CD8^+$ T cells receive the needed stimuli and gain a fully activated status, they are able to eliminate adjacent cancer cells that participate in the four cell-type interaction by releasing the mutant neoantigens that are digested and presented by the nearby APC to be targeted while stimulating the T cells in the cluster. It is also postulated that the $CD8^+$ T cells enter the cluster because they recognize cross-presented antigen on the APC. The four cell-type interactions might occur everywhere in the treated solid tumor and are needed for tumor eradication and could also cause upregulation of MHC by IFN-γ (Ward, Koeppen et al. 1990, Wu, Schreiber et al. 2011) and increased antigen expression for more efficient recognition by $CD8^+$ T cells. Direct CD4-CD8 cell-cell contact maybe required for both T cell subsets to become properly activated. The molecular pathways of this interaction was not studied in this dissertation and could involve pathways such as CD40/CD40L and CD27/CD70 which are important for T cell priming in LN (Agematsu, Kobata et al. 1995, Zhong, Roberts et al. 2001, de Goer de Herve, Dembele et al. 2010) but might also play a major role in activation at the effector phase. The pathways needed on the $CD4^+$ T cell side for example could be studied by using $CD4^+$ T cells from CD40 knockout (van Essen, Kikutani et al. 1995) or from CD27 knockout (Hendriks, Gravestein et al. 2000) mice, as both mice strains show impaired $CD4^+$ T cell help.

In another study a required four cell-type interaction was also shown (Arina, Karrison et al. 2017) and a collaborative effect of $CD4^+$ and $CD8^+$ T cells was needed to eradicate established solid tumors. In this study however, $CD8^+$ T cells targeted the highly over-expressed model antigen SIY cross-presented on cells of the tumor stroma and were not able to recognize the cancer cells directly. The $CD8^+$ T cells caused tumor destruction followed by a long-term stable disease but were not able to eliminate cancers which is similar to results obtained with $CD4^+$ T cells in the 6132A tumor model. Interestingly, the used allogeneic $CD4^+$ T cells had no observable anti-tumor effect although they were able to recognize tumor stroma and the cancer cells directly *in vivo* which is also similar to results gathered with $CD8^+$ T cells in the 6132A tumor model. Importantly, the seemingly ineffective $CD4^+$ T cells were still required for tumor eradication. The authors from the Arina et al. publication show that tumor stroma recognition by $CD4^+$ T cells was needed for tumor eradication since MHC class II negative hosts did not reject cancers when treated with the combination of $CD4^+$ and $CD8^+$ T cells. This results suggests that APCs are needed for successful T cell stimulation and indicates that in the Arina et al. study cancer cell recognition together with APC mediated CD4-CD8 interactions are essential for tumor eradication. It appears to be the inverted situation compared to the 6132A model but still hints to the basic principle of a four cell-type interaction needed for eradication of solid tumors.

MHC class I loss is a common mechanism of escape from immunotherapy (Connor and Stern 1990, Kaklamanis, Townsend et al. 1994, Blades, Keating et al. 1995, Korkolopoulou, Kaklamanis et al. 1996) and a H-$2D^k$-negative 6132A variant was also isolated after treatment with anti-6132A-A4-transduced $CD8^+$ T cells. Thus, occurrence of escape needs to be thwarted for immunotherapy to be effective (Garrido, Aptsiauri et al. 2016, Garrido, Ruiz-Cabello et al. 2017). It remains unclear whether the combinational treatment used in this thesis reduces the chance of such an escape because mouse and not human cancers were used. In contrast to the mouse tumor models used in this thesis that harbor two alleles of each MHC haplotype, human cancers usually harbor only one allele of a certain MHC haplotype, which makes escape due to MHC loss more likely. One way to circumvent the issue of MHC loss could be to use a CAR instead of a TCR which allows T cells to target the mutant neoantigen directly and independent of MHC presentation. However, CAR T cells have shown some success against solid tumors in mouse models (Textor, Listopad et al. 2014) but little to no efficiency in the treatment of solid tumor in human patients (Yeku, Li et al. 2017, D'Aloia, Zizzari et al. 2018) and ideas of combinations of CAR-$CD8^+$ with CAR-$CD4^+$ T cells improved therapy only against hematopoietic cancers (Turtle, Hanafi et al. 2016, Turtle, Hanafi et al. 2016, O'Rourke, Nasrallah et al. 2017). The disadvantage of CAR T cells could be their inability to recognize APCs in the tumor stroma.

According to the four-cell interaction hypothesis the combination of CAR-CD8$^+$ with CAR-CD4$^+$ T cells would not involve targeting the stroma and it would lack the APC-T cell interactions needed for activation. An approach against solid tumors could be using stroma recognizing, TCR-transduced CD4$^+$ T cells together with cancer cell-recognizing CAR-transduced CD8$^+$ T cells. However, this scenario would only work if no direct CD4-CD8 interactions are required, since TCR-CD4$^+$ T cells would act on stroma only and CAR-CD8$^+$ T cells would operate on cancer cells only because the CAR-CD8$^+$ T cells would have no reason to bind to an APC by recognizing cross-presented antigen. Thus, the APC would not mediate the CD4-CD8 interaction if needed for complete CD8$^+$ T cell activation and successful tumor eradication. Therefore, a more successful approach to destroy MHC class I-negative cancer cells could be the use of APC recognizing CD4$^+$ T cells together with CD8$^+$ T cells that are expressing both, a TCR and a CAR. These double-transduced CD8$^+$ T cells would recognize tumor stromal APCs which cross-present cancer-specific antigens with their TCR and recognize the MHC class I-negative cancer cells with their CAR. Tumor stroma recognizing CD4$^+$ T cells would still engage APCs and a four-cell type interaction between CD4$^+$ with CD8$^+$ T cells together with APC and cancer cells would again be possible and could achieve tumor eradication.

7.7 Connection between TCRs and their T cell origin in mouse models

The mutant-neoantigen specific TCRs used in this thesis were isolated from either CD8$^+$ or CD4$^+$ T cell clones and were transferred by TCR-transduction into the same T cell types. The proposed four-cell type interaction is based on the knowledge that CD4$^+$ T cells were required for the CD8$^+$ T cells to eradicate the cancer. This does not prove that both types of T cells are always essential for tumor eradication of other cancers, for which TCR-redirected therapy of only CD8$^+$ T cells could arguably be as efficient as a combination of CD4$^+$ and CD8$^+$ T cells. It was shown that CD8$^+$ T cells targeting only tumor stroma can also induce tumor regression followed by growth arrest (Zhang, Zhang et al. 2008) but this study targeted a largely over-expressed model antigen. Additionally, high-affinity TCRs can activate T cells without the need of costimulatory molecules such as CD8 (Kerry, Buslepp et al. 2003) or CD4 (Nishimura, Avichezer et al. 1999) but their efficiency in eradicating established tumors remained unknown. A possible combination of anti-mRPL9-transduced CD8$^+$ T cells with anti-6132A-A1-transduced CD8$^+$ T cells could also be able to eradicate established 6132A tumors. Conversely, the combination of anti-6132A-A1-transduced CD4$^+$ T cells together with anti-6132A-A1-transduced CD8$^+$ T cells would also be able to recognize both, tumor stroma and cancer cells directly and close CD4-CD8 interactions could also still be possible (Kuball, Schmitz et al. 2005) in a four cell-type interaction. It would be

valuable to understand whether TCRs only deliver T cells to their targets (cancer cells or tumor stroma) and direct the T cells to the cluster for proper activation or whether TCR function depends also on the correct T cell subtype ($CD4^+$ and/or $CD8^+$) the TCR is being transferred in for effective therapy.

The TCRs used in this dissertation were generated from immunized, healthy immune competent mice. Due to the immunization process, damaged tissue and an inflamed environment with immunological danger signals are created which leads to activation of the innate and adaptive immune system (Schreiber, Rowley et al. 2006). It is discussed that the successful activation of the immune response relies on the release of danger signals that occur in the event of tissue damage (Janeway 1992). Only initially, tumors may develop without the generation of danger signals and that an immune response may not occur. However, during development cancers eventually cause tissue damage by destruction of blood vessels due to growth into capillary blood supply. This results into cell necrosis and apoptosis that releases associated molecular patterns such as PAMP's and DAMP's (Demaria, Pikarsky et al. 2010) that can activate the immune response. Nonetheless, the immune response from immune tumor-free mice and cancer bearing mice could be very different including the TCRs generated. Thus, it is not known whether tumor-bearing mice would be able to generate therapeutically useful TCRs as well. In order to examine that question, a system of tumor development in immune competent mice and in the absent of tissue damage would be needed. In an optimized scenario, mutant neoantigen expression is induced (Shockett and Schatz 1996) after the tumor is established and danger signals caused by the cancer cell injection have vanished. In this situation, the immune response to a particular mutant neoantigen, e.g. mRPL9 or mDDX5 which are valuable T cell targets, could be studied and compared to immunized mice. However, those systems of antigen induction have their own bias towards apoptosis resistant cancer cells (Moullan, Mouchiroud et al. 2015) and compromised T cell activation (Ottina, Peperzak et al. 2017, Schmitt, Schulze-Osthoff et al. 2018).

The mouse strains used in this thesis were immune compromised $Rag^{-/-}$ mice and not immune-competent wild-type mice. Therefore, it cannot be excluded that the endogenous adaptive immune system influences the success of adoptive T cell transfer. It is reported that especially $CD4^+$ Tregs suppress successful immune responses in the tumor microenvironment (Chen, Pittet et al. 2005, Jarnicki, Lysaght et al. 2006, Darrasse-Jeze, Bergot et al. 2009). Successful adoptive T cell transfer in immune-competent mice requires lymphodepletion of the recipient prior to adoptive transfer (Fefer 1969, Cheever, Greenberg et al. 1980) and especially $CD4^+$ Tregs are very susceptible to lymphodepletion regimens such as cyclophosphamide (North 1982). Therefore, $CD8^+$ T cells could benefit from the remaining endogenous $CD4^+$ helper T cells

and adoptive T cell transfer of $CD8^+$ T cells only might therefore be more effective in wild-type mice compared to $Rag^{-/-}$ mice. It could also be argued that in tumor-bearing wild-type mice, the endogenous $CD8^+$ T cell response is not functional because the required help from $CD4^+$ T cells is missing. Therefore, treatment with $CD4^+$ T cells only could also be already sufficient to achieve tumor eradication in wild type mice. Finally, an important consideration should also be given to the fact that $Rag^{-/-}$ mice are B cell deficient and lack IgA secretion, which could change the gut microbiome composition. In recent studies, it is reported that the gut microbiome in patients influences the success of immunotherapy in different kinds of cancer (Gopalakrishnan, Spencer et al. 2018, Matson, Fessler et al. 2018, Routy, Le Chatelier et al. 2018) which cannot be excluded from the data presented in this thesis.

7.8 Relevance for clinical translation

In this doctoral dissertation it was shown that curative effects with adoptive T cell therapy against cancer can be achieved with just two TCR clonotypes: one being a stroma-recognizing $CD4^+$TCR and the second being a cancer cell-recognizing $CD8^+$TCR. The finding that these two TCR clonotypes can be essential and sufficient for eradication of unmanipulated solid tumors shows that simplifications for TCR gene therapy are possible without sacrificing efficacy of adoptively transferring mutant neoantigen-specific TCR-transduced T cells. The mechanistic principle behind this success is the hypothesized four-cell type interaction as a requirement for tumor eradication.

8. References

Abelin, J. G., D. Harjanto, M. Malloy, P. Suri, T. Colson, S. P. Goulding, A. L. Creech, L. R. Serrano, G. Nasir, Y. Nasrullah, C. D. McGann, D. Velez, Y. S. Ting, A. Poran, D. A. Rothenberg, S. Chhangawala, A. Rubinsteyn, J. Hammerbacher, R. B. Gaynor, E. F. Fritsch, J. Greshock, R. C. Oslund, D. Barthelme, T. A. Addona, C. M. Arieta and M. S. Rooney (2019). "Defining HLA-II Ligand Processing and Binding Rules with Mass Spectrometry Enhances Cancer Epitope Prediction." Immunity **51**(4): 766-779 e717.

Agata, Y., A. Kawasaki, H. Nishimura, Y. Ishida, T. Tsubata, H. Yagita and T. Honjo (1996). "Expression of the PD-1 antigen on the surface of stimulated mouse T and B lymphocytes." Int Immunol **8**(5): 765-772.

Agematsu, K., T. Kobata, K. Sugita, T. Hirose, S. F. Schlossman and C. Morimoto (1995). "Direct cellular communications between CD45R0 and CD45RA T cell subsets via CD27/CD70." J Immunol **154**(8): 3627-3635.

Ahmed, K. A., L. Wang and J. Xiang (2012). "A new dynamic model of three cell interactions for CTL responses." Oncoimmunology **1**(8): 1430-1432.

Ahrends, T., A. Spanjaard, B. Pilzecker, N. Babala, A. Bovens, Y. Xiao, H. Jacobs and J. Borst (2017). "CD4(+) T Cell Help Confers a Cytotoxic T Cell Effector Program Including Coinhibitory Receptor Downregulation and Increased Tissue Invasiveness." Immunity **47**(5): 848-861 e845.

Ajore, R., D. Raiser, M. McConkey, M. Joud, B. Boidol, B. Mar, G. Saksena, D. M. Weinstock, S. Armstrong, S. R. Ellis, B. L. Ebert and B. Nilsson (2017). "Deletion of ribosomal protein genes is a common vulnerability in human cancer, especially in concert with TP53 mutations." EMBO Mol Med **9**(4): 498-507.

Alexandrov, L. B., S. Nik-Zainal, D. C. Wedge, S. A. Aparicio, S. Behjati, A. V. Biankin, G. R. Bignell, N. Bolli, A. Borg, A. L. Borresen-Dale, S. Boyault, B. Burkhardt, A. P. Butler, C. Caldas, H. R. Davies, C. Desmedt, R. Eils, J. E. Eyfjord, J. A. Foekens, M. Greaves, F. Hosoda, B. Hutter, T. Ilicic, S. Imbeaud, M. Imielinski, N. Jager, D. T. Jones, D. Jones, S. Knappskog, M. Kool, S. R. Lakhani, C. Lopez-Otin, S. Martin, N. C. Munshi, H. Nakamura, P. A. Northcott, M. Pajic, E.

Papaemmanuil, A. Paradiso, J. V. Pearson, X. S. Puente, K. Raine, M. Ramakrishna, A. L. Richardson, J. Richter, P. Rosenstiel, M. Schlesner, T. N. Schumacher, P. N. Span, J. W. Teague, Y. Totoki, A. N. Tutt, R. Valdes-Mas, M. M. van Buuren, L. van 't Veer, A. Vincent-Salomon, N. Waddell, L. R. Yates, I. Australian Pancreatic Cancer Genome, I. B. C. Consortium, I. M.-S. Consortium, I. PedBrain, J. Zucman-Rossi, P. A. Futreal, U. McDermott, P. Lichter, M. Meyerson, S. M. Grimmond, R. Siebert, E. Campo, T. Shibata, S. M. Pfister, P. J. Campbell and M. R. Stratton (2013). "Signatures of mutational processes in human cancer." Nature **500**(7463): 415-421.

Alspach, E., D. M. Lussier, A. P. Miceli, I. Kizhvatov, M. DuPage, A. M. Luoma, W. Meng, C. F. Lichti, E. Esaulova, A. N. Vomund, D. Runci, J. P. Ward, M. M. Gubin, R. F. V. Medrano, C. D. Arthur, J. M. White, K. C. F. Sheehan, A. Chen, K. W. Wucherpfennig, T. Jacks, E. R. Unanue, M. N. Artyomov and R. D. Schreiber (2019). "MHC-II neoantigens shape tumour immunity and response to immunotherapy." Nature **574**(7780): 696-701.

Amsterdam, A., K. C. Sadler, K. Lai, S. Farrington, R. T. Bronson, J. A. Lees and N. Hopkins (2004). "Many ribosomal protein genes are cancer genes in zebrafish." PLoS Biol **2**(5): E139.

Anderson, H. A., E. M. Hiltbold and P. A. Roche (2000). "Concentration of MHC class II molecules in lipid rafts facilitates antigen presentation." Nat Immunol **1**(2): 156-162.

Aoki, M., E. Blazek and P. K. Vogt (2001). "A role of the kinase mTOR in cellular transformation induced by the oncoproteins P3k and Akt." Proc Natl Acad Sci U S A **98**(1): 136-141.

Arens, R., K. Tesselaar, P. A. Baars, G. M. van Schijndel, J. Hendriks, S. T. Pals, P. Krimpenfort, J. Borst, M. H. van Oers and R. A. van Lier (2001). "Constitutive CD27/CD70 interaction induces expansion of effector-type T cells and results in IFNgamma-mediated B cell depletion." Immunity **15**(5): 801-812.

Arina, A., C. Idel, E. M. Hyjek, M. L. Alegre, Y. Wang, V. P. Bindokas, R. R. Weichselbaum and H. Schreiber (2016). "Tumor-associated fibroblasts predominantly come from local and not circulating precursors." Proc Natl Acad Sci U S A **113**(27): 7551-7556.

Arina, A., T. Karrison, E. Galka, K. Schreiber, R. R. Weichselbaum and H. Schreiber (2017). "Transfer of Allogeneic CD4+ T Cells Rescues CD8+ T Cells in Anti-PD-L1-Resistant Tumors Leading to Tumor Eradication." Cancer Immunol Res **5**(2): 127-136.

Arina, A., K. Schreiber, D. C. Binder, T. G. Karrison, R. B. Liu and H. Schreiber (2014). "Adoptively transferred immune T cells eradicate established tumors despite cancer-induced immune suppression." J Immunol **192**(3): 1286-1293.

Austyn, J. M. and S. Gordon (1981). "F4/80, a monoclonal antibody directed specifically against the mouse macrophage." Eur J Immunol **11**(10): 805-815.

Bai, X. F., J. Liu, O. Li, P. Zheng and Y. Liu (2003). "Antigenic drift as a mechanism for tumor evasion of destruction by cytolytic T lymphocytes." J Clin Invest **111**(10): 1487-1496.

Bai, X. F., J. Q. Liu, P. S. Joshi, L. Wang, L. Yin, J. Labanowska, N. Heerema, P. Zheng and Y. Liu (2006). "Different lineages of P1A-expressing cancer cells use divergent modes of immune evasion for T-cell adoptive therapy." Cancer Res **66**(16): 8241-8249.

Baldwin, R. W. (1955). "Immunity to methylcholanthrene-induced tumours in inbred rats following atrophy and regression of the implanted tumours." Br J Cancer **9**(4): 652-657.

Barth, R. J., Jr., J. J. Mule, P. J. Spiess and S. A. Rosenberg (1991). "Interferon gamma and tumor necrosis factor have a role in tumor regressions mediated by murine CD8+ tumor-infiltrating lymphocytes." J Exp Med **173**(3): 647-658.

Basombrio, M. A. (1970). "Search for common antigenicities among twenty-five sarcomas induced by methylcholanthrene." Cancer Res **30**(10): 2458-2462.

Basombrio, M. A. and R. T. Prehn (1972). "Studies on the basis for diversity and time of appearance of antigens in chemically induced tumors." Natl Cancer Inst Monogr **35**: 117-124.

Bates, G. J., S. M. Nicol, B. J. Wilson, A. M. Jacobs, J. C. Bourdon, J. Wardrop, D. J. Gregory, D. P. Lane, N. D. Perkins and F. V. Fuller-Pace (2005). "The DEAD box protein p68: a novel transcriptional coactivator of the p53 tumour suppressor." EMBO J **24**(3): 543-553.

Beck-Engeser, G. B., P. A. Monach, D. Mumberg, F. Yang, S. Wanderling, K. Schreiber, R. Espinosa, 3rd, M. M. Le Beau, S. C. Meredith and H. Schreiber (2001). "Point mutation in essential genes with loss or mutation of the second allele: relevance to the retention of tumor-specific antigens." J Exp Med **194**(3): 285-300.

Binnewies, M., E. W. Roberts, K. Kersten, V. Chan, D. F. Fearon, M. Merad, L. M. Coussens, D. I. Gabrilovich, S. Ostrand-Rosenberg, C. C. Hedrick, R. H. Vonderheide, M. J. Pittet, R. K. Jain, W. Zou, T. K. Howcroft, E. C. Woodhouse, R. A. Weinberg and M. F. Krummel (2018). "Understanding the tumor immune microenvironment (TIME) for effective therapy." Nat Med **24**(5): 541-550.

Bjorkman, P. J., M. A. Saper, B. Samraoui, W. S. Bennett, J. L. Strominger and D. C. Wiley (1987). "Structure of the human class I histocompatibility antigen, HLA-A2." Nature **329**(6139): 506-512.

Blades, R. A., P. J. Keating, L. J. McWilliam, N. J. George and P. L. Stern (1995). "Loss of HLA class I expression in prostate cancer: implications for immunotherapy." Urology **46**(5): 681-686; discussion 686-687.

Borst, J., S. Alexander, J. Elder and C. Terhorst (1983). "The T3 complex on human T lymphocytes involves four structurally distinct glycoproteins." J Biol Chem **258**(8): 5135-5141.

Bos, R. and L. A. Sherman (2010). "CD4+ T-cell help in the tumor milieu is required for recruitment and cytolytic function of CD8+ T lymphocytes." Cancer Res **70**(21): 8368-8377.

Bouzin, C. and O. Feron (2007). "Targeting tumor stroma and exploiting mature tumor vasculature to improve anti-cancer drug delivery." Drug Resist Updat **10**(3): 109-120.

Brandes, M., K. Willimann and B. Moser (2005). "Professional antigen-presentation function by human gammadelta T Cells." Science **309**(5732): 264-268.

Bretscher, P. and M. Cohn (1970). "A theory of self-nonself discrimination." Science **169**(3950): 1042-1049.

Bretscher, P. A. (1999). "A two-step, two-signal model for the primary activation of precursor helper T cells." Proc Natl Acad Sci U S A **96**(1): 185-190.

Bretscher, P. A. (2019). "The history of the two-signal model of lymphocyte activation: A personal perspective." Scand J Immunol **89**(6): e12762.

Briesemeister, D., D. Sommermeyer, C. Loddenkemper, R. Loew, W. Uckert, T. Blankenstein and T. Kammertoens (2011). "Tumor rejection by local interferon gamma induction in established tumors is associated with blood vessel destruction and necrosis." Int J Cancer **128**(2): 371-378.

Brioli, A., L. Melchor, M. Cavo and G. J. Morgan (2014). "The impact of intra-clonal heterogeneity on the treatment of multiple myeloma." Br J Haematol **165**(4): 441-454.

Brown, E. L., J. L. Wooters, C. R. Ferenz, C. M. O'Brien, R. M. Hewick and S. H. Herrmann (1994). "Characterization of peptide binding to the murine MHC class I H-2Kk molecule. Sequencing of the bound peptides and direct binding of synthetic peptides to isolated class I molecules." J Immunol **153**(7): 3079-3092.

Brown, J. H., T. S. Jardetzky, J. C. Gorga, L. J. Stern, R. G. Urban, J. L. Strominger and D. C. Wiley (1993). "Three-dimensional structure of the human class II histocompatibility antigen HLA-DR1." Nature **364**(6432): 33-39.

Brugnoni, D., P. Airo, R. Marino, L. D. Notarangelo, R. A. van Lier and R. Cattaneo (1997). "CD70 expression on T-cell subpopulations: study of normal individuals and patients with chronic immune activation." Immunol Lett **55**(2): 99-104.

Bullock, T. N. and H. Yagita (2005). "Induction of CD70 on dendritic cells through CD40 or TLR stimulation contributes to the development of CD8+ T cell responses in the absence of CD4+ T cells." J Immunol **174**(2): 710-717.

Bunnell, B. A., L. M. Muul, R. E. Donahue, R. M. Blaese and R. A. Morgan (1995). "High-efficiency retroviral-mediated gene transfer into human and nonhuman primate peripheral blood lymphocytes." Proc Natl Acad Sci U S A **92**(17): 7739-7743.

Cameron, B. J., A. B. Gerry, J. Dukes, J. V. Harper, V. Kannan, F. C. Bianchi, F. Grand, J. E. Brewer, M. Gupta, G. Plesa, G. Bossi, A. Vuidepot, A. S. Powlesland, A. Legg, K. J. Adams, A. D. Bennett, N. J. Pumphrey, D. D. Williams, G. Binder-Scholl, I. Kulikovskaya, B. L. Levine, J. L. Riley, A. Varela-Rohena, E. A. Stadtmauer, A. P. Rapoport, G. P. Linette, C. H. June, N. J. Hassan, M. Kalos and B. K. Jakobsen (2013). "Identification of a Titin-derived HLA-A1-presented peptide as a cross-reactive target for engineered MAGE A3-directed T cells." Sci Transl Med **5**(197): 197ra103.

Carlsson, E., K. Krohn, K. Ovaska, P. Lindberg, V. Hayry, P. Maliniemi, A. Lintulahti, M. Korja, R. Kivisaari, S. Hussein, S. Sarna, K. Niiranen, S. Hautaniemi, H. Haapasalo and A. Ranki (2013). "Neuron navigator 3 alterations in nervous system tumors associate with tumor malignancy grade and prognosis." Genes Chromosomes Cancer **52**(2): 191-201.

Carreno, B. M., V. Magrini, M. Becker-Hapak, S. Kaabinejadian, J. Hundal, A. A. Petti, A. Ly, W. R. Lie, W. H. Hildebrand, E. R. Mardis and G. P. Linette (2015). "Cancer immunotherapy. A dendritic cell vaccine increases the breadth and diversity of melanoma neoantigen-specific T cells." Science **348**(6236): 803-808.

Cella, M., D. Scheidegger, K. Palmer-Lehmann, P. Lane, A. Lanzavecchia and G. Alber (1996). "Ligation of CD40 on dendritic cells triggers production of high levels of interleukin-12 and enhances T cell stimulatory capacity: T-T help via APC activation." J Exp Med **184**(2): 747-752.

Chang, T. W., P. C. Kung, S. P. Gingras and G. Goldstein (1981). "Does OKT3 monoclonal antibody react with an antigen-recognition structure on human T cells?" Proc Natl Acad Sci U S A **78**(3): 1805-1808.

Chavez, J. C., C. Bachmeier and M. A. Kharfan-Dabaja (2019). "CAR T-cell therapy for B-cell lymphomas: clinical trial results of available products." Ther Adv Hematol **10**: 2040620719841581.

Cheever, M. A., P. D. Greenberg and A. Fefer (1980). "Specificity of adoptive chemoimmunotherapy of established syngeneic tumors." J Immunol **125**(2): 711-714.

Chen, M. L., M. J. Pittet, L. Gorelik, R. A. Flavell, R. Weissleder, H. von Boehmer and K. Khazaie (2005). "Regulatory T cells suppress tumor-specific CD8 T cell cytotoxicity through TGF-beta signals in vivo." Proc Natl Acad Sci U S A **102**(2): 419-424.

Chien, Y. H. and M. M. Davis (1993). "How alpha beta T-cell receptors 'see' peptide/MHC complexes." Immunol Today **14**(12): 597-602.

Chien, Y. H., N. R. Gascoigne, J. Kavaler, N. E. Lee and M. M. Davis (1984). "Somatic recombination in a murine T-cell receptor gene." Nature **309**(5966): 322-326.

Clevers, H., B. Alarcon, T. Wileman and C. Terhorst (1988). "The T cell receptor/CD3 complex: a dynamic protein ensemble." Annu Rev Immunol **6**: 629-662.

Cohen, M. C. and S. Cohen (1996). "Cytokine function: a study in biologic diversity." Am J Clin Pathol **105**(5): 589-598.

Cohen, S., P. E. Bigazzi and T. Yoshida (1974). "Commentary. Similarities of T cell function in cell-mediated immunity and antibody production." Cell Immunol **12**(1): 150-159.

Cohen-Dvashi, H., N. Ben-Chetrit, R. Russell, S. Carvalho, M. Lauriola, S. Nisani, M. Mancini, N. Nataraj, M. Kedmi, L. Roth, W. Kostler, A. Zeisel, A. Yitzhaky, J. Zylberg, G. Tarcic, R. Eilam, Y. Wigelman, R. Will, S. Lavi, Z. Porat, S. Wiemann, S. Ricardo, F. Schmitt, C. Caldas and Y. Yarden (2015). "Navigator-3, a modulator of cell migration, may act as a suppressor of breast cancer progression." EMBO Mol Med **7**(3): 299-314.

Collaborators, G. B. D. C. o. D. (2017). "Global, regional, and national age-sex specific mortality for 264 causes of death, 1980-2016: a systematic analysis for the Global Burden of Disease Study 2016." Lancet **390**(10100): 1151-1210.

Connor, M. E. and P. L. Stern (1990). "Loss of MHC class-I expression in cervical carcinomas." Int J Cancer **46**(6): 1029-1034.

Cresswell, P. (1994). "Assembly, transport, and function of MHC class II molecules." Annu Rev Immunol **12**: 259-293.

D'Agostino, M. and N. Raje (2020). "Anti-BCMA CAR T-cell therapy in multiple myeloma: can we do better?" Leukemia **34**(1): 21-34.

D'Aloia, M. M., I. G. Zizzari, B. Sacchetti, L. Pierelli and M. Alimandi (2018). "CAR-T cells: the long and winding road to solid tumors." Cell Death Dis **9**(3): 282.

Darrasse-Jeze, G., A. S. Bergot, A. Durgeau, F. Billiard, B. L. Salomon, J. L. Cohen, B. Bellier, K. Podsypanina and D. Klatzmann (2009). "Tumor emergence is sensed by self-specific CD44hi memory Tregs that create a dominant tolerogenic environment for tumors in mice." J Clin Invest **119**(9): 2648-2662.

Das, K., D. Eisel, C. Lenkl, A. Goyal, S. Diederichs, E. Dickes, W. Osen and S. B. Eichmuller (2017). "Generation of murine tumor cell lines deficient in MHC molecule surface expression using the CRISPR/Cas9 system." PLoS One **12**(3): e0174077.

Davila, M. L. and R. J. Brentjens (2016). "CD19-Targeted CAR T cells as novel cancer immunotherapy for relapsed or refractory B-cell acute lymphoblastic leukemia." Clin Adv Hematol Oncol **14**(10): 802-808.

Davis, M. M. and P. J. Bjorkman (1988). "T-cell antigen receptor genes and T-cell recognition." Nature **334**(6181): 395-402.

de Bruin, E. C., N. McGranahan, R. Mitter, M. Salm, D. C. Wedge, L. Yates, M. Jamal-Hanjani, S. Shafi, N. Murugaesu, A. J. Rowan, E. Gronroos, M. A. Muhammad, S. Horswell, M. Gerlinger, I. Varela, D. Jones, J. Marshall, T. Voet, P. Van Loo, D. M. Rassl, R. C. Rintoul, S. M. Janes, S. M. Lee, M. Forster, T. Ahmad, D. Lawrence, M. Falzon, A. Capitanio, T. T. Harkins, C. C. Lee, W. Tom, E. Teefe, S. C. Chen, S. Begum, A. Rabinowitz, B. Phillimore, B. Spencer-Dene, G. Stamp, Z. Szallasi, N. Matthews, A. Stewart, P. Campbell and C. Swanton (2014). "Spatial and temporal diversity in genomic instability processes defines lung cancer evolution." Science **346**(6206): 251-256.

de Goer de Herve, M. G., B. Dembele, M. Vallee, F. Herr, A. Cariou and Y. Taoufik (2010). "Direct CD4 help provision following interaction of memory CD4 and CD8 T cells with distinct antigen-presenting dendritic cells." J Immunol **185**(2): 1028-1036.

Delorme, E. J. and P. Alexander (1964). "Treatment of Primary Fibrosarcoma in the Rat with Immune Lymphocytes." Lancet **2**(7351): 117-120.

Demaria, S., E. Pikarsky, M. Karin, L. M. Coussens, Y. C. Chen, E. M. El-Omar, G. Trinchieri, S. M. Dubinett, J. T. Mao, E. Szabo, A. Krieg, G. J. Weiner, B. A. Fox, G. Coukos, E. Wang, R. T. Abraham, M. Carbone and M. T. Lotze (2010). "Cancer and inflammation: promise for biologic therapy." J Immunother **33**(4): 335-351.

Dembic, Z., W. Haas, S. Weiss, J. McCubrey, H. Kiefer, H. von Boehmer and M. Steinmetz (1986). "Transfer of specificity by murine alpha and beta T-cell receptor genes." Nature **320**(6059): 232-238.

Demotz, S., H. M. Grey and A. Sette (1990). "The minimal number of class II MHC-antigen complexes needed for T cell activation." Science **249**(4972): 1028-1030.

Doench, J. G., N. Fusi, M. Sullender, M. Hegde, E. W. Vaimberg, K. F. Donovan, I. Smith, Z. Tothova, C. Wilen, R. Orchard, H. W. Virgin, J. Listgarten and D. E. Root (2016). "Optimized sgRNA design to maximize activity and minimize off-target effects of CRISPR-Cas9." Nat Biotechnol **34**(2): 184-191.

Dong, H., S. E. Strome, D. R. Salomao, H. Tamura, F. Hirano, D. B. Flies, P. C. Roche, J. Lu, G. Zhu, K. Tamada, V. A. Lennon, E. Celis and L. Chen (2002). "Tumor-associated B7-H1 promotes T-cell apoptosis: a potential mechanism of immune evasion." Nat Med **8**(8): 793-800.

Dong, H., G. Zhu, K. Tamada and L. Chen (1999). "B7-H1, a third member of the B7 family, co-stimulates T-cell proliferation and interleukin-10 secretion." Nat Med **5**(12): 1365-1369.

Dubey, P., R. C. Hendrickson, S. C. Meredith, C. T. Siegel, J. Shabanowitz, J. C. Skipper, V. H. Engelhard, D. F. Hunt and H. Schreiber (1997). "The immunodominant antigen of an ultraviolet-induced regressor tumor is generated by a somatic point mutation in the DEAD box helicase p68." J Exp Med **185**(4): 695-705.

Dudley, M. E., J. R. Wunderlich, P. F. Robbins, J. C. Yang, P. Hwu, D. J. Schwartzentruber, S. L. Topalian, R. Sherry, N. P. Restifo, A. M. Hubicki, M. R. Robinson, M. Raffeld, P. Duray, C. A.

Seipp, L. Rogers-Freezer, K. E. Morton, S. A. Mavroukakis, D. E. White and S. A. Rosenberg (2002). "Cancer regression and autoimmunity in patients after clonal repopulation with antitumor lymphocytes." Science **298**(5594): 850-854.

Dudley, M. E., J. R. Wunderlich, J. C. Yang, R. M. Sherry, S. L. Topalian, N. P. Restifo, R. E. Royal, U. Kammula, D. E. White, S. A. Mavroukakis, L. J. Rogers, G. J. Gracia, S. A. Jones, D. P. Mangiameli, M. M. Pelletier, J. Gea-Banacloche, M. R. Robinson, D. M. Berman, A. C. Filie, A. Abati and S. A. Rosenberg (2005). "Adoptive cell transfer therapy following non-myeloablative but lymphodepleting chemotherapy for the treatment of patients with refractory metastatic melanoma." J Clin Oncol **23**(10): 2346-2357.

Durrant, L. G., K. C. Ballantyne, N. C. Armitage, R. A. Robins, R. Marksman, J. D. Hardcastle and R. W. Baldwin (1987). "Quantitation of MHC antigen expression on colorectal tumours and its association with tumour progression." Br J Cancer **56**(4): 425-432.

Dutt, S., A. Narla, K. Lin, A. Mullally, N. Abayasekara, C. Megerdichian, F. H. Wilson, T. Currie, A. Khanna-Gupta, N. Berliner, J. L. Kutok and B. L. Ebert (2011). "Haploinsufficiency for ribosomal protein genes causes selective activation of p53 in human erythroid progenitor cells." Blood **117**(9): 2567-2576.

Eberlein, T. J., M. Rosenstein and S. A. Rosenberg (1982). "Regression of a disseminated syngeneic solid tumor by systemic transfer of lymphoid cells expanded in interleukin 2." J Exp Med **156**(2): 385-397.

Eichmann, K., J. I. Jonsson, I. Falk and F. Emmrich (1987). "Effective activation of resting mouse T lymphocytes by cross-linking submitogenic concentrations of the T cell antigen receptor with either Lyt-2 or L3T4." Eur J Immunol **17**(5): 643-650.

Engels, B., H. Cam, T. Schuler, S. Indraccolo, M. Gladow, C. Baum, T. Blankenstein and W. Uckert (2003). "Retroviral vectors for high-level transgene expression in T lymphocytes." Hum Gene Ther **14**(12): 1155-1168.

Engels, B., A. S. Chervin, A. J. Sant, D. M. Kranz and H. Schreiber (2012). "Long-term persistence of CD4(+) but rapid disappearance of CD8(+) T cells expressing an MHC class I-restricted TCR of nanomolar affinity." Mol Ther **20**(3): 652-660.

Engels, B., V. H. Engelhard, J. Sidney, A. Sette, D. C. Binder, R. B. Liu, D. M. Kranz, S. C. Meredith, D. A. Rowley and H. Schreiber (2013). "Relapse or eradication of cancer is predicted by peptide-major histocompatibility complex affinity." Cancer Cell **23**(4): 516-526.

Erkan, M., S. Hausmann, C. W. Michalski, A. A. Fingerle, M. Dobritz, J. Kleeff and H. Friess (2012). "The role of stroma in pancreatic cancer: diagnostic and therapeutic implications." Nat Rev Gastroenterol Hepatol **9**(8): 454-467.

Eshhar, Z., T. Waks, G. Gross and D. G. Schindler (1993). "Specific activation and targeting of cytotoxic lymphocytes through chimeric single chains consisting of antibody-binding domains and the gamma or zeta subunits of the immunoglobulin and T-cell receptors." Proc Natl Acad Sci U S A **90**(2): 720-724.

Fancello, L., K. R. Kampen, I. J. Hofman, J. Verbeeck and K. De Keersmaecker (2017). "The ribosomal protein gene RPL5 is a haploinsufficient tumor suppressor in multiple cancer types." Oncotarget **8**(9): 14462-14478.

Feau, S., Z. Garcia, R. Arens, H. Yagita, J. Borst and S. P. Schoenberger (2012). "The CD4(+) T-cell help signal is transmitted from APC to CD8(+) T-cells via CD27-CD70 interactions." Nat Commun **3**: 948.

Fefer, A. (1969). "Immunotherapy and chemotherapy of Moloney sarcoma virus-induced tumors in mice." Cancer Res **29**(12): 2177-2183.

Foley, E. J. (1953). "Antigenic properties of methylcholanthrene-induced tumors in mice of the strain of origin." Cancer Res **13**(12): 835-837.

Fortier, S., T. MacRae, M. Bilodeau, T. Sargeant and G. Sauvageau (2015). "Haploinsufficiency screen highlights two distinct groups of ribosomal protein genes essential for embryonic stem cell fate." Proc Natl Acad Sci U S A **112**(7): 2127-2132.

Freiberg, S. M., S. (1997). "On the Growth Rates of Human Malignant Tumors: Implications for Medical Decision Making." Journal of Surgical Oncology **65**: 284 - 297.

Fuller-Pace, F. V. (2013). "The DEAD box proteins DDX5 (p68) and DDX17 (p72): multi-tasking transcriptional regulators." Biochim Biophys Acta **1829**(8): 756-763.

Gajewski, T. F., H. Schreiber and Y. X. Fu (2013). "Innate and adaptive immune cells in the tumor microenvironment." Nat Immunol **14**(10): 1014-1022.

Garboczi, D. N., P. Ghosh, U. Utz, Q. R. Fan, W. E. Biddison and D. C. Wiley (1996). "Structure of the complex between human T-cell receptor, viral peptide and HLA-A2." Nature **384**(6605): 134-141.

Garcia, K. C., M. Degano, R. L. Stanfield, A. Brunmark, M. R. Jackson, P. A. Peterson, L. Teyton and I. A. Wilson (1996). "An alphabeta T cell receptor structure at 2.5 A and its orientation in the TCR-MHC complex." Science **274**(5285): 209-219.

Garrido, F., N. Aptsiauri, E. M. Doorduijn, A. M. Garcia Lora and T. van Hall (2016). "The urgent need to recover MHC class I in cancers for effective immunotherapy." Curr Opin Immunol **39**: 44-51.

Garrido, F., F. Ruiz-Cabello and N. Aptsiauri (2017). "Rejection versus escape: the tumor MHC dilemma." Cancer Immunol Immunother **66**(2): 259-271.

Gerlinger, M., A. J. Rowan, S. Horswell, M. Math, J. Larkin, D. Endesfelder, E. Gronroos, P. Martinez, N. Matthews, A. Stewart, P. Tarpey, I. Varela, B. Phillimore, S. Begum, N. Q. McDonald, A. Butler, D. Jones, K. Raine, C. Latimer, C. R. Santos, M. Nohadani, A. C. Eklund, B. Spencer-Dene, G. Clark, L. Pickering, G. Stamp, M. Gore, Z. Szallasi, J. Downward, P. A. Futreal and C. Swanton (2012). "Intratumor heterogeneity and branched evolution revealed by multiregion sequencing." N Engl J Med **366**(10): 883-892.

Ghosh, S., S. B. Koralov, I. Stevanovic, M. S. Sundrud, Y. Sasaki, K. Rajewsky, A. Rao and M. R. Muller (2010). "Hyperactivation of nuclear factor of activated T cells 1 (NFAT1) in T cells

attenuates severity of murine autoimmune encephalomyelitis." Proc Natl Acad Sci U S A **107**(34): 15169-15174.

Gil-Torregrosa, B. C., A. M. Lennon-Dumenil, B. Kessler, P. Guermonprez, H. L. Ploegh, D. Fruci, P. van Endert and S. Amigorena (2004). "Control of cross-presentation during dendritic cell maturation." Eur J Immunol **34**(2): 398-407.

Globerson, A. and M. Feldman (1964). "Antigenic Specificity of Benzo(a)Pyrene-Induced Sarcomas." J Natl Cancer Inst **32**: 1229-1243.

Gompertz, B. (1825). "On the Nature of the Function Expressive of the Law of Human Mortality, and on a New Mode of Determining the Value of Life Contingencies." Philosophical Transactions of the Royal Society of London **115**: 513 - 583.

Goodman, A. M., S. Kato, L. Bazhenova, S. P. Patel, G. M. Frampton, V. Miller, P. J. Stephens, G. A. Daniels and R. Kurzrock (2017). "Tumor Mutational Burden as an Independent Predictor of Response to Immunotherapy in Diverse Cancers." Mol Cancer Ther **16**(11): 2598-2608.

Gopalakrishnan, V., C. N. Spencer, L. Nezi, A. Reuben, M. C. Andrews, T. V. Karpinets, P. A. Prieto, D. Vicente, K. Hoffman, S. C. Wei, A. P. Cogdill, L. Zhao, C. W. Hudgens, D. S. Hutchinson, T. Manzo, M. Petaccia de Macedo, T. Cotechini, T. Kumar, W. S. Chen, S. M. Reddy, R. Szczepaniak Sloane, J. Galloway-Pena, H. Jiang, P. L. Chen, E. J. Shpall, K. Rezvani, A. M. Alousi, R. F. Chemaly, S. Shelburne, L. M. Vence, P. C. Okhuysen, V. B. Jensen, A. G. Swennes, F. McAllister, E. Marcelo Riquelme Sanchez, Y. Zhang, E. Le Chatelier, L. Zitvogel, N. Pons, J. L. Austin-Breneman, L. E. Haydu, E. M. Burton, J. M. Gardner, E. Sirmans, J. Hu, A. J. Lazar, T. Tsujikawa, A. Diab, H. Tawbi, I. C. Glitza, W. J. Hwu, S. P. Patel, S. E. Woodman, R. N. Amaria, M. A. Davies, J. E. Gershenwald, P. Hwu, J. E. Lee, J. Zhang, L. M. Coussens, Z. A. Cooper, P. A. Futreal, C. R. Daniel, N. J. Ajami, J. F. Petrosino, M. T. Tetzlaff, P. Sharma, J. P. Allison, R. R. Jenq and J. A. Wargo (2018). "Gut microbiome modulates response to anti-PD-1 immunotherapy in melanoma patients." Science **359**(6371): 97-103.

Govindan, R. (2014). "Cancer. Attack of the clones." Science **346**(6206): 169-170.

Govindan, R., L. Ding, M. Griffith, J. Subramanian, N. D. Dees, K. L. Kanchi, C. A. Maher, R. Fulton, L. Fulton, J. Wallis, K. Chen, J. Walker, S. McDonald, R. Bose, D. Ornitz, D. Xiong, M. You, D. J. Dooling, M. Watson, E. R. Mardis and R. K. Wilson (2012). "Genomic landscape of non-small cell lung cancer in smokers and never-smokers." Cell **150**(6): 1121-1134.

Gravestein, L. A., J. D. Nieland, A. M. Kruisbeek and J. Borst (1995). "Novel mAbs reveal potent co-stimulatory activity of murine CD27." Int Immunol **7**(4): 551-557.

Gray, P. W. and D. V. Goeddel (1983). "Cloning and expression of murine immune interferon cDNA." Proc Natl Acad Sci U S A **80**(19): 5842-5846.

Greenberg, P. D., D. E. Kern and M. A. Cheever (1985). "Therapy of disseminated murine leukemia with cyclophosphamide and immune Lyt-1+,2- T cells. Tumor eradication does not require participation of cytotoxic T cells." J Exp Med **161**(5): 1122-1134.

Grewal, I. S., J. Xu and R. A. Flavell (1995). "Impairment of antigen-specific T-cell priming in mice lacking CD40 ligand." Nature **378**(6557): 617-620.

Gross, G., T. Waks and Z. Eshhar (1989). "Expression of immunoglobulin-T-cell receptor chimeric molecules as functional receptors with antibody-type specificity." Proc Natl Acad Sci U S A **86**(24): 10024-10028.

Gross, L. (1943). "Intradermal Immunization of C3H Mice against a Sarcoma That Originated in an Animal of the Same Line." Cancer Research(3): 326 - 333.

Gupta, P. B., C. M. Fillmore, G. Jiang, S. D. Shapira, K. Tao, C. Kuperwasser and E. S. Lander (2011). "Stochastic state transitions give rise to phenotypic equilibrium in populations of cancer cells." Cell **146**(4): 633-644.

Haldane, J. B. (2004). "The rate of spontaneous mutation of a human gene. 1935." J Genet **83**(3): 235-244.

Hansen, J. M., P.; Nowinski, R. C. (1980). "Monoelonal Antibodies Identifying a Novel T-Cell Antigen and Ia Antigens of Human Lymphocytes." Immunogenetics **10**: 247 - 260.

Harding, C. V. and E. R. Unanue (1990). "Quantitation of antigen-presenting cell MHC class II/peptide complexes necessary for T-cell stimulation." Nature **346**(6284): 574-576.

Haupt, Y., R. Maya, A. Kazaz and M. Oren (1997). "Mdm2 promotes the rapid degradation of p53." Nature **387**(6630): 296-299.

Hedrick, S. M., D. I. Cohen, E. A. Nielsen and M. M. Davis (1984). "Isolation of cDNA clones encoding T cell-specific membrane-associated proteins." Nature **308**(5955): 149-153.

Hendriks, J., L. A. Gravestein, K. Tesselaar, R. A. van Lier, T. N. Schumacher and J. Borst (2000). "CD27 is required for generation and long-term maintenance of T cell immunity." Nat Immunol **1**(5): 433-440.

Honjo, K., X. Xu and R. P. Bucy (2004). "CD4+ T-cell receptor transgenic T cells alone can reject vascularized heart transplants through the indirect pathway of alloantigen recognition." Transplantation **77**(3): 452-455.

Huang, J., M. Brameshuber, X. Zeng, J. Xie, Q. J. Li, Y. H. Chien, S. Valitutti and M. M. Davis (2013). "A single peptide-major histocompatibility complex ligand triggers digital cytokine secretion in CD4(+) T cells." Immunity **39**(5): 846-857.

Hundal, J., B. M. Carreno, A. A. Petti, G. P. Linette, O. L. Griffith, E. R. Mardis and M. Griffith (2016). "pVAC-Seq: A genome-guided in silico approach to identifying tumor neoantigens." Genome Med **8**(1): 11.

Ibe, S., Z. Qin, T. Schuler, S. Preiss and T. Blankenstein (2001). "Tumor rejection by disturbing tumor stroma cell interactions." J Exp Med **194**(11): 1549-1559.

Inaba, K., S. Turley, F. Yamaide, T. Iyoda, K. Mahnke, M. Inaba, M. Pack, M. Subklewe, B. Sauter, D. Sheff, M. Albert, N. Bhardwaj, I. Mellman and R. M. Steinman (1998). "Efficient presentation of phagocytosed cellular fragments on the major histocompatibility complex class II products of dendritic cells." J Exp Med **188**(11): 2163-2173.

Ishida, Y., Y. Agata, K. Shibahara and T. Honjo (1992). "Induced expression of PD-1, a novel member of the immunoglobulin gene superfamily, upon programmed cell death." EMBO J **11**(11): 3887-3895.

Jackson, A. L. and L. A. Loeb (1998). "The mutation rate and cancer." Genetics **148**(4): 1483-1490.

Janeway, C. A., Jr. (1989). "Approaching the asymptote? Evolution and revolution in immunology." Cold Spring Harb Symp Quant Biol **54 Pt 1**: 1-13.

Janeway, C. A., Jr. (1992). "The immune system evolved to discriminate infectious nonself from noninfectious self." Immunol Today **13**(1): 11-16.

Janeway, C. A., Jr., S. Haque, L. A. Smith and K. Saizawa (1987). "The role of the murine L3T4 molecule in T cell activation: differential effects of anti-L3T4 on activation by monoclonal anti-receptor antibodies." J Mol Cell Immunol **3**(2): 121-131.

Jarnicki, A. G., J. Lysaght, S. Todryk and K. H. Mills (2006). "Suppression of antitumor immunity by IL-10 and TGF-beta-producing T cells infiltrating the growing tumor: influence of tumor environment on the induction of CD4+ and CD8+ regulatory T cells." J Immunol **177**(2): 896-904.

Jerne, N. K. (1960). "Immunological speculations." Annu Rev Microbiol **14**: 341-358.

June, C. H., J. A. Bluestone, L. M. Nadler and C. B. Thompson (1994). "The B7 and CD28 receptor families." Immunol Today **15**(7): 321-331.

Kaklamanis, L., A. Townsend, I. A. Doussis-Anagnostopoulou, N. Mortensen, A. L. Harris and K. C. Gatter (1994). "Loss of major histocompatibility complex-encoded transporter associated with antigen presentation (TAP) in colorectal cancer." Am J Pathol **145**(3): 505-509.

Kammertoens, T., C. Friese, A. Arina, C. Idel, D. Briesemeister, M. Rothe, A. Ivanov, A. Szymborska, G. Patone, S. Kunz, D. Sommermeyer, B. Engels, M. Leisegang, A. Textor, H. J. Fehling, M. Fruttiger, M. Lohoff, A. Herrmann, H. Yu, R. Weichselbaum, W. Uckert, N. Hubner, H.

Gerhardt, D. Beule, H. Schreiber and T. Blankenstein (2017). "Tumour ischaemia by interferon-gamma resembles physiological blood vessel regression." Nature **545**(7652): 98-102.

Kappler, J. W., N. Roehm and P. Marrack (1987). "T cell tolerance by clonal elimination in the thymus." Cell **49**(2): 273-280.

Kelly, P. N., A. Dakic, J. M. Adams, S. L. Nutt and A. Strasser (2007). "Tumor growth need not be driven by rare cancer stem cells." Science **317**(5836): 337.

Kerry, S. E., J. Buslepp, L. A. Cramer, R. Maile, L. L. Hensley, A. I. Nielsen, P. Kavathas, B. J. Vilen, E. J. Collins and J. A. Frelinger (2003). "Interplay between TCR affinity and necessity of coreceptor ligation: high-affinity peptide-MHC/TCR interaction overcomes lack of CD8 engagement." J Immunol **171**(9): 4493-4503.

Keskin, D. B., A. J. Anandappa, J. Sun, I. Tirosh, N. D. Mathewson, S. Li, G. Oliveira, A. Giobbie-Hurder, K. Felt, E. Gjini, S. A. Shukla, Z. Hu, L. Li, P. M. Le, R. L. Allesoe, A. R. Richman, M. S. Kowalczyk, S. Abdelrahman, J. E. Geduldig, S. Charbonneau, K. Pelton, J. B. Iorgulescu, L. Elagina, W. Zhang, O. Olive, C. McCluskey, L. R. Olsen, J. Stevens, W. J. Lane, A. M. Salazar, H. Daley, P. Y. Wen, E. A. Chiocca, M. Harden, N. J. Lennon, S. Gabriel, G. Getz, E. S. Lander, A. Regev, J. Ritz, D. Neuberg, S. J. Rodig, K. L. Ligon, M. L. Suva, K. W. Wucherpfennig, N. Hacohen, E. F. Fritsch, K. J. Livak, P. A. Ott, C. J. Wu and D. A. Reardon (2019). "Neoantigen vaccine generates intratumoral T cell responses in phase Ib glioblastoma trial." Nature **565**(7738): 234-239.

Khandelwal, S. and P. A. Roche (2010). "Distinct MHC class II molecules are associated on the dendritic cell surface in cholesterol-dependent membrane microdomains." J Biol Chem **285**(46): 35303-35310.

Klein, G., H. O. Sjogren, E. Klein and K. E. Hellstrom (1960). "Demonstration of resistance against methylcholanthrene-induced sarcomas in the primary autochthonous host." Cancer Res **20**: 1561-1572.

Koch, F., U. Stanzl, P. Jennewein, K. Janke, C. Heufler, E. Kampgen, N. Romani and G. Schuler (1996). "High level IL-12 production by murine dendritic cells: upregulation via MHC class II and CD40 molecules and downregulation by IL-4 and IL-10." J Exp Med **184**(2): 741-746.

Kochenderfer, J. N. and S. A. Rosenberg (2013). "Treating B-cell cancer with T cells expressing anti-CD19 chimeric antigen receptors." Nat Rev Clin Oncol **10**(5): 267-276.

Kochenderfer, J. N., W. H. Wilson, J. E. Janik, M. E. Dudley, M. Stetler-Stevenson, S. A. Feldman, I. Maric, M. Raffeld, D. A. Nathan, B. J. Lanier, R. A. Morgan and S. A. Rosenberg (2010). "Eradication of B-lineage cells and regression of lymphoma in a patient treated with autologous T cells genetically engineered to recognize CD19." Blood **116**(20): 4099-4102.

Kokolo, M. and M. Bach-Elias (2017). "Downregulation of p68 RNA Helicase (DDX5) Activates a Survival Pathway Involving mTOR and MDM2 Signals." Folia Biol (Praha) **63**(2): 52-59.

Korkolopoulou, P., L. Kaklamanis, F. Pezzella, A. L. Harris and K. C. Gatter (1996). "Loss of antigen-presenting molecules (MHC class I and TAP-1) in lung cancer." Br J Cancer **73**(2): 148-153.

Kowolik, C. M., M. S. Topp, S. Gonzalez, T. Pfeiffer, S. Olivares, N. Gonzalez, D. D. Smith, S. J. Forman, M. C. Jensen and L. J. Cooper (2006). "CD28 costimulation provided through a CD19-specific chimeric antigen receptor enhances in vivo persistence and antitumor efficacy of adoptively transferred T cells." Cancer Res **66**(22): 10995-11004.

Kreiter, S., M. Vormehr, N. van de Roemer, M. Diken, M. Lower, J. Diekmann, S. Boegel, B. Schrors, F. Vascotto, J. C. Castle, A. D. Tadmor, S. P. Schoenberger, C. Huber, O. Tureci and U. Sahin (2015). "Mutant MHC class II epitopes drive therapeutic immune responses to cancer." Nature **520**(7549): 692-696.

Kuball, J., F. W. Schmitz, R. H. Voss, E. A. Ferreira, R. Engel, P. Guillaume, S. Strand, P. Romero, C. Huber, L. A. Sherman and M. Theobald (2005). "Cooperation of human tumor-reactive CD4+ and CD8+ T cells after redirection of their specificity by a high-affinity p53A2.1-specific TCR." Immunity **22**(1): 117-129.

Kula, T., M. H. Dezfulian, C. I. Wang, N. S. Abdelfattah, Z. C. Hartman, K. W. Wucherpfennig, H. K. Lyerly and S. J. Elledge (2019). "T-Scan: A Genome-wide Method for the Systematic Discovery of T Cell Epitopes." Cell **178**(4): 1016-1028 e1013.

Kumamoto, Y., L. M. Mattei, S. Sellers, G. W. Payne and A. Iwasaki (2011). "CD4+ T cells support cytotoxic T lymphocyte priming by controlling lymph node input." Proc Natl Acad Sci U S A **108**(21): 8749-8754.

Laird, A. K. (1964). "Dynamics of Tumor Growth." Br J Cancer **13**: 490-502.

Lanitis, E., D. Dangaj, M. Irving and G. Coukos (2017). "Mechanisms regulating T-cell infiltration and activity in solid tumors." Ann Oncol **28**(suppl_12): xii18-xii32.

Lawrence, M. S., P. Stojanov, C. H. Mermel, J. T. Robinson, L. A. Garraway, T. R. Golub, M. Meyerson, S. B. Gabriel, E. S. Lander and G. Getz (2014). "Discovery and saturation analysis of cancer genes across 21 tumour types." Nature **505**(7484): 495-501.

Lawrence, M. S., P. Stojanov, P. Polak, G. V. Kryukov, K. Cibulskis, A. Sivachenko, S. L. Carter, C. Stewart, C. H. Mermel, S. A. Roberts, A. Kiezun, P. S. Hammerman, A. McKenna, Y. Drier, L. Zou, A. H. Ramos, T. J. Pugh, N. Stransky, E. Helman, J. Kim, C. Sougnez, L. Ambrogio, E. Nickerson, E. Shefler, M. L. Cortes, D. Auclair, G. Saksena, D. Voet, M. Noble, D. DiCara, P. Lin, L. Lichtenstein, D. I. Heiman, T. Fennell, M. Imielinski, B. Hernandez, E. Hodis, S. Baca, A. M. Dulak, J. Lohr, D. A. Landau, C. J. Wu, J. Melendez-Zajgla, A. Hidalgo-Miranda, A. Koren, S. A. McCarroll, J. Mora, B. Crompton, R. Onofrio, M. Parkin, W. Winckler, K. Ardlie, S. B. Gabriel, C. W. M. Roberts, J. A. Biegel, K. Stegmaier, A. J. Bass, L. A. Garraway, M. Meyerson, T. R. Golub, D. A. Gordenin, S. Sunyaev, E. S. Lander and G. Getz (2013). "Mutational heterogeneity in cancer and the search for new cancer-associated genes." Nature **499**(7457): 214-218.

Ledbetter, J. A., C. H. June, L. S. Grosmaire and P. S. Rabinovitch (1987). "Crosslinking of surface antigens causes mobilization of intracellular ionized calcium in T lymphocytes." Proc Natl Acad Sci U S A **84**(5): 1384-1388.

Leisegang, M., B. Engels, K. Schreiber, P. Y. Yew, K. Kiyotani, C. Idel, A. Arina, J. Duraiswamy, R. R. Weichselbaum, W. Uckert, Y. Nakamura and H. Schreiber (2016). "Eradication of Large

Solid Tumors by Gene Therapy with a T-Cell Receptor Targeting a Single Cancer-Specific Point Mutation." Clin Cancer Res **22**(11): 2734-2743.

Leisegang, M., T. Kammertoens, W. Uckert and T. Blankenstein (2016). "Targeting human melanoma neoantigens by T cell receptor gene therapy." J Clin Invest **126**(3): 854-858.

Leko, V., L. A. McDuffie, Z. Zheng, J. J. Gartner, T. D. Prickett, A. B. Apolo, P. K. Agarwal, S. A. Rosenberg and Y. C. Lu (2019). "Identification of Neoantigen-Reactive Tumor-Infiltrating Lymphocytes in Primary Bladder Cancer." J Immunol **202**(12): 3458-3467.

Lennerz, V., M. Fatho, C. Gentilini, R. A. Frye, A. Lifke, D. Ferel, C. Wolfel, C. Huber and T. Wolfel (2005). "The response of autologous T cells to a human melanoma is dominated by mutated neoantigens." Proc Natl Acad Sci U S A **102**(44): 16013-16018.

Linnemann, C., M. M. van Buuren, L. Bies, E. M. Verdegaal, R. Schotte, J. J. Calis, S. Behjati, A. Velds, H. Hilkmann, D. E. Atmioui, M. Visser, M. R. Stratton, J. B. Haanen, H. Spits, S. H. van der Burg and T. N. Schumacher (2015). "High-throughput epitope discovery reveals frequent recognition of neo-antigens by CD4+ T cells in human melanoma." Nat Med **21**(1): 81-85.

Linsley, P. S., J. L. Greene, P. Tan, J. Bradshaw, J. A. Ledbetter, C. Anasetti and N. K. Damle (1992). "Coexpression and functional cooperation of CTLA-4 and CD28 on activated T lymphocytes." J Exp Med **176**(6): 1595-1604.

Liu, J., H. Dang and X. W. Wang (2018). "The significance of intertumor and intratumor heterogeneity in liver cancer." Exp Mol Med **50**(1): e416.

Livak, K. J. and T. D. Schmittgen (2001). "Analysis of relative gene expression data using real-time quantitative PCR and the 2(-Delta Delta C(T)) Method." Methods **25**(4): 402-408.

Loeffler, M., J. A. Kruger, A. G. Niethammer and R. A. Reisfeld (2006). "Targeting tumor-associated fibroblasts improves cancer chemotherapy by increasing intratumoral drug uptake." J Clin Invest **116**(7): 1955-1962.

Lohrum, M. A., R. L. Ludwig, M. H. Kubbutat, M. Hanlon and K. H. Vousden (2003). "Regulation of HDM2 activity by the ribosomal protein L11." Cancer Cell **3**(6): 577-587.

Lu, Y. C., X. Yao, J. S. Crystal, Y. F. Li, M. El-Gamil, C. Gross, L. Davis, M. E. Dudley, J. C. Yang, Y. Samuels, S. A. Rosenberg and P. F. Robbins (2014). "Efficient identification of mutated cancer antigens recognized by T cells associated with durable tumor regressions." Clin Cancer Res **20**(13): 3401-3410.

Lu, Y. C., Z. Zheng, P. F. Robbins, E. Tran, T. D. Prickett, J. J. Gartner, Y. F. Li, S. Ray, Z. Franco, V. Bliskovsky, P. C. Fitzgerald and S. A. Rosenberg (2018). "An Efficient Single-Cell RNA-Seq Approach to Identify Neoantigen-Specific T Cell Receptors." Mol Ther **26**(2): 379-389.

Luo, Y., H. Zhou, J. Krueger, C. Kaplan, S. H. Lee, C. Dolman, D. Markowitz, W. Wu, C. Liu, R. A. Reisfeld and R. Xiang (2006). "Targeting tumor-associated macrophages as a novel strategy against breast cancer." J Clin Invest **116**(8): 2132-2141.

Luria, S. E. and M. Delbruck (1943). "Mutations of Bacteria from Virus Sensitivity to Virus Resistance." Genetics **28**(6): 491-511.

Mackensen, A., N. Meidenbauer, S. Vogl, M. Laumer, J. Berger and R. Andreesen (2006). "Phase I study of adoptive T-cell therapy using antigen-specific CD8+ T cells for the treatment of patients with metastatic melanoma." J Clin Oncol **24**(31): 5060-5069.

Maliniemi, P., E. Carlsson, A. Kaukola, K. Ovaska, K. Niiranen, O. Saksela, L. Jeskanen, S. Hautaniemi and A. Ranki (2011). "NAV3 copy number changes and target genes in basal and squamous cell cancers." Exp Dermatol **20**(11): 926-931.

Mao, Y., E. T. Keller, D. H. Garfield, K. Shen and J. Wang (2013). "Stromal cells in tumor microenvironment and breast cancer." Cancer Metastasis Rev **32**(1-2): 303-315.

Martinez, M. and E. K. Moon (2019). "CAR T Cells for Solid Tumors: New Strategies for Finding, Infiltrating, and Surviving in the Tumor Microenvironment." Front Immunol **10**: 128.

Matson, V., J. Fessler, R. Bao, T. Chongsuwat, Y. Zha, M. L. Alegre, J. J. Luke and T. F. Gajewski (2018). "The commensal microbiome is associated with anti-PD-1 efficacy in metastatic melanoma patients." Science **359**(6371): 104-108.

Matsushita, H., M. D. Vesely, D. C. Koboldt, C. G. Rickert, R. Uppaluri, V. J. Magrini, C. D. Arthur, J. M. White, Y. S. Chen, L. K. Shea, J. Hundal, M. C. Wendl, R. Demeter, T. Wylie, J. P. Allison, M. J. Smyth, L. J. Old, E. R. Mardis and R. D. Schreiber (2012). "Cancer exome analysis reveals a T-cell-dependent mechanism of cancer immunoediting." Nature **482**(7385): 400-404.

Mavilio, F., G. Ferrari, S. Rossini, N. Nobili, C. Bonini, G. Casorati, C. Traversari and C. Bordignon (1994). "Peripheral blood lymphocytes as target cells of retroviral vector-mediated gene transfer." Blood **83**(7): 1988-1997.

McDuffie, M., W. Born, P. Marrack and J. Kappler (1986). "The role of the T-cell receptor in thymocyte maturation: effects in vivo of anti-receptor antibody." Proc Natl Acad Sci U S A **83**(22): 8728-8732.

Miceli, M. C. and J. R. Parnes (1991). "The roles of CD4 and CD8 in T cell activation." Semin Immunol **3**(3): 133-141.

Mitchison, N. A. and C. O'Malley (1987). "Three-cell-type clusters of T cells with antigen-presenting cells best explain the epitope linkage and noncognate requirements of the in vivo cytolytic response." Eur J Immunol **17**(11): 1579-1583.

Monach, P. A., S. C. Meredith, C. T. Siegel and H. Schreiber (1995). "A unique tumor antigen produced by a single amino acid substitution." Immunity **2**(1): 45-59.

Moretta, A., A. Poggi, D. Olive, C. Bottino, C. Fortis, G. Pantaleo and L. Moretta (1987). "Selection and characterization of T-cell variants lacking molecules involved in T-cell activation (T3 T-cell receptor, T44, and T11): analysis of the functional relationship among different pathways of activation." Proc Natl Acad Sci U S A **84**(6): 1654-1658.

Morgan, R. A., N. Chinnasamy, D. Abate-Daga, A. Gros, P. F. Robbins, Z. Zheng, M. E. Dudley, S. A. Feldman, J. C. Yang, R. M. Sherry, G. Q. Phan, M. S. Hughes, U. S. Kammula, A. D. Miller,

C. J. Hessman, A. A. Stewart, N. P. Restifo, M. M. Quezado, M. Alimchandani, A. Z. Rosenberg, A. Nath, T. Wang, B. Bielekova, S. C. Wuest, N. Akula, F. J. McMahon, S. Wilde, B. Mosetter, D. J. Schendel, C. M. Laurencot and S. A. Rosenberg (2013). "Cancer regression and neurological toxicity following anti-MAGE-A3 TCR gene therapy." J Immunother **36**(2): 133-151.

Morgan, R. A., J. C. Yang, M. Kitano, M. E. Dudley, C. M. Laurencot and S. A. Rosenberg (2010). "Case report of a serious adverse event following the administration of T cells transduced with a chimeric antigen receptor recognizing ERBB2." Mol Ther **18**(4): 843-851.

Morita, S., T. Kojima and T. Kitamura (2000). "Plat-E: an efficient and stable system for transient packaging of retroviruses." Gene Ther **7**(12): 1063-1066.

Moullan, N., L. Mouchiroud, X. Wang, D. Ryu, E. G. Williams, A. Mottis, V. Jovaisaite, M. V. Frochaux, P. M. Quiros, B. Deplancke, R. H. Houtkooper and J. Auwerx (2015). "Tetracyclines Disturb Mitochondrial Function across Eukaryotic Models: A Call for Caution in Biomedical Research." Cell Rep **10**(10): 1681-1691.

Mumberg, D., P. A. Monach, S. Wanderling, M. Philip, A. Y. Toledano, R. D. Schreiber and H. Schreiber (1999). "CD4(+) T cells eliminate MHC class II-negative cancer cells in vivo by indirect effects of IFN-gamma." Proc Natl Acad Sci U S A **96**(15): 8633-8638.

Muranski, P., A. Boni, P. A. Antony, L. Cassard, K. R. Irvine, A. Kaiser, C. M. Paulos, D. C. Palmer, C. E. Touloukian, K. Ptak, L. Gattinoni, C. Wrzesinski, C. S. Hinrichs, K. W. Kerstann, L. Feigenbaum, C. C. Chan and N. P. Restifo (2008). "Tumor-specific Th17-polarized cells eradicate large established melanoma." Blood **112**(2): 362-373.

Muul, L. M., P. J. Spiess, E. P. Director and S. A. Rosenberg (1987). "Identification of specific cytolytic immune responses against autologous tumor in humans bearing malignant melanoma." J Immunol **138**(3): 989-995.

Narla, A. and B. L. Ebert (2010). "Ribosomopathies: human disorders of ribosome dysfunction." Blood **115**(16): 3196-3205.

Nishimura, H., M. Nose, H. Hiai, N. Minato and T. Honjo (1999). "Development of lupus-like autoimmune diseases by disruption of the PD-1 gene encoding an ITIM motif-carrying immunoreceptor." Immunity **11**(2): 141-151.

Nishimura, M. I., D. Avichezer, M. C. Custer, C. S. Lee, C. Chen, M. R. Parkhurst, R. A. Diamond, P. F. Robbins, D. J. Schwartzentruber and S. A. Rosenberg (1999). "MHC class I-restricted recognition of a melanoma antigen by a human CD4+ tumor infiltrating lymphocyte." Cancer Res **59**(24): 6230-6238.

North, R. J. (1982). "Cyclophosphamide-facilitated adoptive immunotherapy of an established tumor depends on elimination of tumor-induced suppressor T cells." J Exp Med **155**(4): 1063-1074.

Norton, L. (1988). "A Gompertzian model of human breast cancer growth." Cancer Res **48**(24 Pt 1): 7067-7071.

Nowell, P. C. (1976). "The clonal evolution of tumor cell populations." Science **194**(4260): 23-28.

O'Rourke, D. M., M. P. Nasrallah, A. Desai, J. J. Melenhorst, K. Mansfield, J. J. D. Morrissette, M. Martinez-Lage, S. Brem, E. Maloney, A. Shen, R. Isaacs, S. Mohan, G. Plesa, S. F. Lacey, J. M. Navenot, Z. Zheng, B. L. Levine, H. Okada, C. H. June, J. L. Brogdon and M. V. Maus (2017). "A single dose of peripherally infused EGFRvIII-directed CAR T cells mediates antigen loss and induces adaptive resistance in patients with recurrent glioblastoma." Sci Transl Med **9**(399).

Oldford, S. A., J. D. Robb, P. H. Watson and S. Drover (2004). "HLA-DRB alleles are differentially expressed by tumor cells in breast carcinoma." Int J Cancer **112**(3): 399-406.

Olson, M. R., D. S. McDermott and S. M. Varga (2012). "The initial draining lymph node primes the bulk of the CD8 T cell response and influences memory T cell trafficking after a systemic viral infection." PLoS Pathog **8**(12): e1003054.

Otahal, P., S. C. Hutchinson, L. M. Mylin, M. J. Tevethia, S. S. Tevethia and T. D. Schell (2005). "Inefficient cross-presentation limits the CD8+ T cell response to a subdominant tumor antigen epitope." J Immunol **175**(2): 700-712.

Ott, P. A., Z. Hu, D. B. Keskin, S. A. Shukla, J. Sun, D. J. Bozym, W. Zhang, A. Luoma, A. Giobbie-Hurder, L. Peter, C. Chen, O. Olive, T. A. Carter, S. Li, D. J. Lieb, T. Eisenhaure, E. Gjini, J. Stevens, W. J. Lane, I. Javeri, K. Nellaiappan, A. M. Salazar, H. Daley, M. Seaman, E. I. Buchbinder, C. H. Yoon, M. Harden, N. Lennon, S. Gabriel, S. J. Rodig, D. H. Barouch, J. C. Aster, G. Getz, K. Wucherpfennig, D. Neuberg, J. Ritz, E. S. Lander, E. F. Fritsch, N. Hacohen and C. J. Wu (2017). "An immunogenic personal neoantigen vaccine for patients with melanoma." Nature **547**(7662): 217-221.

Ottina, E., V. Peperzak, K. Schoeler, E. Carrington, R. Sgonc, M. Pellegrini, S. Preston, M. J. Herold, A. Strasser and A. Villunger (2017). "DNA-binding of the Tet-transactivator curtails antigen-induced lymphocyte activation in mice." Nat Commun **8**(1): 1028.

Panic, L., S. Tamarut, M. Sticker-Jantscheff, M. Barkic, D. Solter, M. Uzelac, K. Grabusic and S. Volarevic (2006). "Ribosomal protein S6 gene haploinsufficiency is associated with activation of a p53-dependent checkpoint during gastrulation." Mol Cell Biol **26**(23): 8880-8891.

Paul, W. E. and R. A. Seder (1994). "Lymphocyte responses and cytokines." Cell **76**(2): 241-251.

Phan, G. Q., J. C. Yang, R. M. Sherry, P. Hwu, S. L. Topalian, D. J. Schwartzentruber, N. P. Restifo, L. R. Haworth, C. A. Seipp, L. J. Freezer, K. E. Morton, S. A. Mavroukakis, P. H. Duray, S. M. Steinberg, J. P. Allison, T. A. Davis and S. A. Rosenberg (2003). "Cancer regression and autoimmunity induced by cytotoxic T lymphocyte-associated antigen 4 blockade in patients with metastatic melanoma." Proc Natl Acad Sci U S A **100**(14): 8372-8377.

Philip, M., L. Fairchild, L. Sun, E. L. Horste, S. Camara, M. Shakiba, A. C. Scott, A. Viale, P. Lauer, T. Merghoub, M. D. Hellmann, J. D. Wolchok, C. S. Leslie and A. Schietinger (2017). "Chromatin states define tumour-specific T cell dysfunction and reprogramming." Nature **545**(7655): 452-456.

Philip, M., A. Schietinger and H. Schreiber (2010). "Ribosomal versus non-ribosomal cellular antigens: factors determining efficiency of indirect presentation to CD4+ T cells." Immunology **130**(4): 494-503.

Pisco, A. O. and S. Huang (2015). "Non-genetic cancer cell plasticity and therapy-induced stemness in tumour relapse: 'What does not kill me strengthens me'." Br J Cancer **112**(11): 1725-1732.

Postow, M. A. (2015). "Managing immune checkpoint-blocking antibody side effects." Am Soc Clin Oncol Educ Book: 76-83.

Prehn, R. T. and J. M. Main (1957). "Immunity to methylcholanthrene-induced sarcomas." J Natl Cancer Inst **18**(6): 769-778.

Qin, Z. and T. Blankenstein (2000). "CD4+ T cell--mediated tumor rejection involves inhibition of angiogenesis that is dependent on IFN gamma receptor expression by nonhematopoietic cells." Immunity **12**(6): 677-686.

Quezada, S. A., T. R. Simpson, K. S. Peggs, T. Merghoub, J. Vider, X. Fan, R. Blasberg, H. Yagita, P. Muranski, P. A. Antony, N. P. Restifo and J. P. Allison (2010). "Tumor-reactive CD4(+) T cells develop cytotoxic activity and eradicate large established melanoma after transfer into lymphopenic hosts." J Exp Med **207**(3): 637-650.

Ran, F. A., P. D. Hsu, J. Wright, V. Agarwala, D. A. Scott and F. Zhang (2013). "Genome engineering using the CRISPR-Cas9 system." Nat Protoc **8**(11): 2281-2308.

Ribas, A. and J. D. Wolchok (2018). "Cancer immunotherapy using checkpoint blockade." Science **359**(6382): 1350-1355.

Ridge, J. P., F. Di Rosa and P. Matzinger (1998). "A conditioned dendritic cell can be a temporal bridge between a CD4+ T-helper and a T-killer cell." Nature **393**(6684): 474-478.

Rohaan, M. W., J. H. van den Berg, P. Kvistborg and J. Haanen (2018). "Adoptive transfer of tumor-infiltrating lymphocytes in melanoma: a viable treatment option." J Immunother Cancer **6**(1): 102.

Rosenberg, S. A. and M. E. Dudley (2009). "Adoptive cell therapy for the treatment of patients with metastatic melanoma." Curr Opin Immunol **21**(2): 233-240.

Rosenberg, S. A., B. S. Packard, P. M. Aebersold, D. Solomon, S. L. Topalian, S. T. Toy, P. Simon, M. T. Lotze, J. C. Yang, C. A. Seipp and et al. (1988). "Use of tumor-infiltrating lymphocytes and interleukin-2 in the immunotherapy of patients with metastatic melanoma. A preliminary report." N Engl J Med **319**(25): 1676-1680.

Rosenberg, S. A., J. C. Yang, R. M. Sherry, U. S. Kammula, M. S. Hughes, G. Q. Phan, D. E. Citrin, N. P. Restifo, P. F. Robbins, J. R. Wunderlich, K. E. Morton, C. M. Laurencot, S. M. Steinberg, D. E. White and M. E. Dudley (2011). "Durable complete responses in heavily pretreated patients with metastatic melanoma using T-cell transfer immunotherapy." Clin Cancer Res **17**(13): 4550-4557.

Roser, M., Ritchie, H. (2020). "Cancer." Published online at OurWorldInData.org.

Routy, B., E. Le Chatelier, L. Derosa, C. P. M. Duong, M. T. Alou, R. Daillere, A. Fluckiger, M. Messaoudene, C. Rauber, M. P. Roberti, M. Fidelle, C. Flament, V. Poirier-Colame, P. Opolon, C. Klein, K. Iribarren, L. Mondragon, N. Jacquelot, B. Qu, G. Ferrere, C. Clemenson, L. Mezquita, J. R. Masip, C. Naltet, S. Brosseau, C. Kaderbhai, C. Richard, H. Rizvi, F. Levenez, N. Galleron, B. Quinquis, N. Pons, B. Ryffel, V. Minard-Colin, P. Gonin, J. C. Soria, E. Deutsch, Y. Loriot, F. Ghiringhelli, G. Zalcman, F. Goldwasser, B. Escudier, M. D. Hellmann, A. Eggermont, D. Raoult, L. Albiges, G. Kroemer and L. Zitvogel (2018). "Gut microbiome influences efficacy of PD-1-based immunotherapy against epithelial tumors." Science **359**(6371): 91-97.

Rowley, D. A. and F. W. Fitch (2012). "The road to the discovery of dendritic cells, a tribute to Ralph Steinman." Cell Immunol **273**(2): 95-98.

Sade-Feldman, M., K. Yizhak, S. L. Bjorgaard, J. P. Ray, C. G. de Boer, R. W. Jenkins, D. J. Lieb, J. H. Chen, D. T. Frederick, M. Barzily-Rokni, S. S. Freeman, A. Reuben, P. J. Hoover, A. C. Villani, E. Ivanova, A. Portell, P. H. Lizotte, A. R. Aref, J. P. Eliane, M. R. Hammond, H. Vitzthum, S. M. Blackmon, B. Li, V. Gopalakrishnan, S. M. Reddy, Z. A. Cooper, C. P. Paweletz, D. A. Barbie, A. Stemmer-Rachamimov, K. T. Flaherty, J. A. Wargo, G. M. Boland, R. J. Sullivan, G. Getz and N. Hacohen (2018). "Defining T Cell States Associated with Response to Checkpoint Immunotherapy in Melanoma." Cell **175**(4): 998-1013 e1020.

Sadelain, M., R. Brentjens, I. Riviere and J. Park (2015). "CD19 CAR Therapy for Acute Lymphoblastic Leukemia." Am Soc Clin Oncol Educ Book: e360-363.

Sahin, U., E. Derhovanessian, M. Miller, B. P. Kloke, P. Simon, M. Lower, V. Bukur, A. D. Tadmor, U. Luxemburger, B. Schrors, T. Omokoko, M. Vormehr, C. Albrecht, A. Paruzynski, A. N. Kuhn, J. Buck, S. Heesch, K. H. Schreeb, F. Muller, I. Ortseifer, I. Vogler, E. Godehardt, S. Attig, R. Rae, A. Breitkreuz, C. Tolliver, M. Suchan, G. Martic, A. Hohberger, P. Sorn, J. Diekmann, J. Ciesla, O. Waksmann, A. K. Bruck, M. Witt, M. Zillgen, A. Rothermel, B. Kasemann, D. Langer, S. Bolte, M. Diken, S. Kreiter, R. Nemecek, C. Gebhardt, S. Grabbe, C. Holler, J. Utikal, C. Huber, C. Loquai and O. Tureci (2017). "Personalized RNA mutanome vaccines mobilize poly-specific therapeutic immunity against cancer." Nature **547**(7662): 222-226.

Samelson, L. E., T. Lindsten, B. J. Fowlkes, P. van den Elsen, C. Terhorst, M. M. Davis, R. N. Germain and R. H. Schwartz (1985). "Expression of genes of the T-cell antigen receptor complex in precursor thymocytes." Nature **315**(6022): 765-768.

Sathyanarayanan, V. and S. S. Neelapu (2015). "Cancer immunotherapy: Strategies for personalization and combinatorial approaches." Mol Oncol **9**(10): 2043-2053.

Schenten, D. and R. Medzhitov (2011). "The control of adaptive immune responses by the innate immune system." Adv Immunol **109**: 87-124.

Schietinger, A., A. Arina, R. B. Liu, S. Wells, J. Huang, B. Engels, V. Bindokas, T. Bartkowiak, D. Lee, A. Herrmann, D. W. Piston, M. J. Pittet, P. C. Lin, T. Zal and H. Schreiber (2013). "Longitudinal confocal microscopy imaging of solid tumor destruction following adoptive T cell transfer." Oncoimmunology **2**(11): e26677.

Schietinger, A., J. J. Delrow, R. S. Basom, J. N. Blattman and P. D. Greenberg (2012). "Rescued tolerant CD8 T cells are preprogrammed to reestablish the tolerant state." Science **335**(6069): 723-727.

Schietinger, A., M. Philip, V. E. Krisnawan, E. Y. Chiu, J. J. Delrow, R. S. Basom, P. Lauer, D. G. Brockstedt, S. E. Knoblaugh, G. J. Hammerling, T. D. Schell, N. Garbi and P. D. Greenberg

(2016). "Tumor-Specific T Cell Dysfunction Is a Dynamic Antigen-Driven Differentiation Program Initiated Early during Tumorigenesis." Immunity **45**(2): 389-401.

Schietinger, A., M. Philip, R. B. Liu, K. Schreiber and H. Schreiber (2010). "Bystander killing of cancer requires the cooperation of CD4(+) and CD8(+) T cells during the effector phase." J Exp Med **207**(11): 2469-2477.

Schmitt, A., K. Schulze-Osthoff and S. Hailfinger (2018). "Correspondence: T cells are compromised in tetracycline transactivator transgenic mice." Cell Death Differ **25**(3): 634-636.

Schoenberger, S. P., R. E. Toes, E. I. van der Voort, R. Offringa and C. J. Melief (1998). "T-cell help for cytotoxic T lymphocytes is mediated by CD40-CD40L interactions." Nature **393**(6684): 480-483.

Schreiber, K., A. Arina, B. Engels, M. T. Spiotto, J. Sidney, A. Sette, T. Karrison, R. R. Weichselbaum, D. A. Rowley and H. Schreiber (2012). "Spleen cells from young but not old immunized mice eradicate large established cancers." Clin Cancer Res **18**(9): 2526-2533.

Schreiber, K., T. G. Karrison, S. P. Wolf, K. Kiyotani, M. Steiner, E. R. Littmann, E. G. Pamer, T. Kammertoens, H. Schreiber and M. Leisegang (2020). "Impact of TCR Diversity on the Development of Transplanted or Chemically Induced Tumors." Cancer Immunol Res **8**(2): 192-202.

Schreiber, K., D. A. Rowley, G. Riethmuller and H. Schreiber (2006). "Cancer immunotherapy and preclinical studies: why we are not wasting our time with animal experiments." Hematol Oncol Clin North Am **20**(3): 567-584.

Schreiber, K., T. H. Wu, W. M. Kast and H. Schreiber (2001). "Tracking the common ancestry of antigenically distinct cancer variants." Clin Cancer Res **7**(3 Suppl): 871s-875s.

Schumacher, T. N. and R. D. Schreiber (2015). "Neoantigens in cancer immunotherapy." Science **348**(6230): 69-74.

Seung, L. P., D. A. Rowley, P. Dubey and H. Schreiber (1995). "Synergy between T-cell immunity and inhibition of paracrine stimulation causes tumor rejection." Proc Natl Acad Sci U S A **92**(14): 6254-6258.

Sha, W. C., C. A. Nelson, R. D. Newberry, D. M. Kranz, J. H. Russell and D. Y. Loh (1988). "Positive and negative selection of an antigen receptor on T cells in transgenic mice." Nature **336**(6194): 73-76.

Shaffer, S. M., M. C. Dunagin, S. R. Torborg, E. A. Torre, B. Emert, C. Krepler, M. Beqiri, K. Sproesser, P. A. Brafford, M. Xiao, E. Eggan, I. N. Anastopoulos, C. A. Vargas-Garcia, A. Singh, K. L. Nathanson, M. Herlyn and A. Raj (2017). "Rare cell variability and drug-induced reprogramming as a mode of cancer drug resistance." Nature **546**(7658): 431-435.

Sharma, G., C. M. Rive and R. A. Holt (2019). "Rapid selection and identification of functional CD8(+) T cell epitopes from large peptide-coding libraries." Nat Commun **10**(1): 4553.

Sharma, S. V., D. Y. Lee, B. Li, M. P. Quinlan, F. Takahashi, S. Maheswaran, U. McDermott, N. Azizian, L. Zou, M. A. Fischbach, K. K. Wong, K. Brandstetter, B. Wittner, S. Ramaswamy, M. Classon and J. Settleman (2010). "A chromatin-mediated reversible drug-tolerant state in cancer cell subpopulations." Cell **141**(1): 69-80.

Shockett, P. E. and D. G. Schatz (1996). "Diverse strategies for tetracycline-regulated inducible gene expression." Proc Natl Acad Sci U S A **93**(11): 5173-5176.

Shoji, S., C. M. Dambacher, Z. Shajani, J. R. Williamson and P. G. Schultz (2011). "Systematic chromosomal deletion of bacterial ribosomal protein genes." J Mol Biol **413**(4): 751-761.

Sim, G. K., J. Yague, J. Nelson, P. Marrack, E. Palmer, A. Augustin and J. Kappler (1984). "Primary structure of human T-cell receptor alpha-chain." Nature **312**(5996): 771-775.

Skipper, H. E. (1971). "Cancer chemotherapy is many things: G.H.A. Clowes Memorial Lecture." Cancer Res **31**(9): 1173-1180.

Smith, C. M., N. S. Wilson, J. Waithman, J. A. Villadangos, F. R. Carbone, W. R. Heath and G. T. Belz (2004). "Cognate CD4(+) T cell licensing of dendritic cells in CD8(+) T cell immunity." Nat Immunol **5**(11): 1143-1148.

Sonenberg, N. (1993). "Translation factors as effectors of cell growth and tumorigenesis." Curr Opin Cell Biol **5**(6): 955-960.

Spiotto, M. T., D. A. Rowley and H. Schreiber (2004). "Bystander elimination of antigen loss variants in established tumors." Nat Med **10**(3): 294-298.

Spiotto, M. T., P. Yu, D. A. Rowley, M. I. Nishimura, S. C. Meredith, T. F. Gajewski, Y. X. Fu and H. Schreiber (2002). "Increasing tumor antigen expression overcomes "ignorance" to solid tumors via crosspresentation by bone marrow-derived stromal cells." Immunity **17**(6): 737-747.

Steel, G. G. (1984). "Clonogenic tumour cells." J Cell Physiol Suppl **3**: 21-27.

Sun, C., L. Wang, S. Huang, G. J. Heynen, A. Prahallad, C. Robert, J. Haanen, C. Blank, J. Wesseling, S. M. Willems, D. Zecchin, S. Hobor, P. K. Bajpe, C. Lieftink, C. Mateus, S. Vagner, W. Grernrum, I. Hofland, A. Schlicker, L. F. Wessels, R. L. Beijersbergen, A. Bardelli, F. Di Nicolantonio, A. M. Eggermont and R. Bernards (2014). "Reversible and adaptive resistance to BRAF(V600E) inhibition in melanoma." Nature **508**(7494): 118-122.

Taupier, M. A., J. F. Kearney, P. J. Leibson, M. R. Loken and H. Schreiber (1983). "Nonrandom escape of tumor cells from immune lysis due to intraclonal fluctuations in antigen expression." Cancer Res **43**(9): 4050-4056.

Textor, A., J. J. Listopad, L. L. Wuhrmann, C. Perez, A. Kruschinski, M. Chmielewski, H. Abken, T. Blankenstein and J. Charo (2014). "Efficacy of CAR T-cell therapy in large tumors relies upon stromal targeting by IFNgamma." Cancer Res **74**(23): 6796-6805.

Tivol, E. A., F. Borriello, A. N. Schweitzer, W. P. Lynch, J. A. Bluestone and A. H. Sharpe (1995). "Loss of CTLA-4 leads to massive lymphoproliferation and fatal multiorgan tissue destruction, revealing a critical negative regulatory role of CTLA-4." Immunity **3**(5): 541-547.

Tomlinson, I. P., M. R. Novelli and W. F. Bodmer (1996). "The mutation rate and cancer." Proc Natl Acad Sci U S A **93**(25): 14800-14803.

Tonegawa, S. (1983). "Somatic generation of antibody diversity." Nature **302**(5909): 575-581.

Tran, E., P. F. Robbins and S. A. Rosenberg (2017). "'Final common pathway' of human cancer immunotherapy: targeting random somatic mutations." Nat Immunol **18**(3): 255-262.

Tran, E., S. Turcotte, A. Gros, P. F. Robbins, Y. C. Lu, M. E. Dudley, J. R. Wunderlich, R. P. Somerville, K. Hogan, C. S. Hinrichs, M. R. Parkhurst, J. C. Yang and S. A. Rosenberg (2014). "Cancer immunotherapy based on mutation-specific CD4+ T cells in a patient with epithelial cancer." Science **344**(6184): 641-645.

Turajlic, S., K. Litchfield, H. Xu, R. Rosenthal, N. McGranahan, J. L. Reading, Y. N. S. Wong, A. Rowan, N. Kanu, M. Al Bakir, T. Chambers, R. Salgado, P. Savas, S. Loi, N. J. Birkbak, L. Sansregret, M. Gore, J. Larkin, S. A. Quezada and C. Swanton (2017). "Insertion-and-deletion-derived tumour-specific neoantigens and the immunogenic phenotype: a pan-cancer analysis." Lancet Oncol **18**(8): 1009-1021.

Turtle, C. J., L. A. Hanafi, C. Berger, T. A. Gooley, S. Cherian, M. Hudecek, D. Sommermeyer, K. Melville, B. Pender, T. M. Budiarto, E. Robinson, N. N. Steevens, C. Chaney, L. Soma, X. Chen, C. Yeung, B. Wood, D. Li, J. Cao, S. Heimfeld, M. C. Jensen, S. R. Riddell and D. G. Maloney (2016). "CD19 CAR-T cells of defined CD4+:CD8+ composition in adult B cell ALL patients." J Clin Invest **126**(6): 2123-2138.

Turtle, C. J., L. A. Hanafi, C. Berger, M. Hudecek, B. Pender, E. Robinson, R. Hawkins, C. Chaney, S. Cherian, X. Chen, L. Soma, B. Wood, D. Li, S. Heimfeld, S. R. Riddell and D. G. Maloney (2016). "Immunotherapy of non-Hodgkin's lymphoma with a defined ratio of CD8+ and CD4+ CD19-specific chimeric antigen receptor-modified T cells." Sci Transl Med **8**(355): 355ra116.

Valkenburg, K. C., A. E. de Groot and K. J. Pienta (2018). "Targeting the tumour stroma to improve cancer therapy." Nat Rev Clin Oncol **15**(6): 366-381.

van Essen, D., H. Kikutani and D. Gray (1995). "CD40 ligand-transduced co-stimulation of T cells in the development of helper function." Nature **378**(6557): 620-623.

Van Wauwe, J. P., J. R. De Mey and J. G. Goossens (1980). "OKT3: a monoclonal anti-human T lymphocyte antibody with potent mitogenic properties." J Immunol **124**(6): 2708-2713.

Veatch, J. R., S. M. Lee, M. Fitzgibbon, I. T. Chow, B. Jesernig, T. Schmitt, Y. Y. Kong, J. Kargl, A. M. Houghton, J. A. Thompson, M. McIntosh, W. W. Kwok and S. R. Riddell (2018). "Tumor-infiltrating BRAFV600E-specific CD4+ T cells correlated with complete clinical response in melanoma." J Clin Invest **128**(4): 1563-1568.

Vogelstein, B., E. R. Fearon, S. R. Hamilton, S. E. Kern, A. C. Preisinger, M. Leppert, Y. Nakamura, R. White, A. M. Smits and J. L. Bos (1988). "Genetic alterations during colorectal-tumor development." N Engl J Med **319**(9): 525-532.

Vogelstein, B., N. Papadopoulos, V. E. Velculescu, S. Zhou, L. A. Diaz, Jr. and K. W. Kinzler (2013). "Cancer genome landscapes." Science **339**(6127): 1546-1558.

Vogt, P. K. (2001). "PI 3-kinase, mTOR, protein synthesis and cancer." Trends Mol Med **7**(11): 482-484.

Walker, B. A., C. P. Wardell, L. Chiecchio, E. M. Smith, K. D. Boyd, A. Neri, F. E. Davies, F. M. Ross and G. J. Morgan (2011). "Aberrant global methylation patterns affect the molecular pathogenesis and prognosis of multiple myeloma." Blood **117**(2): 553-562.

Walker, B. A., C. P. Wardell, L. Melchor, A. Brioli, D. C. Johnson, M. F. Kaiser, F. Mirabella, L. Lopez-Corral, S. Humphray, L. Murray, M. Ross, D. Bentley, N. C. Gutierrez, R. Garcia-Sanz, J. San Miguel, F. E. Davies, D. Gonzalez and G. J. Morgan (2014). "Intraclonal heterogeneity is a critical early event in the development of myeloma and precedes the development of clinical symptoms." Leukemia **28**(2): 384-390.

Walker, B. A., C. P. Wardell, L. Melchor, S. Hulkki, N. E. Potter, D. C. Johnson, K. Fenwick, I. Kozarewa, D. Gonzalez, C. J. Lord, A. Ashworth, F. E. Davies and G. J. Morgan (2012).

"Intraclonal heterogeneity and distinct molecular mechanisms characterize the development of t(4;14) and t(11;14) myeloma." Blood **120**(5): 1077-1086.

Wang, B., C. C. Norbury, R. Greenwood, J. R. Bennink, J. W. Yewdell and J. A. Frelinger (2001). "Multiple paths for activation of naive CD8+ T cells: CD4-independent help." J Immunol **167**(3): 1283-1289.

Ward, P. L., H. Koeppen, T. Hurteau and H. Schreiber (1989). "Tumor antigens defined by cloned immunological probes are highly polymorphic and are not detected on autologous normal cells." J Exp Med **170**(1): 217-232.

Ward, P. L., H. K. Koeppen, T. Hurteau, D. A. Rowley and H. Schreiber (1990). "Major histocompatibility complex class I and unique antigen expression by murine tumors that escaped from CD8+ T-cell-dependent surveillance." Cancer Res **50**(13): 3851-3858.

Waterhouse, P., J. M. Penninger, E. Timms, A. Wakeham, A. Shahinian, K. P. Lee, C. B. Thompson, H. Griesser and T. W. Mak (1995). "Lymphoproliferative disorders with early lethality in mice deficient in Ctla-4." Science **270**(5238): 985-988.

Wehrens, E. J., G. Mijnheer, C. L. Duurland, M. Klein, J. Meerding, J. van Loosdregt, W. de Jager, B. Sawitzki, P. J. Coffer, B. Vastert, B. J. Prakken and F. van Wijk (2011). "Functional human regulatory T cells fail to control autoimmune inflammation due to PKB/c-akt hyperactivation in effector cells." Blood **118**(13): 3538-3548.

Wei, S. C., J. H. Levine, A. P. Cogdill, Y. Zhao, N. A. S. Anang, M. C. Andrews, P. Sharma, J. Wang, J. A. Wargo, D. Pe'er and J. P. Allison (2017). "Distinct Cellular Mechanisms Underlie Anti-CTLA-4 and Anti-PD-1 Checkpoint Blockade." Cell **170**(6): 1120-1133 e1117.

Whiteside, T. L. (2008). "The tumor microenvironment and its role in promoting tumor growth." Oncogene **27**(45): 5904-5912.

Wolf, M., A. Schimpl and T. Hunig (2001). "Control of T cell hyperactivation in IL-2-deficient mice by CD4(+)CD25(-) and CD4(+)CD25(+) T cells: evidence for two distinct regulatory mechanisms." Eur J Immunol **31**(6): 1637-1645.

Wölfel, T., M. Hauer, J. Schneider, M. Serrano, C. Wölfel, E. Klehmann-Hieb, E. De Plaen, T. Hankeln, K. H. Meyer zum Buschenfelde and D. Beach (1995). "A p16INK4a-insensitive CDK4 mutant targeted by cytolytic T lymphocytes in a human melanoma." Science **269**: 1281-1284.

Wortzel, R. D., C. Philipps and H. Schreiber (1983). "Multiple tumour-specific antigens expressed on a single tumour cell." Nature **304**(5922): 165-167.

Wu, T. H., K. Schreiber, A. Arina, N. N. Khodarev, E. V. Efimova, D. A. Rowley, R. R. Weichselbaum and H. Schreiber (2011). "Progression of cancer from indolent to aggressive despite antigen retention and increased expression of interferon-gamma inducible genes." Cancer Immun **11**: 2.

Yanagi, Y., Y. Yoshikai, K. Leggett, S. P. Clark, I. Aleksander and T. W. Mak (1984). "A human T cell-specific cDNA clone encodes a protein having extensive homology to immunoglobulin chains." Nature **308**(5955): 145-149.

Yang, L., C. Lin and Z. R. Liu (2005). "Phosphorylations of DEAD box p68 RNA helicase are associated with cancer development and cell proliferation." Mol Cancer Res **3**(6): 355-363.

Yarchoan, M., A. Hopkins and E. M. Jaffee (2017). "Tumor Mutational Burden and Response Rate to PD-1 Inhibition." N Engl J Med **377**(25): 2500-2501.

Yeku, O., X. Li and R. J. Brentjens (2017). "Adoptive T-Cell Therapy for Solid Tumors." Am Soc Clin Oncol Educ Book **37**: 193-204.

Yossef, R., E. Tran, D. C. Deniger, A. Gros, A. Pasetto, M. R. Parkhurst, J. J. Gartner, T. D. Prickett, G. Cafri, P. F. Robbins and S. A. Rosenberg (2018). "Enhanced detection of neoantigen-reactive T cells targeting unique and shared oncogenes for personalized cancer immunotherapy." JCI Insight **3**(19).

Yost, K. E., A. T. Satpathy, D. K. Wells, Y. Qi, C. Wang, R. Kageyama, K. L. McNamara, J. M. Granja, K. Y. Sarin, R. A. Brown, R. K. Gupta, C. Curtis, S. L. Bucktrout, M. M. Davis, A. L. S. Chang and H. Y. Chang (2019). "Clonal replacement of tumor-specific T cells following PD-1 blockade." Nat Med **25**(8): 1251-1259.

Zacharakis, N., H. Chinnasamy, M. Black, H. Xu, Y. C. Lu, Z. Zheng, A. Pasetto, M. Langhan, T. Shelton, T. Prickett, J. Gartner, L. Jia, K. Trebska-McGowan, R. P. Somerville, P. F. Robbins, S. A. Rosenberg, S. L. Goff and S. A. Feldman (2018). "Immune recognition of somatic mutations leading to complete durable regression in metastatic breast cancer." Nat Med **24**(6): 724-730.

Zhang, B., T. Karrison, D. A. Rowley and H. Schreiber (2008). "IFN-gamma- and TNF-dependent bystander eradication of antigen-loss variants in established mouse cancers." J Clin Invest **118**(4): 1398-1404.

Zhang, B., Y. Zhang, N. A. Bowerman, A. Schietinger, Y. X. Fu, D. M. Kranz, D. A. Rowley and H. Schreiber (2008). "Equilibrium between host and cancer caused by effector T cells killing tumor stroma." Cancer Res **68**(5): 1563-1571.

Zhang, J., J. Fujimoto, J. Zhang, D. C. Wedge, X. Song, J. Zhang, S. Seth, C. W. Chow, Y. Cao, C. Gumbs, K. A. Gold, N. Kalhor, L. Little, H. Mahadeshwar, C. Moran, A. Protopopov, H. Sun, J. Tang, X. Wu, Y. Ye, W. N. William, J. J. Lee, J. V. Heymach, W. K. Hong, S. Swisher, Wistuba, II and P. A. Futreal (2014). "Intratumor heterogeneity in localized lung adenocarcinomas delineated by multiregion sequencing." Science **346**(6206): 256-259.

Zhong, W., A. D. Roberts and D. L. Woodland (2001). "Antibody-independent antiviral function of memory CD4+ T cells in vivo requires regulatory signals from CD8+ effector T cells." J Immunol **167**(3): 1379-1386.

9. Publications

Wolf, S. P., A. Anastasopoulou, K. Schreiber, K. Borutta, B. Engels, P. Yew, K. Kiyotani, Y. Nakamura, M. Leisegang and H. Schreiber. (2020). “One stroma-recognizing $CD4^+$TCR and one cancer-recognizing $CD8^+$TCR are essential and sufficient for tumor eradication.” Immunity submitted.

Sharma, P., V. Marada, Q. Cai, M. Kizerwetter, Y. He, **S. P. Wolf**, K. Schreiber, H. Clausen, H. Schreiber and D. M. Kranz (2020). "Structure-guided engineering of the affinity and specificity of CARs against Tn-glycopeptides." Proc Natl Acad Sci U S A **117**(26): 15148-15159.

Diehl, M. I., **S. P. Wolf**, V. Bindokas and H. Schreiber. (2020). “Automated cell cluster analysis provides insight into multi-cell-type interactions between immune cells and their targets.” Exp Cell Res: 112014.

Bottinger, P., K. Schreiber, E. Hyjek, T. Krausz, M. T. Spiotto, M. Steiner, C. Idel, H. Booras, G. Beck-Engeser, J. Riederer, G. Willimsky, **S. P. Wolf**, T. Karrison, E. Jensen, R. R. Weichselbaum, Y. Nakamura, P. Y. Yew, P. F. Lambert, T. Kurita, K. Kiyotani, M. Leisegang and H. Schreiber (2020). "Cooperation of genes in HPV16 E6/E7-dependent cervico-vaginal carcinogenesis trackable by endoscopy and independent of exogenous estrogens or carcinogens." Carcinogenesis.

Schreiber, K., T. G. Karrison, **S. P. Wolf**, K. Kiyotani, M. Steiner, E. R. Littmann, E. G. Pamer, T. Kammertoens, H. Schreiber and M. Leisegang (2020). "Impact of TCR Diversity on the Development of Transplanted or Chemically Induced Tumors." Cancer Immunol Res **8**(2): 192-202.

He, Y., K. Schreiber, **S. P. Wolf**, F. Wen, C. Steentoft, J. Zerweck, M. Steiner, P. Sharma, H. M. Shepard, A. Posey, C. H. June, U. Mandel, H. Clausen, M. Leisegang, S. C. Meredith, D. M. Kranz and H. Schreiber (2019). "Multiple cancer-specific antigens are targeted by a chimeric antigen receptor on a single cancer cell." JCI Insight **4**(23).

10. Appendix

10.1 Abbreviations

APC	–	Antigen Presenting Cell
ATT	–	Adoptive T Cell Transfer
BCR	–	B Cell receptor
CAR	–	Chimeric Antigen Receptor
CTL	–	Cytolytic T Lymphocyte
CTLA4	–	Cytotoxic T Lymphocyte Associated Protein 4
DC	–	Dendritic Cell
DNA	–	Deoxyribonucleic Acid
ER	–	Endoplasmic Reticulum
i.p.	–	Intraperitoneal Injection
LN	–	Lymph Node
mAb	–	Monoclonal Antibody
MHC	–	Major Histocompatibility Complex
nsSNV	–	Nonsynonymous Single Nucleotide Variant
PAMP	–	Pathogen Associated Molecular Pattern
PBL	–	Peripheral Blood Lymphocytes
PD-1	–	Programmed Cell Death Protein 1
PD-L1	–	Programmed Cell Death Protein Ligand 1
pMHC	–	Peptide MHC
PRR	–	Pattern Recognition Receptor
RNA	–	Ribonucleic Acid
s.c.	–	Subcutaneous Injection
TAM	–	Tumor Associated Macrophage
TCR	–	T Cell Receptor
TIL	–	Tumor Infiltrating Lymphocyte
Treg	–	Regulatory $CD4^+$ T cell

10.2 List of figures

10.3 List of tables

Statement of authorship

I, Steven Wolf, hereby confirm that the present thesis with the title “Combining effects of one tumor-stroma recognizing TCR with one cancer-cell specific TCR for eradication of solid tumors” was written independently with the help of the cited literature and references.

Furthermore, I assure that the present thesis, in its current or similar form was not submitted to another university or elsewhere.